UNIVERSITY OF MODENA AND REGGIO EMILIA

Dipartimento di Scienze della Vita

PhD Program in
Molecular and Regenerative Medicine

XXXIV Cycle

COMBINATION OF CHEMO AND GENE THERAPY IN LOCALLY ADVANCED PANCREATIC CANCER: TOWARDS THE CLINICAL SETTINGS

PhD program coordinator:
Prof. Michele De Luca

Tutor:
Prof. Massimo Dominici

PhD Candidate:

Dr. Andrea Spallanzani

ABSTRACT

Locally advanced pancreatic cancer (LAPC) represents a future challenge with an increasing incidence. Currently despite important efforts in developing pioneering targeted therapies, PC has today the highest mortality rate of all major cancers. Chemotherapy alone or chemo-radiotherapy aim to control locally advanced pancreatic cancer (LAPC) but fail in major cytoreduction to reach a R0 surgery. In preclinical studies the co-administration of Gemcitabine (GEM) and Nab-paclitaxel (Nab-PTX) increased the intra-tumoral concentrations of both drugs inducing stromal damage. In our pre-clinical experience we reported both in vitro and in vivo model the anti-cancer effect of RR001: an anti-neoplastic gene-therapy strategy based on human adipose mesenchymal stromal/stem cells engineered to secrete proapoptotic soluble (s)-TRAIL protein. To enhance the rational of treating pancreatic adenocarcinoma (PDAC) with RR001, 58 specimens were collected from pancreatic cancer patients (primary tumor or liver metastases) highlighting the histological positivity of TRAIL functional receptors in 100% of the specimens. Afterwards we have focused on overcoming gemcitabine and TRAIL resistance, confirming both in vitro and in a vivo-like PC model the synergistic anti-cancer activity of the trio-combination of GEM + Nab-PTX + RR001. This combination induces PDAC death associated with stroma damage: pre-treatment with gemcitabine and nab-paclitaxel overcame TRAIL resistance. With these assumptions we have designed a phase I/IIa trial in LAPC aim to determine the safety, feasibility and dose finding of intra-tumoral injection of the RR001 administered by ultrasound (US) guided injections in combination with standard of care therapy based on GEM/Nab-PTX. Secondly, the trial will explore the efficacy of this combination (radiological or histological for operated patients) researching liquid and tissue predictive biomarkers: the levels of sTRAIL, tumor/stromal ratio and lymphocytes infiltration before and after RR001 in histological specimens. The trial has been approved by local ethical committee on July 2021 and will soon be ready to enroll.

RIASSUNTO

Il carcinoma pancreatico localmente avanzato (LAPC) rappresenta una sfida futura a causa della crescente incidenza, dell'aggressività della patologia e dell'assenza di trattamenti target innovativi che lo classificano attualmente come la neoplasia con il più alto tasso di mortalità tra i tumori prevalenti. La sola chemioterapia o il trattamento di associazione chemio-radioterapico hanno come principale endpoint il controllo locale e sistemico di malattia ma raramente ottengono una citoriduzione maggiore tale da consentire di raggiungere un intervento chirurgico radicale con margine di resezione negativo (R0). Studi preclinici condotti in vivo su modelli murini, ottenuti utilizzando sia linee cellulari che cellule primarie di carcinoma pancreatico, hanno evidenziato un aumento dell'effetto antitumorale mediato dalla gemcitabina (GEM) quando somministrata in combinazione con Nab-Paclitaxel (Nab-PTX) rispetto al trattamento in monoterapia. Tali studi hanno inoltre riportato un significativo incremento delle concentrazioni intra-tumorali sia di Nab-PTX che di GEM, quando co-somministrati provocando un danno sul compartimento stromale, determinando un calo della quota di fibroblasti associati al tumore (CAF). Nella nostra esperienza preclinica abbiamo riportato sia in vitro che in vivo l'attività anti-neoplastica di RR001: un prodotto medicinale a base di cellule umane autologhe geneticamente modificate per veicolare molecola antitumorale TRAIL solubile (sTRAIL). Per analizzare il razionale del trattamento del PC con RR001, sono stati raccolti 58 campioni da pazienti con cancro del pancreas (tumore primario o metastasi epatiche) evidenziando la positività istologica dei recettori funzionali TRAIL nel 100% dei campioni. Successivamente ci siamo concentrati sul superamento della resistenza alla gemcitabina e a TRAIL, confermando sia in vitro che in un modello in vivo su cloni cellulari resistenti a TRAIL, l'attività sinergica antitumorale della trio-combinazione di GEM + Nab-PTX + RR001. In conclusione questa combinazione induce la morte cellulare nei tessuti analizzati inducendo inoltre un significativo danno stromale: nello specifico il pre-trattamento con GEM e Nab-PTX ha superato la resistenza a TRAIL. Con questi presupposti abbiamo delineato uno studio di fase I/IIa in pazienti con LAPC con lo scopo di determinare la sicurezza, la fattibilità e la dose massima tollerabile di RR01 somministrato tramite iniezioni intratumorali eseguite su guida ecografica in combinazione con la chemioterapia standard con GEM /Nab-PTX. Saranno valutati secondariamente anche endpoint correlati all'efficacia di questa combinazione come risposta radiologica o istologica per pazienti operati e la sopravvivenza, ricercando biomarcatori predittivi di risposta liquidi e tissutali: i livelli di

sTRAIL, il rapporto tumore/stromale e l'infiltrazione linfocitaria prima e dopo RR001 nei campioni istologici. La sperimentazione è stata approvata dal comitato etico locale nel luglio 2021 e sarà presto pronta per iniziare l'arruolamento.

ABBREVIATIONS AND ACRONYMS

5-FU 5- fluorouracil
AD-MSCs Adipose mesenchymal stromal cells
ADEX Aberrantly differentiated endocrine and exocrine
ADSC Human stromal cells obtained from adipose tissue
ASIs Angiotensin system inhibitors
BID BH3 interacting domain death agonist
BLI Bioluminescence
CA Celiac artery
CA. Laser ablation and cryoablation
CTL Control
DcR1 Decoy Receptor 1
DcR2 Decoy Receptor 2
DFS Disease free survival
DiR Deep infrared fluorescent
DISC Death-inducing signaling complex
DR4 Death Receptor 4
DR5 Death Receptor 5
E:T Effector-target
EC Electrochemotherapy
ECM Extracellular matrix
EMT Epithelial to mesenchymal transition
ET-1 Endothelin-1
EVs Extracellular vesicles
FACS Fluorescence activated cell sorting
FADD Fas-associated death domain
FAP Fibroblast activation protein
FN-1 Fibronectin 1
FSP Fibroblast specific protein

GAGs Glycosaminoglycans

Gal-1 Glycoprotein galectin 1

GBM Glioblastoma multiforme

GEM Gemcitabine

GM-CSF Granulocyte macrophage colony stimulating factor

GNP Gemcitabine + Nab-paclitaxel

H&E Hematoxylin and eosin

HpMSCs Human pancreas-derived MSCs

IFN Interferon

IHC Immunohistochemical

IRAK4 IL-1 receptor-associated kinase 4

IRE Irreversible electroporation

ICAFs Inflammatory CAFs

LAPC Locally advanced pancreatic cancer

LOX Lysyl oxidase

MDSCs Marrow-derived suppressor cell

MSC-TRAIL MSC producing TRAIL

MSCs Mesenchimal stromal cells

MSCstTRAIL MSCs transfected with the secreting form of TRAIL

MWA Microwave ablation

MyCAFs Myofibroblastic CAFs

Nab-PTX Nab-paclitaxel

NAL-IRI Nanoliposomal irinotecan

NSCLC Non small cell lung cancer

OPG Osteoprotegerin

OS Overall survival

PARP Poly adenosine diphosphate-ribose polymerase

PCs Pancreatic stellate cells

PDAC. Pancreatic adenocarcinoma

PDGF Platelet-derived growth factor

PIF. Interstistial fluid pressure

pMMR Proficient miss-match repair

PRs Partial responses

PV Portal vein

RFA Radiofrequency ablation

rhTRAIL Recombinant human TRAIL

ROCK Rho kinase

RT Radiotherapy

SABR Stereotactic ablative body radiation

SHH Sonic hedgehog pathway

SMA Superior mesenteric artery

SMV Superior mesenteric vein

SPARC Secreted protein acidic and rich in cysteine

sTRAIL Soluble TRAIL

T-reg Regulatory T cells

CAFs Cancer-associated fibroblasts

TAM Tumor associated macrophages

TME Tumor microenvironment

TMZ Temozolomide

TNFSF10 TRAIL/Apo2L

TRAIL TNF related apoptosis inducing ligand

TRAIL-R TRAIL receptors

US Ultrasound

VEGF – A Vascular endothelial growth factor A

SUMMARY

1 BACKGROUND

1.1 PANCREATIC DUCTAL ADENOCARCINOMA: AN UNMET NEED

1.1.1 Epidemiology and risk factors

With a worldwide incidence of approximately 500,000 new cases and 466,000 deaths in 2021, pancreatic adenocarcinoma (PDAC) has one of the highest mortality rates in cancers estimating to become the number two leading cause of cancer-related death in 2030 [1] (**Figure 1**). PDAC etiology is a multifactorial process including cigarette smoking and family history as dominant risk factors but also diabetes mellitus, obesity, dietary factors, alcohol abuse, age, ethnicity [2]. Approximately 10% of patients with PDAC have some genetic predisposition and several germline mutations are involved in hereditary forms of pancreatic cancer including BRCA1, BRCA2, PALB2, ATM, CDKN2A, APC, MLH1, MSH2, MSH6, PMS2, PRSS1 and STK11 [3]. Despite the progress in diagnostic and therapeutic approaches, actually the 1 year overall survival (OS) of the disease is about 24% and only 9% of patients are alive after 5 years from diagnosis [4].

1.1.2 Molecular profiling of PDAC

The recently retrospective analysis of the "Know you tumor registry" trial reported that actionable mutations were identified in 26% of 1082 PDAC samples [5]. In a minority of cases, germline or somatic mutations in DNA damage repair genes (DDR) such as BRCA2 (that account for 5-17% of families with familial pancreatic cancer), PALB2 (3% of patients with familial pancreatic cancer) and ATM were identified [6-8]. Many studies have confirmed that PDAC patients carrying gBRCA1-2pv could benefit from platinum-based treatments. [7, 9-11]

The process of carcinogenesis of PDAC is driven by four mutational pathways: kirsten rat sarcoma virus (KRAS), cellular tumor antigen p53 (TP53), cyclin dependent kinase inhibitor 2A (CDKN2A), and SMAD family member 4 (SMAD4) [12-14]. Frequently

the first step is the activation of KRAS which occurs early in carcinogenesis, whereas the later progression of the disease is related to mutations in SMAD4.
In 2016 Bailey et al performed an integrated genomic analysis of 456 patients with PDAC revealing 10 possible activated pathway: KRAS, TGF-β, WNT, NOTCH, ROBO/SLIT signaling, G1/S transition, SWI-SNF, chromatin modification, DNA repair and RNA processing [13]. They defined 4 different transcriptomic subtypes with peculiar histopathological correlation called squamous, pancreatic progenitor, immunogenic and aberrantly differentiated endocrine and exocrine (ADEX) (**Figure 2**). Squamous subtype was characterized by activation of gene pathways involved in inflammation, hypoxia, TGF-B signaling, MYC pathway and autophagy, leading to a complete loss of endodermal identity. Pancreatic progenitor subtype expressed genes involved in early pancreatic development such as PDX1, MNX1, HNF4G, HNF4A, HNF1B, HNF1A, FOXA2, FOXA3 e HES1. ADEX group was characterized by upregulation of genes involved in later stages of pancreatic development and involved in KRAS activation, exocrine (NR5A2 and RBPJL) and endocrine (NEUROD1 and NKX2-2) differentiation. Lastly the immunogenic subtype was characterized by significant immune infiltrate and upregulation of CTLA4 and PD-1 expression that preclude novel immunotherapy approach [13].

1.1.3 Current treatment strategies

According to American Cancer Society, only 10-20% of new cases of pancreatic cancer are classified as resectable or borderline resectable (**Figure 3**). For those patients, surgery combined with adjuvant chemotherapy is the standard of care with 5-year survival rate of 20% [15]. More than an half of new cases are reported as metastatic disease and one third of new diagnosis are defined as locally advanced non resectable disease (LAPC) with poor 5 years OS ranged between 10 to 15% [15]

1.1.3.1 Resectable pancreatic cancer

A commonly accepted definition of potentially resectable pancreatic cancer is a tumor that is limited to the pancreas with no arterial contact (superior mesenteric artery, celiac axis, common hepatic artery); some authors also include superior mesenteric vein involvement ≤90 degrees [16].

Surgical resection offers the only chance of cure for exocrine pancreatic cancer, but only 15 to 20% of cases are potentially resectable at presentation and although the surgical approach, 5-year survival rates are approximatively 10% [17, 18]. Six months of adjuvant treatment with gemcitabine or fluoropyrimidine (fluorouracil plus leucovirin or S-1 in Japan) was the standard of care from 2000 till 2017 with significant benefit in overall survival. However, recurrence rates remain high despite adjuvant treatment, with 69 to 75% of patients having a relapse within 2 years [17, 18].

Few improvement in adjuvant treatment were reported in 2017 with the ESPAC-4 trial [19]. The trial confirmed a significant OS benefit in patients treated with adjuvant poli-chemotherapy with capecitabine and gemcitabine versus gemcitabine alone. The median OS for patients in the gemcitabine plus capecitabine group was 28·0 months (95% CI 23·5-31·5) compared with 25·5 months (95% CI 22·7-27·9) in the gemcitabine group (HR 0·82 [95% CI 0·68-0·98], p=0·032) [19]. Following the same direction of an intensive chemotherapy regimen in adjuvant setting, a recent phase III landmark randomized controlled trial showed a significant improvement in median OS in selected patients treated with adjuvant polychemotherapy with modified FOLFIRINOX regimen versus gemcitabine alone [20]. The median OS was 54.4 months in the modified-FOLFIRINOX group and 35.0 months in the gemcitabine group (HR 0.64; 95% CI, 0.48 to 0.86; P=0.003). The authors concluded that the PRODIGE-24 trial report a significant improvement in OS compared with previous results obtained with capecitabine-gemcitabine combination due to a better patients selection.

The main limit of adjuvant therapy is that unfortunately not all patients could receive an effective treatment due to surgical complications so also in early disease setting, the role of neoadjuvant therapy is under investigation with the aim of enhancing R0 resection rate, allowing early therapy for micro-metastases and improving patient selection for better surgical outcomes. The addition of neoadjuvant therapy improved survival in borderline resectable and locally advanced pancreatic cancer settings but there are few published trials that included only resectable disease [21, 22]. In the recent SWOG S1505 phase II trial, two years OS were 47% and 48% with perioperative FOLFIRINOX and Gemcitabine – Nab paclitaxel respectively without any improvement compared with historical cohorts based on upfront surgery [23]. In a metanalysis included 6 trials enrolling 469 patients with resectable pancreatic cancer, neoadjuvant chemotherapy significantly improved OS (HR 0.75; 95% CI 0.58-0.98; P = 0.033) and DFS (HR 0.73; 95% CI 0.59-0.89; P = 0.002) compared to upfront surgery [24].

Based on these recent results, the role of neoadjuvant treatment in resectable disease is still debated.

1.1.3.2 Borderline resectable pancreatic cancer

The International Association of Pancreatology defined the borderline resectable disease with anatomic, biological and conditional factors [25]. The anatomical definition is a tumor contact 180 ° or greater or invasion of the superior mesenteric vein (SMV) or portal vein (PV) with bilateral narrowing or occlusion and not exceeding the inferior border of the duodenum. In case of arterial invasion, the definition is a tumor contact with the superior mesenteric artery (SMA) and/or celiac artery (CA) less than 180° without showing stenosis or deformity. Biological criteria included clinical findings suspicious for metastatic disease (CA 19.9>500 ng/ml, enlarged lymph-nodes). The conditional factors are related to patients performance status.

In borderline resectable setting, preoperative chemoradiotherapy might increase the R0 resection rate through tumor downstaging. A meta-analysis from Versteijne et al evaluated the role of preoperative chemo(radio)therapy in resectable or borderline resectable PDAC showed a prolonged OS in pre-treated group when compared with immediate surgery (18.8 v 14.8 months) [26]. These data were recently confirmed in a subsequent metanalysis on almost 1000 patients with resectable or borderline resectable disease. In the latter group in particular neoadjuvant treatment reduced the risk of death of almost 40% versus upfront surgery (HR 0.61, 95% CI 0.44-0.85; p = 0.004) [27, 28]. Although the difference in median OS was only 1.4 months (15.7 months *v* 14.3 months), the 5-year OS rate was 20.5% (95% CI, 14.2 to 29.8) with neoadjuvant chemoradiotherapy and 6.5% (95% CI, 3.1 to 13.7) with upfront surgery.

1.1.3.3 Locally advanced pancreatic cancer

Worldwide, various criteria for locally advanced pancreatic cancer (LAPC) diagnosis are used. National Comprehensive Cancer Network (NCCN) criteria define a tumor with >180° of arterial contact or un-reconstructable venous involvement as unresectable [16]. Patients with LAPC have typically an extensive vascular involvement with a peri-operative morbidity of 54% and a mortality rate of 12% in upfront resections. Taken this into account, together with a high recurrence rate and no proven survival benefit, an upfront resection is not deemed beneficial for patients with LAPC [29].

Historically, patients with LAPC were treated as patients with stage IV disease with a palliative chemotherapy approach. The standard of care in this setting provides a polychemotherapy approach with or without radiotherapy aim to obtain local and systemic control and a resectable disease. Polychemotherapy regimens are the same used in metastatic setting: FOLFIRINOX or GEM + Nab-PTX.

In a recent metanalysis on 653 patients with LAPC treated with FOLFIRINOX, median OS and PFS ranged from 10,0 to 32.7 months and 3.0 to 25.3 months [30]. After FOLFIRINOX the resection rate was 34% with 88% rate of radical surgery (R0 resection) [30].

In the phase II LAPACT trial, 107 patients with LAPC were enrolled and treated with 6 months of GEM – Nab-PTX polychemotherapy. Median PFS was 10 months and median OS was 19 months [31]. The overall response rate was 33% with a tumor resection conversion in only 15% of patients (16 of 107).

The landmark role of resection in LAPC setting was enhanced in the phase II NEOLAP trial that randomized 168 patients to 4 cycles of chemotherapy with GEM + Nab-PTX or a sequential approach with 2 cycles of this regimen followed by 4 cycles with FOLFIRINOX. No differences in terms of efficacy and safety of these 2 approaches were reported with mOS 17.2 vs 22.5 months (HR 0.73, p 0,268). R0 resection was feasible in 46 over 168 patients (27%). Overall survival was doubled in patients who underwent R0 resection reaching more than 2 years and it was comparable to patients with resectable disease at diagnosis (median OS 27.4 months) [32].

Patients with stable disease or partial response during cytoreductive chemotherapy and not eligible for surgery are potential candidates for stereotactic radiation or ablative therapies due to the feasibility of EUS-guided approaches [33, 34].

Stereotactic ablative body radiation (SABR) is based on an highly dose of radiation (6 - 25 Gy) on the target region with few applications (1-5 days) limiting the dose to the surrounding organs [35].

Radiofrequency ablation (RFA), microwave ablation (MWA), laser ablation and cryoablation (CA) are considered thermal ablative strategies while irreversible electroporation (IRE) and electrochemotherapy (EC) are considered non-thermal treatments.

RFA can be performed during surgery, percutaneously or using endoscopic ultrasound through needle electrodes to apply high-frequency alternating current to solid tumors generating high temperatures obtaining necrosis, and protein denaturation within the

tumor [36]. Recent experiences reported an improved OS over 2 years when combining RFA and chemotherapy vs systemic treatment alone.

CA induces rapid argon-gas-based freezing and thawing of target lesions causing cellular destruction by vascular-mediated cytotoxicity, endothelial damage, and cell death [36].

MWA causes heat by oscillation of predominantly H_20- molecules in an electromagnetic field. This technique has advantages over RFA in the ease of setup and larger ablation zones in a shorter period [36].

IRE can be applied on the pancreatic gland via laparotomy or percutaneously by image-guided puncture. Through electrodes inserted into the tumor, an electric field across the cell membrane is created, rendering cellular membranes irreversibly porous and effectively breaking down the membrane barrier activating the apoptotic pathway leading to cell death. IRE has the ability to preserve the extracellular matrix and surrounding organs [37].

Electrochemotherapy is a new non-thermal technique that exploits the combination of reversible electroporation and chemotherapeutic drugs (bleomycin) avoiding possible thermal injury to the peripancreatic vessels. Also this treatment is feasible by percutaneous EUS-guided approach [38].

There has been an increase in the regional/ intra-tumoral administration of cell-based and viral vector-based clinical trials over the last decades. Various approaches have been evaluated for intra-tumoral injection to improve local delivery of anti-cancer treatment in combination with systemic therapies. These developments involved also PDAC patients with few published trials with intratumorally delivered anti-cancer agents including lymphocytes, dendritic cells, fibroblasts allogeneic tumor cells and vaccines demonstrating the feasibility and the safety of the approach.(**Table 1**)

1.1.3.4 Metastatic pancreatic cancer

Systemic chemotherapy is the only approach that demonstrated an improve in disease related symptoms and quality of life in metastatic PDAC setting [16]. The current standard first-line regimen has evolved over the years from fluoropyrimidine alone to gemcitabine to the current standard of care FOLFIRINOX or GEM-Nab-PTX. FOLFIRINOX and GEM-Nab-PTX are both effective first-line chemotherapy regimen based on PRODIGE 4-ACCORD11 and MPACT trials. In the phase III PRODIGE 4-ACCORD 11 trial, OS was significantly increased in FOLFIRINOX arm versus previous standard of care gemcitabine (11,1 months versus 6,8 months; HR 0.57; 95% CI, 0.45 to

0.73; P<0.001) in selected good performance status patients without previous serious comorbidities [39]. Also, in the phase III randomized MPACT trial enrolling 861 patients, the combination treatment of GEM-Nab-PTX was superior to gemcitabine alone. Median OS was 8.5 months in the GEM-Nab-PTX arm vs 6.7 months in the control arm (HR, 0.72; 95% CI, 0.62–0.83; p < 0.001) [40]. Actually, there are no published prospective randomized studies comparing FOLFIRINOX to GEM-Nab-PTX but only retrospective studies that suggested greater activity for FOLFIRINOX in patients with better ECOG PS and general fitness [41]. In a recent Italian meta-analysis on 3813 patients, no evidence of a statistical OS or PFS benefit with FOLFIRINOX as opposed to GEM-Nab-PTX as a first-line therapy in metastatic PDAC was reported, highlighting the need for a prospective study to answer this question. [42]

In patients with germinal BRCA mutation and disease control after first line platinum-based chemotherapy, the role of olaparib (a PARP inhibitor) has been evaluated in the phase III POLO trial [43]. One hundred and fifty-seven patients with gBRCAm were randomized to receive either olaparib or placebo. The median PFS was significantly improved in the olaparib group (7.4 versus 3.8 months, HR 0.53; 95% CI [0.35–0.82]; p = 0.004). Final OS results were recently presented and showed no difference between the two arms (19.0 in the olaparib arm versus 19.2 months in the placebo arm, p = 0.3487) [11] and so for this reason actually AIFA has not authorized the use of olaparib in this setting yet.

After first line treatment failure, less than a half of patients with advanced PDAC proceed to second-line therapy. Recently nanoliposomal irinotecan (NAL-IRI) , a novel formulation of irinotecan has been evaluated in the phase III NAPOLI-1 trial showing longer OS in the combination arm (NAL-IRI + 5-FU) vs 5-FU alone (median, 6.1 versus 4.2 months; HR, 0.75; p = 0.012) [44]. Previously the CONKO-003 trial showed a statistically significant OS benefit with FOLFOX in comparison with 5-FU/leucovorin alone [45]. Actually the main international guidelines suggest the choice of second line treatment depending on previous first line regimen, ECOG PS, co-morbidities and organ function [16].

1.1.3.5 New Horizons

Mutations in KRAS are found in more than 90% of advanced PDAC so only less than 10% of patients are KRAS wt [14]. Nimotuzumab, an anti-EGFR monoclonal antibody,

obtained survival benefit in a phase IIb randomized trial including 192 patients in combination with gemcitabine in first line setting (mOS 8.6 versus 6.0 months; HR 0.69; p = 0.03; median PFS 5.1 versus 3.4 months; HR 0.68; p = 0.02). The most impressive result was the 1 year OS rate : 53.8% versus 15.8% (HR 0.32; p = 0.026). As expected KRAS wt patients experienced a significantly better OS than those with KRAS mutations (11.6 versus 5.6 months, P = 0.03) [46].

At ASCO 2022 the results of the confirmatory phase III NOTABLE trial were reported. The trial randomized 92 Chinese patients with KRAS wt metastatic PDAC to nimotuzumab /gemcitabine vs gemcitabine alone [47]. Median OS was longer for patients in the nimotuzumab/gemcitabine group (10.9 months) compared to those who received gemcitabine plus placebo (8.5 months). The 1-year overall survival rate was 43.6% in the nimotuzumab/gemcitabine group vs 26.8% in the placebo/gemcitabine group; 3-year rates were 13.9% vs. 2.7%, respectively. With these promising results, a confirmatory trial in the Western countries is awaiting.

In the same setting of KRAS wt disease, several molecular actionable alterations are in evaluation such as NRTK (<1%), ROS1 fusions, NRG1 fusions, ALK rearrangement (<1%) and BRAF mutations. [48]

As we previously reported, 90% of mPDAC are KRAS mutated. In patients with KRAS G12C mutation the activity of Adagrasib and Sotorasib was explored in phase I/II trials with promising results (DCR of 85-100% and mPFS of 4-6 months) although the limited number of patients (10 treated with adagrasib and 38 treated with sotorasib). [49, 50]

One of the most recent explored target is the mitochondrial metabolism in tumor cells. A new compound called Devimistat (CPI-613) targets the mitochondrial tricarboxylic acid (TCA) cycle, through the inhibition of two of its major enzyme complexes: pyruvate dehydrogenase complex (PDC) and α-ketoglutarate dehydrogenase (KGDH). Encouraging results came from a phase I study on CPI-613 combined with FOLFIRINOX with an ORR of 61% (95% CI, 36–83%) led to the start of the AVENGER phase III trial, which evaluated modified FOLFIRINOX with or without CPI-613 in the first-line setting [51, 52].

The role of immunotherapy in pancreatic cancer is still marginal and limited to patients with mismatch repair deficiency (<1%) without any benefit in previous report in pMMR patients. In fact in a phase II trial, 27 patients with advanced PDAC received ipilimumab with no objective response [53]. Also the combination of the anti-PD-L1 durvalumab and the anti-CTLA4 tremelimumab in a second-line setting was disappointing, with an ORR

of 3.1% (95% CI, 0.008–16.22) for combination therapy and 0% (95% CI, 0.00–10.58) for monotherapy [54].

The source for immunotherapeutic vaccine is still ongoing. The most interesting data are related to GVAX, an heterologous whole-cell vaccine composed of 2 allogeneic PDAC cell lines modified to secrete GM-CSF. GVAX, is able to induce T cells infiltration and develop of tertiary lymphoid structures to convert the non-immunogenic PDAC tumor microenvironment (TME) in an immunogenic neoplasm [55].

In a phase II trial, 60 patients treated with combination of GVAX and gemcitabine reported mDFS of 17.3 months and mOS of 24.8 months with no benefit compared to standard treatment group [56]. So the synergic effect of GVAX in combination with anti-CTLA4 ipilimumab was tested in a small group of metastatic pre-treated PDAC patients observing a marginal benefit in overall survival compared to ipilimumab alone (5.7 months vs 3.6 months) [57]. Other treatment options based on immunomodulation such as CAR-T cells have been explored. A phase I trial using CAR T targeting mesothelin in advanced PDAC showed preliminary anticancer activity [58]. Recently a durable response with 72% reduction of cancer volume according to RECIST criteria was reported in a patient with metastatic PDAC treated by TCR-transduced T cells against KRAS G12D mutation suggesting a possible combinatory approach with both T-cell immunotherapy and specific small molecule inhibitor [59]. Furthermore, CD40 agonist role was tested in combination with gemcitabine: in a phase I trial an objective response rate in almost 20% of advanced pretreated PDAC patients was reported so phase II trials with this approach are awaiting [60].

1.2 DISSECTING TUMOR STROMA IN PDAC

In PDAC cancerogenesis the role of stroma is peculiar: it mediates tumor progression acting on cancer cells and influencing TME [61]. With its fibrotic nature, on one side it complicates the delivery of systemic chemotherapy but on the other side it contains neoplastic cells in primary tumor site avoiding metastatic spread of the disease [61].

The main components of pancreatic cancer stroma are extracellular matrix (ECM), vasculature and cancer-associated fibroblasts (CAFs) with constant interactions mediated by an inflammatory infiltrate and immune cells (**Figure 4**) [62, 63].

1.2.1 ECM

ECM is a 3-dimensional network composed by collagen fibers, proteoglycans and multi-adhesive matrix proteins secreted by PDAC cells [64]. Pancreatic cancer cells are surrounded by a marked desmoplastic reaction within the tumor stroma due to type I, III and IV collagen production enhanced by CAFs activity [65]. Collagen I is the most abundant in PDAC stroma and it represents the main actor in this desmoplastic reaction. High levels of collagen I are associated with significant poor median OS compared to low density highlighting its pro-cancerogenis role (6.4 months vs 14.6 months) [66]. Also high level of collagen IV and fibrillar collagen V stimulate cancer cell proliferation with inhibition of apoptosis [67]. However when C-terminal prodomains are cleaved, collagen I may suppress tumor cell proliferation in the same way as collagen III [68].

In addition to collagen, ECM composition also includes integrin, proteoglycans and glycoproteins. Integrins are transmembrane receptors that bind ECM glycoproteins. Also integrin are involved in the metastatic cascade by promoting the expression of matrix metalloproteinases that process extracellular matrix components, cell surface proteins, and immune modulators facilitating the release of cancers cells within the TME [69].

Proteoglycans are a glycoprotein subclass present not only in extracellular locations but also in cell membranes to transduce extracellular signals [70]. They regulate the hydration level of the interstitial fluid by interactions with hyaluronic acid and stimulate tissue repairing. They are composed by core proteins linked to glycosaminoglycans (GAGs) among which the most important are heparan sulfate and hyaluronic acid. High interstitial fluid pressure (PIF) resulting from high level of hyaluronic acid, complicates the trans-capillary transport and diffusion of drugs within the tumor [71].

The glycoprotein galectin 1 (GAL1) and Fibronectin 1 (FN1) are upregulated proteoglycans in PDAC TME and enable tumor cells to infiltrate the basement membrane stimulating the interactions between integrins and ECM collagens and inducing stroma cell activation through TGF-B release [72, 73] .

Also secreted protein acidic and rich in cysteine (SPARC) is a landmark class of glycoprotein in the PDAC TME that regulate ECM organization by binding collagens I-III-IV and V. [74]

ECM plays several roles beyond acting as a barrier for tumor cells [70]. Few researches highlighted the pro-cancerogenesis role of ECM by repleting tumor stroma resulting in proliferation of aggressive cancers but a recent report confirmed that stroma and ECM activity mediated by CAFs may slow down tumor growth [70]. Firstly, ECM contributes

to epithelial to mesenchymal transition (EMT). In pancreatic cancer in particular, the stiffness of the surrounding ECM has driven EMT in colture cells through nuclear translocation of the transcription factors YAP and TAZ [75]. The authors observed an upregulation of mesenchymal markers (vimentin) such as a downregulation of epithelial markers (E-cadherin). This heterogeneous composition of ECM through interactions between stroma and tumor cells strongly contribute to tumor cell heterogeneity.

ECM can also act as a barrier shielding cancer cells from therapeutic agents [76]. The transport of drugs in an abundant and fibrotic ECM is significantly hindered and the presence of an altered neo-angiogenesis and hypoxia through TME further compromises this process. Five lysyl oxidase isoenzymes (LOX and LOXL 1-4) are the main actors in the creation of cross-link between collagen fibers and glycoprotein [77]. The upregulation of these isoenzymes could be modulated by activation of various pathways such as TGF-b signaling or by radiotherapy [78, 79]. Rossow et al reported that upregulation of LOX and LOXL levels enhance collagen accumulation and stabilization creating a fibrotic ECM where the diffusion of the drugs is significantly hampered [80]. In vitro study on breast, ovarian and colorectal cancer cells, inhibition of lysyl oxidases improved oxygenation and reduced vascular endothelial growth factor A (VEGF-A) expression with positive effects on vasculature maturation [80].

The interaction between fibronectin or laminin with integrin b1 prevents G2/M arrest in response to radiation or chemotherapy by upregulation of p21 and p27 and downregulation of cyclins A, B, and E [81]. The same interaction might upregulate an anti-apoptotic signaling through ILK/AkT/NFkB pathway confering resistance to 5-FU effect in oral squamous carcinoma cells [82]. Interfering with integrin b1 pathway by targeting integrin b1 or downstream PI3K/AKT signaling enhanced the efficacy of radiotherapy in cultured breast cells [83, 84] .

The high density of ECM can also determine the distribution and the infiltration of immune cells into the tumor [85]. Hypoxia and metabolic stress condition induced by high fibrotic stroma upregulate the secretion of immunosuppressive factors like IL-10, TGFb, prostaglandin E2 and VEGF-A that inhibit the infiltration of CD8+ cytotoxic lymphocytes and natural killer cells and attract regulatory T cells (T-reg) and tumor associated macrophages (TAM) [86]. The protective role of ECM and the limited activity of CD8+ and natural killer cells complicate the efficacy of immunotherapeutic approaches that required to get both the drug (characterized by large diameter molecules) and T lymphocytes into the tumor. In PDAC model in particular, hyaluronic acid

enhances the collagen role in reducing the infiltration of drugs and immune cells into the tumor [87].

Recently the interest in the ECM has been renewed due to the possible therapeutic role of target therapies towards its components. TGF-β signaling was studied as a therapeutic target of pancreatic ECM. In pancreatic stroma TGF-β pathway stimulation activates pancreatic stellate cells supporting fibrosis and immune evasion [88]. A preclinical coculture model using Galunisertib (LY2157299 monohydrate), an oral TKI acting against chimeric TGFβRI-ALK5 kinase, revealed that this mechanism can be blocked [89]. In a phase Ib trial comparing Galunisertib in combination with gemcitabine versus gemcitabine alone, marginal improving in median OS in the combination group was reported (8.9 vs 7.1 months) [90]. In addition, a phase Ib trial looking into the synergic activity of Galunsertib and an anti-PD-L1 inhibitor (Durvalumab) resulted in one partial response and 7 out of 32 patient showing stable disease (disease control rate 25%), warranting further consideration for PDAC patients [91].

Rho kinase (ROCK) inhibition resulted in a disorganized ECM that countered cancer cell migration and invasion in vitro. ROCK inhibitors alter PDAC cell cytoskeletal and CAFs contractility favoring drug delivery and inhibit PDAC metastases in vitro and vivo model. With this assumption a phase I trial with AT13148 (anti-ROCK kinase inhibitor) was designed but early stopped due to high toxicity of the drug [92, 93]. Also vitamin D receptor ligand (calcipotriol) reported activity on PDAC stroma composition decreasing inflammation and improving gemcitabine activity so several studies in combination with chemotherapies and immunotherapies are ongoing [94, 95].

Another recently explored strategy to overcome ECM inducted chemo-resistance is the reduction of the interstitial fluid pressure within the TME to weaken tumor angiogenesis and permeability. A new drug called PEGPH20 (a Hyaluronidase encapsulated by polyethylene glycol) has been developed to improve hyaluronic acid degradation. Based on preclinical evidence supporting the efficacy in reducing interstitial fluid pressure, the role of PEGPH20 was explored in a phase Ib-II trial in combination with mFOLFIRINOX in 138 patients with metastatic PDAC [96]. Unfortunately in the combination arm, significant detrimental effects in terms of median OS (7,7 vs 14,4 months) associated with a worst safety profile (45% of treatment related adverse serious events) were reported. The efficacy of PEGPH20 in metastatic PDAC was explored also in combination with GEM-Nab-PTX in a phase III randomized controlled trial in patients with high tumour levels of hyaluronic acid [97]. After enrolling 494 patients, randomized

2:1 to chemo + PEGPH20 or placebo, the median OS was 11.2 months for the first group versus 11.5 months for the other one (HR 1.00; 95% CI, 0.80 to 1.27; $p = .97$). With these disheartening results, no more efforts on PEGPH20 role in PDAC will be made.

1.2.2 Vasculature

PDAC is a hypo vascular tumour characterized by impaired micro vessel integrity and poor perfused vessels [98]. These altered characteristics of the tumour vasculature negatively affect drug distribution and promote the development of hypoxic microenvironment thus impacting on therapeutic outcomes [99]. Therefore, new therapeutic strategies aiming to induce normalization of tumour blood vessels may result in improved tumour perfusion, reduced hypoxia, and drug delivery thus enhancing the treatment response [62].

In preclinical experiences, anti-VEGF strategies reduced human PDAC cell lines growth although no phase II and III clinical has reported positive results with this approach [100-103]. New approaches investigating tumor vasculature normalization are emerging with the aim to improve drug delivery and to sensitize to immunotherapy. In a phase II trial the combination of losartan (angiotensin system inhibitors that decompress vessels in preclinical models) and chemo-radiotherapy resulted in a remarkably high fraction (61%) of R0 resection with increased pathological response and improved mOS versus standard treatment alone [104].

Also in early setting, in 299 resected patients with PDAC, the chronic use of angiotensin system inhibitors (ASIs) was associated with improved mOS in both univariate (median OS, 36.3 vs. 19.3 months, $P = 0.011$) and adjusted multivariate (HR, 0.505; 95% CI, 0.339-0.750; $P = 0.001$) analyses [105]. In RNA seq analysis in tumors of ASIs users a normalized extracellular matrix and a reduced expression of genes involved in PDAC progression (e.g., WNT and Notch signaling) were reported. The role of ASIs was also associated with an increased expression of genes linked with the activity of T cells and antigen-presenting cells suggesting an immunomodulatory action [105]. There is no standard role for ASIs in PDAC patients but few trials exploring this strategy are ongoing.

1.2.3 Myeloid and lymphatic cells

Myeloid cells under the influence of PDAC components act as cancerogenic factors blocking T cell regulation functions and promoting cancer stemness, angiogenesis and stroma deposition [106]. In particular in PDAC the most investigated myeloid cells are marrow-derived suppressor cell (MDSCs) and tumor associated macrophages (TAMs) [107].

MDSCs are immature bone-marrow derived cells infiltrating PDAC TME under the influence of granulocyte macrophage colony stimulating factor production (GM-CSF) and hypoxia-inducible factor 1 secreted by PDAC cells. They suppress T lymphocytes through direct contact or through a combination of multiple major mediators (COX2, TGF-B, IL-10) determining STAT3 activation, PD-1 and PD-L1 up-regulation [108].

TAMs is the major leukocyte population reported in cancers and they are attracted into PDAC TME by IL-4 and colony stimulating factor-1 production in stroma during cancerogenesis. TAMs play an important role in mediating adaptive immune response in cancer through the secretion of immunosuppressive and pro-angiogenic factors (IL-6, IL-10, TGF-B, VEGF). Interestingly, macrophages can have both anti and proinflammatory roles, which is often linked to their M1 or M2 polarization status [109]. Hyaluronic acid and Col I expression could drive M2 polarization (pro-tumorigenic phenotype) while high fibronectin expression enhance the M1 polarization with cytotoxic activity [110]. Based on this assumption, TAMs levels correlate with early metastasis, tumor recurrence and reduced overall survival [111]. About the lymphatic cells, immunohistochemical analysis suggests that there is a lack of functional CD8+T cells in human tumors although CD4+ and CD8+ T cells were presents in PDAC specimen.[112]

1.2.4 CAFs

Another landmark component [113] of PDAC stroma are CAFs. Fibroblasts are supportive cells of mesenchymal origin that are placed in every solid organ as supportive structure but they are also involved in biological activity such as secreting ECM proteins and soluble factors. They are active players during all the phases of PDAC development: initiation, local evolution and systemic spreading [114]. They are also involved in chemo-resistance both acting as physical barrier to drug diffusion but also inducing biological events through secretion of soluble factors and exosomes, remodeling extracellular

matrix, and reprogramming metabolic processes in tumor through epigenetic modifications. It has been demonstrated that during treatment with gemcitabine, cancer cells collect exosomes (micro RNAs-containing lipid extracellular vesicles) secreting by CAFs within TME that promote proliferation by suppression of PTEN, upregulation of ROS detoxifying genes or downregulation of DCK (gene involved in gemcitabine metabolization) [115, 116].

CAFs are characterized by overexpression of fibroblast specific protein (FSP) and fibroblast activation protein (FAP) but also malignant tumors markers such as stromelyisin 1 (SL-1), thrombospondin-1 (TSP-1) and pro-tumorigenic growth factors including HGF, EGF, FGF [117]. In addiction CAFs can degrade ECM with degrading enzymes production, promoting the release of pro-angiogenic factors such as VEGF and TGF-b involved in endothelial cells activation and regulation of tumor angiogenesis [118].

Various hypothesis on the origin of CAFs have been proposed and the currently accepted theory is the derivation both from resident precursors and from a circulating pool of mesenchymal progenitors cells (originating in bone marrow and adipose tissue) [119-121]. Particularly in PDAC, the heterogeneity of CAFs described in the TME along with the complex and still obscure role-played by these cells in tumor outcomes and patient prognosis lead the researchers to consider CAFs as novel potential therapeutic target in PDAC treatment [122]. Recently Helms et al developed a mouse model in which they could track and specifically ablate pancreatic stellate cells (PSCs) within the pancreas, revealing their unique lipid-storing origin. They found that PSCs give rise to CAFs but that this PSC-derived CAF population was numerically minor, suggesting additional and yet undefined cellular origins for most PDAC CAFs. Importantly, PSC-derived CAFs played significant, nonredundant roles in modulation of the tumour microenvironment, including production of specific components of the ECM, suggesting that these cells or their critical regulators may be therapeutic targets [123].

The hypoxia generated by CAFs within TME resulted in a overexpression of platelet-derived growth factor (PDGF) and VEGF, representing homing and mitogenic factors for mesenchymal stromal cells (MSCs) . Thus, MSCs can migrate into the tumor site and promote vasculogenesis empowering the pro-angiogenic potential of CAFs [124].

In a recent molecular categorization, CAFs were classified as myofibroblastic CAFs (myCAFs) and inflammatory CAFS (iCAFs) [62].

MyCAFS are pancreatic stellate cells (PCSs): fibroblasts present in the periductal, periacinar and perivascular space of the normal pancreas assuming a myofibroblastic gene expression profile in cocolture with KPC mouse-derived organoids [125].

Sonic hedgehog (Shh) pathway is involved in the activation of MyCAFS. Inhibition of hedgehog signaling can reduce or even reverse PSCs activation, leading to improved outcomes in chronic pancreatitis. The pharmacological inhibition of Shh in KPC mice resulted in poor differentiated cancer cells affecting animal survival [126]. Unfortunately this preclinical results were not confirmed in clinical setting where the combination of Shh inhibitor (Vismodegib) and chemotherapy failed in improving oncological outcomes in a phase II trial [127].

ICAFs express IL-6, IL-8 and other inflammatory cytokines instead of upregulation of myofibroblastic gene [128, 129].

Based on its proinflammatory action, also IL-6 secreted by iCAFs under the pressure of cancer cells is a pro-cancerogenesis mediator through STAT pathway. Patients with high level of IL-6 in human plasma have a major risk of developing liver metastases, cachexia and a systemic immunoevasion state caused by high glucocorticoid levels [130]. Antoon et al recently reported tumor formation delayed in vitro and in vivo pancreatic model with an anti-IL6 receptor antibody (tocilizumab) [131]. Based on these preclinical results, an interesting approach of targeting both IL-6 and PDL-1 is currently under way [132].

Based on its role in iCAFS pathogenesis, also JAK-STAT pathway was targeted with JAK1-2 inhibitor. JAK2/STAT3 pathway is activated in pancreatic tumor cells and contributes to cell proliferation and malignant transformation as well as inflammatory signaling in TME [133]. The use of AZD1480 (a JAK/STAT inhibitor) in combination with gemcitabine enhanced in vivo drug delivery and tumor response in mouse model of PDAC. These effects were mediated by tumor stromal remodeling without stromal collagen depletion underlining the dynamic link between stroma and pancreatic cancer cells [134]. In ICAFs of patients with PDAC, IL-1 receptor-associated kinase 4 (IRAK4) is highly activated in contrast to normal human tissue enhancing cancerogenesis and stromal fibrosis. One of the main actors of this activation is IL1-B product by CAFs and by tumor cells whereas inhibiting IL1B-IRAK4 activation disrupted tumor stroma enhancing chemo-sensitivity in vivo [135]. Actually, a combination approach of chemotherapy and IL-1R target is evaluating in a clinical trial [136].

Another possible target actually in evaluation as a potential treatment strategy is CXCL-12 (ligand for CXCR4), an iCAFs derived molecule. A phase I-II trials in PDAC patients

with the combination of pembrolizumab and NOX-A12 (a CXCL-12 inhibitor) is under way and at the same time, the activity of BL-8040 (a CXCR4 inhibitor) has been explored in 15 mPDAC patients gemcitabine-resistant with partial response in a third of patients (4/15) [137].

1.3 MESENCHIMAL STROMAL CELL

MSCs are multipotent progenitor cells, able to migrate and engraft into TME and becoming part of the stromal compartment [138]. MSCs have significant differentiation capacities that allow the evolution into myogenic, adipocytic, osteogenic, chondrogenic lineages [139]. According to the minimal criteria presented by the International Society for Cellular Therapy (ISCT), MSCs are cells with plastic adherent properties in standard culture conditions and they express CD105 (known as endoglin), CD73 (known as ecto-50-nucleotidase) and CD90 (known as Thy-1) surface markers [140].

MSCs can be isolated from different tissues such as placenta, dental pulp, gingiva but the main sources are bone marrow and adipose tissue [141]. MSCs were reported in a variety of non-hematopoietic tissues where they maintained a proliferative capacity [142].

MSCs are considered to be poorly immunogenic but they possess immunological functions with autocrine and paracrine activities [143, 144]. In injured tissue MSCs differentiate into connective tissue elements and perform as main actors in regulating angiogenesis and secreting cytokines and growth factors. In particular in PDAC setting, BM-MSCs are attracted by pancreatic islets ex vivo and in vivo, and the chemokine SDF-1 plays a relevant role in this migration [145].

Based on this assumptions, MSCs may recognized cancer tissue as damaged tissue with inflammation and homing to tumor site to be incorporated into the tumor architecture as stromal MSCs or CAFs [146]. Many factors could be involved in MSCs tumor migration such as tumor-cell receptors, ECM and soluble cancer-derived factors (TNF-alfa, IL-1, SDF-1) [147].

MSCs can be recruited into the developing tumor and assume a CAF-like phenotype under the influence of the TME [148]. CAFs and MSCs exhibit similar phenotypes reflecting the hypothesis that in tumor tissues, MSCs can differentiate into CAFs and contribute to tumor growth and metastasis, participating in various stages of carcinogenesis [149]. However, compared to MSCs, CAFs secrete significantly higher

levels of TGF-β, VEGF, IL-4, FGF2, IL-6 and IL-10 and express various specific markers such as α-smooth muscle actin (α-SMA), PDGF receptor-β (PDGFR-β), desmin, FSP and FAP [150, 151].

The differences between CAFs and MSC can reflect the capability of MSC to change within the tumor microenvironment under the influence of cancer cells [151].

Huang et al supported the pro-tumogenic hypothesis that the secretion of interleukin-6 (IL-6) from MSCs increased the secretion of endothelin-1 (ET-1) in cancer cells, which activated AKT/ERK pathway in endothelial cells stimulating angiogenesis [152]. Another fundamental pathway involved in this anti-apoptotic activity is WNT-pathway. MSCs can promote metastatic growth and chemo-resistance in cholangiocarcinoma cell colture by the Wnt/catenin signaling pathway that regulate cell survival, differentiation, morphogenesis and proliferation [153].

However, many studies have shown that MSCs could also have tumor-suppressive properties, stimulating an immune-activated microenvironment and inducing apoptosis and cell cycle arrest also in pancreatic cancer [154]. After coculturing pancreatic tumor cancer cells with human stromal cells obtained from adipose tissue (ADSC), cancer cell necrosis following G1-phase arrest was reported without evidence of apoptosis. This report was confirmed in vivo in a human model of PDAC with a single intra-tumoral injection of ADSC [154-156].

The natural and specific ability of MSCs to home and engraft into malignant tissues, along with their immune privileged status, availability, stability, expandability, and proven safety record in clinical trials, make MSCs the ideal cellular vehicle for the delivery of anticancer agents to improve bioavailability versus more conventional approaches [157, 158].

After locally or systemically MSCs injection the main limitations remain the bioavailability and survival in tumor site [159]. In case of locally injection, MSCs can be rejected by TME and with systemic infusion administration only a small amount effectively reaches the cancer site [160, 161]. Current experiences reported that, after endovenous infusion, most MSCs were found in the lung, liver and spleen without any impact in tumor site. Based on these results, one of the major challenge is the research of more efficient target methods to increase therapeutic efficacy reducing the amount of MSCs and the off-target effects [160]. One of this strategy is the physical targeting using surgical procedures or guiding strategies (catheters of external magnets), to place MSCs into the tumor site [162, 163].

Recently, different strategies have also been investigated to manipulate MSCs homing potential: engineering MSCs culture to overexpress homing-related molecules, modifying MSCs membrane to increase homing and manipulating the target tissue [161, 164]. The strategies used to convert MSCs into cellular vehicles for anticancer molecules can be classified into two different types. The first category includes non-genetic modifications of MSCs, such as loading with nanoparticle carriers or drugs. The second consists of approaches based on genetic modification of MSCs to induce the expression of anticancer proteins or suicide genes.

1.3.1 Non genetic modification

In PDAC model, MSCs loaded with chemotherapeutics agents have been tested for their anticancer efficacy both in vitro and in vivo models [165, 166]. Bone marrow or pancreas derived MSC were primed with Gemcitabine (GEM) and the activity of GEM loaded MSCs was tested on CFPAC-1, a human PDAC cell line very sensitive to GEM revealing a strong anti-proliferative effect not inferior to the activity of pure gemcitabine. In contrast, the wild type MSCs (without GEM uptake) had no cytotoxic activity on CFPCA-1 cells [165].

The role of pre-loaded MSCs in pancreatic cancer was evaluated also with Paclitaxel (PTX). Three mechanism of drug loading into MSCs are involved: endocytosis, intracellular transport mediated by hCNT1 and hENT1 transporters and simple diffusion based on chemical characteristics of the drug [167]. The mechanisms driving PTX release by loaded MSCs is mediated by the secretion of extracellular vesicles (EVs) acting as "natural anticancer liposomes" [168]. After confirming the strong resistance to paclitaxel of the murine stromal cell line SR4987 (85% of primed cells survived), a strong cytotoxic activity in CFPAC-1 pancreatic cell lines was reported by using SR4987 CM primed with high dose of paclitaxel [166]. The next step was the evaluation of a new formulation of PTX called PTX-NPs (nanoparticles). Although containing significantly lower doses of PTX, treatment with MSCs carrying PTX-NPs resulted in relevant reduction of tumor growth, increased animal survival, and lower toxicity compared to treatment with PTX solution or free PTX-NPs [169].

1.3.2 Genetic modification

Genetic modification of MSCs is another way to develop effective anticancer therapies.

The first approach is the delivery of suicide genes by MSCs [170]. After manipulation with viral vector, MSCs can secrete specific proteins that convert non active pro-dugs in active anticancer treatment. This pro-drugs are administrated through systemic infusion and, once homing to tumor site, are converted through MSCs activity minimizing the toxicities in the nearby tissue and stimulating the activation of immune cells (cytotoxic T cells and macrophages) [170]. Once activated, the drug metabolites are highly toxic also for the MSCs, reducing the risk of adverse effects due to the their persistence in patients. This approach is ideal for drugs with short half-life or high systemic toxicity such as 5-fluorouracil and ganciclovir [171, 172].

The second approach used in genetic modifications of MSCs is the cell engineering using viral vectors to overexpress anticancer bioactive molecules. In 2002 for the first time, Studeny et al used MSCs for the targeted delivery of interferon-beta [173]. In the following decades other therapeutic genes encoding regulatory proteins and interferons, interleukins, chemokines as well as molecules with pro-apoptotic, antiangiogenic functions (TRAIL, VEGFR1, TNF-a) have been evaluated in preclinical studies [174]. The advantages of the release of these molecules once homing to the tumor site is the direct pro-apoptotic activity on tumor cells and the potentiation of the host inflammatory response by cross-talk with the tumor microenvironment. This process demonstrated antitumor effects in vitro and in vivo model of lung and pancreatic cancer such as glioblastoma, sarcoma and HCC [164, 175-180]. In pancreatic cancer in particular compounds able to modify tumor/stroma interactions allowed a better penetration of molecules into PDAC [181].

Last approach is the incorporation of oncolytic viruses inducing selectively cancer cell death by oncolysis [160]. As we previously reported MSCs are characterized by poor immunogenicity and they have the peculiarity to be able to migrate and engraft into TME and becoming part of the stromal compartment [138]. Based on these assumptions, oncolytic virus delivered by MSCs can reach tumor site without any activation of immune system. Since a high activity of oncolytic adenovirus DNX-2401 was reported in recurrent glioma, a phase I trial with BM-MSC delivering the oncolytic adenovirus DNX-2401 is actually on the line in the same setting to explore the therapeutic potential of this MSC-based delivery strategy[182]. In a mouse model of PDAC the delivery through AD-MSC of an engineered oncolytic adenovirus called OAd Ad5/3-TRAIL expressing TRAIL resulted in a strong anti-cancer activity. [183]

1.4 TRAIL ANTICANCER ACTIVITY IN PDAC

One of the most promising antitumor cytokines is the Tumor Necrosis Factor - Related Apoptosis Inducing Ligand (TRAIL). TRAIL/Apo2L (TNFSF10) is a protein naturally produced by the human body at low levels and expressed by various cells of immune system. Its activity is an immune-mediated physiological reaction of the human body against cancerogenesis thanks to the ability to kill tumor cells by induction of apoptosis without damaging healthy tissues [184].

TRAIL can induce caspase-mediated apoptosis by binding 2 transmembrane functional receptors characterized by a cytoplasmic death domain (Death Receptor 4 – DR4 and Death Receptor 5 – DR5) driving a caspase-8 dependent process of apoptosis (**Figure 5)** [184, 185]. TRAIL also binds membrane-bound receptors called Decoy Receptor 1 (DcR1) and Decoy Receptor 2 (DcR2): the first one acts as a TRAIL-neutralizing decoy-receptor differently from DcR2 that is functional and activates NF-kappa-B mediated pathway. Overexpression experiments displayed the inhibitory potential of DcR1 and DcR2 regarding apoptosis induction by ligand scavenging and/or interaction with the death receptors [185, 186]. Lastly TRAIL can bind osteoprotegerin (OPG) that is a soluble receptor that complicates the interaction of TRAIL with death receptor 4 (DR4) and death receptor 5 (DR5) [187-190].

The activity of TRAIL is based on a trimeric form of the molecule that activates proapoptotic mechanisms binding the trimeric forms of its receptors. Once the bond has happened, DR4 and DR5 recruit the adaptor protein Fas-associated death domain (FADD) to generate the death-inducing signaling complex (DISC) [191]. DISC recruit procaspase 8 and 10 and by proteolysis activates effector caspase 3-6-7 that are the last actors of this "extrinsic apoptosis pathway"[192]. (**Figure 5)**.

In some cell types, the apoptosis process require the interaction between extrinsic apoptosis pathway and "intrinsic or mitochondria-initiated apoptosis pathway". The latter one is activated by caspase-8 that cleaves BID (BH3 interacting domain death agonist) resulting in mitochondrial dysfunction and subsequent release in cell cytoplasm of cytochrome C and second mitochondria-derived activator of caspase (Smac/DIABLO). The apoptosome signaling complex between cytochrome c, procaspase-9 and the adaptor protein Apaf-1 induces the caspase 9 activation that regulates the effector caspase 3-6-7 driving the apoptosis process [193]. Also standard chemo and radiotherapy could induce apoptosis mediated by the intrinsic pathway but, differently from TRAIL, they require

p53 activation [194]. Even though DR4 and DR5 activate the same downstream pathways, cell death may be induced preferentially through one or the other of these receptors depending on the cancer cell type. For instance, in pancreatic and chronic lymphocytic leukemia cells, apoptosis is mainly triggered through DR4 [195].

Previously, the correlation between TRAIL-R and patients prognosis was evaluated in a variety of cancers [196-198].

In the last decade, few reports on the role of TRAIL receptors in PDAC were published. Sanlioglu et al focused on receptor expression (DR4, DR5, DcR1, and DcR2) in tumor tissue and compared this report with receptor expression in healthy pancreatic tissue [199]. They tested 34 PDAC specimens and 31 healthy pancreatic tissues revealing an upregulation of DR4 and DcR2 in cancer tissue compared to the healthy specimens. They also reported an higher DcR2 expression in acinar cells and Langerhans islets from PDAC patients. Gallmeier et al. evaluated 84 consecutive PDAC patients specimens reporting that 77% and 99% of PDAC specimens were positive for DR4 and DR5, while 52% and 69% of specimens were positive for DcR1 and DcR2, respectively. In early stage resected disease, patients with low DR5 expression had poor prognosis (HR 0.44, 95% CI 0.22-0.87 ; p = 0.019) [200].

The high expression of TRAIL-R in PDAC was confirmed also in a subsequent report on 106 PDAC specimen focused on DR4 (93,4% of cases were positive with cytoplasmatic and nuclear localization). Nuclear DR4 expression was significantly higher compared to normal tissue and tumor grading was strictly related to the amount of DR4 positive cells [201]. As in previous report, Gundlach et al confirmed that DR4 and DR5 were mainly intracellularly rather than in the plasma membrane of malignant cells. Also in this report as in the previous one by Gallmeier et al, TRAIL-R expression impact on mOS (20 months for patients with DR4 expression > 80% vs 8 months for patients with DR4 positivity< 80%, p 0,004) [201].

Also our group recently evaluated the expression of TRAIL receptors (DR4, DR5) and TRAIL decoy receptors (DcR1, DcR2 and OPG) on 50 human PDAC specimens [187]. More than 95% of PDAC specimens had histological positivity for both TRAIL functional receptors (DR4 and DR5) and DcR1. Focusing on DcR2 expression, 76% of PDAC samples were negative, and positive specimens had a weak intensity (score 1: 24%). For OPG, 32% of PDAC samples were negative, and positive specimens displayed a weak intensity. In addiction we evaluated TRAIL-R expression on stromal tissue. All PDAC samples stained positive for DR5 in the stromal tissue although 84%, were

negative for DR4 with higher expression of DcR1 and DcR2 (100% of samples) so we could hypothesize a possible TRAIL activity also on stroma components. We evaluated also the correlation between TRAIL-R expression and prognosis: differently from previous reported trials, DR4-DR5 expression was not correlated with survival. However patients with low expression of DcR1 had a worse prognosis than patients with higher expression (HR=0.47; 95% CI=0.26, 0.86; p=0,013). At the same time, patients without any expression of OPG had a lower life expectancy than patients with OPG-positive tumors (HR=0.53; 95% CI=0.28, 0.98; p=0,043) [187].

1.5 TRAIL ACTIVITY IN COMBINATION WITH CHEMOTHERAPY

Despite the attractive tumoricidal potential, TRAIL based therapy may be limited by tumor acquired resistance mechanisms [202]. Hypermetilation, mutation, loss of cell surface expression or defects in caspase protein activation such as overexpression of pro-survival protein (IAP family and Bcl-2 pathway) are involved in this process [203-207].
Some attempts to obtain an improved stability of TRAIL were explored with initial preclinical results: TRAIL conjugates (FLAG-TRAIL, leucine zipper TRAIL and isoleucine sipper TRAIL) or the creation of gene carrier to encapsulate TRAIL plasmids for systemic delivery of the molecule [208-210].
In vivo antitumor activities of TRAIL combined with chemotherapy and radiotherapy have previously been reported in xenograft models of cancer including lung [211], colorectal [212], breast [213], prostate [214], and brain [215]. Actually some clinical experiences with the combination of rhTRAIL and chemotherapy are published and few trials are ongoing (**Table 2**).
PTX is a microtubule-stabilizing agent that leads tumor cells to death, through the involvement of the molecular downregulation of NFK-B and Bcl-2 [216-219]. The administration of the drug in Nanoparticle Album Bound formulation guaranteed an improvement in solubility and bio-availability with higher retention inside the stroma [220]. In addition, PTX has also been reported to up-regulate DR5 expression on cancer cells [221]. In gastric cancer cell lines the combined administration of paclitaxel and TRAIL enhanced the apoptotic process in resistant cancer cells both in vitro and in vivo through activation of mitochondrial apoptotic pathway, upregulation of TRAIL-R and downregulation of antiapoptotic proteins (c-IAP1, c-IAP2, Livin and Mcl-1) [222].

Dorsey et al reported in vitro and in vivo remarkable anticancer activity of the combination of TRAIL and PTX in glioblastoma multiform (GBM) cells lines firstly and then in xenografts derived from GBM cells [223, 224]. In the first phase, they reported an in vitro sensitization to TRAIL by PTX pre-treatment in T98G glioma cells and then studied this effect on SF767 human GBM cell line in mice in xenograft model. Authors assessed anti-cancer activity by multimodality imaging approach including not only bioluminescence but also micro-CT and FDG-PET. The synergistic anticancer activity of rhTRAIL and Nab-PTX was evaluated also on pancreatic Mia Paca-2 cell line and in vivo in Mia Paca-2 cell-xenografted mice [225]. A new formulation of Nab-PTX with incorporated TRAIL (TRAIL/PTX) was developed. On Mia Paca-2 cell line, the inhibitory concentration (IC50) of TRAIL/PTX was significantly lower than Nab-PTX alone. The same efficacy was reported also in Mia Paca-2 cell-xenografted mice: median tumor volumes were 213.9 mm^3, 1126.8 mm^3 and 3080.9 mm^3 in mice treated with TRAIL/PTX, PTX alone or control group respectively. Also the mean weight of tumors was remarkably inferior in the first group (0.18 g vs 0.80 g vs 2.43 g). [225]. (**Figure 7**).

Dulanermin (recombinant human Apo2L/ TRAIL) was evaluated in combination with PTX, carboplatin and bevacizumab in a randomized phase II trial in patients with advanced non small cell lung cancer (NSCLC). No benefit in overall response rate was reported in the combination arm (chemotherapy + dulanermin) vs chemotherapy alone in both squamous NSCLC (38% vs 39%) and non squamous NSCLC patients (40% vs 50%) [226]. Subsequent researches in the same setting was carried out to evaluate the effectiveness of the combination of dulanermin and polychemotherapy with vinorelbine and cisplatin. In a Phase III trial, 452 untreated patients were randomized to combination treatment vs chemotherapy alone. ORR was significantly improve in the dulanermin arm versus placebo arm (46.78% vs 30.00%; p = 0.0019). Median OS was 14.6 months in the dulanermin arm versus 13.9 months in the placebo arm (HR, 0.94; 95% CI, 0.74 to 1.21, p = 0.64) [227].

Another interesting approach is the combination with GEM. The relevance of GEM as single agent or in polychemotherapy regimes as systemic treatment in PDAC has been since years consolidated [19, 228] The synergistic anticancer activity of rhTRAIL or TRAIL-R agonists and GEM has already been reported and in particular this combination therapy was able to empower rhTRAIL activity in sensitive tumors and overcome rhTRAIL-resistant PDAC clones [229, 230]. The activation of both TRAIL intrinsic

pathway and GEM induced an increase in mitochondrial membrane permeabilization activating a tumor cell apoptosis mediated by caspase cascade [231-233]. Lexatumumab, a fully-human agonistic monoclonal antibody that targets and activates DR5, was tested in combination with polychemotherapy (GEM, doxorubicin or FOLFIRI) in a Phase I trial. On 41 patients tumor shrinkage has been observed in the FOLFIRI and doxorubicin arms and stable disease in GEM arm. Good tolerability with no required dose reduction was reported and the only severe adverse events related to lexatumumab were anemia, fatigue and dehydration. Tumor shrinkage has been observed, including confirmed partial responses (PRs) in the FOLFIRI and doxorubicin arms [234].

Recently interesting results with the combination of lexatumumab or GEM and YM155 (a small molecule inhibitor with anti-cancer activity based on suppression of survivin expression at the transcriptional level) were published. Efficacy results were reported in vitro studies in the cultured cells and in vivo studies using xenograft model in mice. Firstly, an upregulation of DR5 expression in pancreatic cancer cells treated with YM155 were revealed and, based on this assumption, a combination treatment with DR5 agonist lexatumumab was tested [235]. Neither YM155 or lexatumumab alone could activate caspase-cascade induced apoptosis but the synergistic effects of the combination could improve anti-cancer activity. Secondary in a cell culture model of pancreatic cancer the activity of YM155 was evaluated in combination with GEM confirming a synergistic effect also with chemotherapy [235].

A similar molecule called Conatumumab (a fully human IgG1 monoclonal antibody with antineoplastic activity mediated by agonist effect against the extracellular domain of human DR5) was evaluated in not pretreated patients with mPDAC in combination with gemcitabine in Phase II trial. Eighty-four patients were randomized to the combination arm or GEM + placebo with 6-month OS rates of 59% (42-73) in the conatumumab arm, and 50% (33-64) in the placebo arm. Based on these preliminary results no subsequent phase III trial were conducted with this strategy [236].

Also Tigatuzumab (CS 1008) as a humanized monoclonal antibody targeting DR5 was tested in combination with GEM in chemo-naïve patients with advanced PDAC. The results were not clinically relevant with an ORR of 13.1% and 45.9% of patients with SD, mPFS was 3.9 months (95% CI, 2.2–5.4 months) and mOS was 8.2 months (95% CI, 5.1–9.6 months) so this approach was not furtherly investigated [237].

Finally Mapatumumab, a fully human agonistic monoclonal antibody that targets DR4, was tested alone or in combination with GEM and cisplatin in a Phase I trial in solid

tumors. The activity of the drug was confirmed in monotherapy (19/49 patients obtained stable disease) and in combination with chemotherapy. Indeed at the dosage of 20 mg/kg in combination with gemcitabine 1,250 mg/m^2 i.v. on days 1 and 8 and cisplatin 80 mg/m^2 i.v. on day 1 of each 21-day cycle, 12 patients obtained a partial response, and 25 patients showed stable disease with a median duration of response of 6 months [238, 239].

1.6 MESENCHIMAL STROMAL CELL PRODUCING TRAIL FOR PDAC TREATMENT

Early-phase clinical trials with rhTRAIL used as a single agent indicated that rhTRAIL can be safely delivered with good toxicity profile [240, 241]. Preclinical evidence suggests that most of PDAC cells are sensitive both *in vitro* and *in vivo* to the action of rhTRAIL [242-244].

Its poor bioavailability profile is responsible for suboptimal therapeutic effects and the need of frequent administrations in patients. Different technological improvements have been so far introduced to ameliorate TRAIL biodistribution, stability and cytotoxic activity including the use of fusion proteins with single-chain variable antibody fragments (scFv), conjugation with nanoparticles and, cell-based methods to express and/or secrete TRAIL [245]. Among these, the use of genetic modified MSC as cellular vehicle for the delivery of TRAIL variants represent one of the main promising and clinical realistic approaches for PDAC patients [174].

Moniri et al isolated and expanded in vivo human pancreas-derived MSCs (hpMSCs) exhibiting positive expression of CD44., CD73., CD95, CD105 and negative of CD34 from human pancreas ductal tissue [240]. They reported an enhanced anticancer activity of MSCs transfected with the secreting form of TRAIL (MSCstTRAIL) compared to the MSCs transfected with the non-secreting form of TRAIL (MSCnsTRAIL). Compared with CM from MSCnsTRAIL, CM from MSCstTRAIL showed more potent inhibition at high concentrations on human pancreatic adenocarcinoma cell lines (BXPC3 and ASPC1) [240]. They confirmed that TRAIL-activity was strictly related to death receptors expression on tumor cells. They suggested that the anticancer properties of MSCstTRAIL were based on a multifactorial process that involved MSCs intrinsic anticancer effect, TRAIL-induced specific tumor cell death and induction of tumor cells TRAIL sensitivity [240]. Mohr et al studied the efficacy of the combined activity of TRAIL and BM-MSCs on primary cancer and disseminated cancer

cells on a human pancreatic cancer mouse model [241]. They confirmed an increased TRAIL pro-apoptotic activity on stable XIAP knockdown clones called Panc1.shXIAP and PancTu1.shXIAP (XIAP expression was silenced to enhance TRAIL sensitivity) obtained from two different TRAIL resistance pancreatic cell lines called Panc1 and PancTu1. Furthermore they used an adenoviral vector called AdsTRAIL to transduce MSCs and obtained MSCsTRAIL. The activity of MSCsTRAIL supernatant were enhanced on Panc1.shXIAP and PancTu1.shXIAP knockdown clones but some apoptosis were reported also in Panc1 and PancTu1. Afterwards they found that the silenting of XIAP reduced the systemic spreading of cancer cells reporting 25% fewer lymph-nodes and lung metastatic lesions. In addiction they confirmed the pro-apoptotic activity of intravenously injection of MSC.sTRAIL in PancTu1.shXIAP mice model and a marked growth retardation in PancTu1.shcontrol mice model [241].

Also our group evaluated TRAIL-AD-MSCs approach on pancreatic rhTRAIL sensitive cell lines (BxPC3), characterized by high expression of DR5 [190]. In this approach MSCs isolated from human adipose tissue by minimally invasive surgical procedures were genetic modified to product membrane bound TRAIL form [246, 247]. TRAIL-AD-MSC were able to induce an apoptosis ratio in line with rhTRAIL group. In microscopic examination, the interaction between TRAIL/GFP AD-MSCs and BxPC3 cells caused a breakdown of tumor islets together with the disruption of adherent BxPC3 cells.

Then to overcome rhTRAIL poor bioavalability we armed AD-MSC with a new soluble multimeric variant of TRAIL called sTRAIL [177]. The gene encoding for the soluble TRAIL was synthetized by linking different domains and cell modification was confirmed by the capacity to release sTRAIL without any impact on AD-MSCs properties. We evaluated sTRAIL cytotoxic activity at 37°C on 3 different PDAC cells lines (BxPC-3, MIA PaCa-2 and PATU-8988T) and on primary PDAC cells isolated from patient biopsy (PK59 EPI). In BxPC-3 cell line, sTRAIL concentrations ranging between 250 and 500 pg/ml, induced 60.6 ± 1.0% of cell death, similar to MIA PaCa-2 line. Contrariwise, PATU-8988T showed a weaker response to sTRAIL and more than half of tumor cells was still viable at 2500 pg/ml of sTRAIL (65±4%). Unexpectedly for the PK59 EPI primary PDAC cells, rhTRAIL activity was superior with apoptosis in 50.9 ± 0.6% of the population versus 37.0 ± 0.5% in the sTRAIL group, 17.5 ± 0.6% of CTL and the 21.2 ± 0.7% of EV control group.

sTRAIL MSC antitumor activity was confirmed also in vivo with 3 doses of empty vector MSC or sTRAIL MSC peritumorally injected in subcutaneously xenografted with $2x10^6$

BxPC3 pancreatic tumor cells mice and compared with 5 mg/kg rhTRAIL intravenously infusions at the same days. We suggested that sTRAIL activity is due to its presence inside the tumor differently from intravenously administered rhTRAIL which activity was hindered by the dense stromal component and, most importantly had poor bioavailability. On contrary, MSC are administered intra-tumor and can still be found at the end of the treatment thus providing a continuous supply of sTRAIL inside the tumor burden.

So far there are no clinical data on the use of TRAIL releasing cells in cancer patients. An academic study (University College of London, London, UK) open Phase I/II study (TACTICAL) using allogeneic bone marrow mesenchymal stromal cells (MSC) for the treatment of non-small cell lung cancer is proposing a combination of standard chemotherapy with MSC producing a TRAIL variant (MSC-TRAIL) [248]. This first-in-human, single-center, dose finding designed trial foresees the delivery of cells in combination with pemetrexed/cisplatin chemotherapy. The patients will receive cisplatin 75 mg/m2 and pemetrexed 500 mg/m2 on day 1 followed by intravenous MSC-TRAIL infusion on day 2 for a total of 3 cycles. In this currently open study, the maximal proposed cell dose has been established at 4 x 108 allogeneic cells intravenously administered 3 times for a total of systemically injected 1.2 billion cells.

1.7 TRAIL-AD MSC IN COMBINATION WITH CHEMOTHERAPY

Based on previous reported data, PDAC represents a promising target for TRAIL-based therapies thanks to the amount of functional and decoy receptors on cancer and stroma cells in primary tumor and liver metastasis [176, 177]. Although we reported preliminary results with this approach, some relevant limitations were still present: rhTRAIL had poor bioavailability profile and suboptimal effect requiring frequent infusions. After reporting the MSC activity in targeting human pancreatic cancer and TRAIL peculiar cytotoxicity in this setting, the step forward was the evaluation of chemotherapy activity in TRAIL resistant model to explore the synergistic effect of this approach. In HCT116 colon cancer cells and in HCT116 xenografts, pre-treatment with 5-fluorouracil enhanced the pro-apoptotic activity of MSC-TRAIL compared to MSC-TRAIL treatment alone [249]. In metastatic renal cell carcinoma and metastatic de-differentiated liposarcoma in vivo model, complete regression of lung nodules in mice was observed with combination of

dodecameric TRAIL secreted by MSCs and Herpes Virus Simplex thymidine kinase (HSV-TK) [250, 251]. Previously the synergistic activity of MSC-TRAIL and taxanes was reported in oral squamous carcinoma and prostate cancer cells [252, 253]. In malignant glioma, the use of valproic acid or compound C (a AMP-activated protein kinase inhibitor) increased TRAIL-induced apoptotic effect [254, 255]. In the same setting, treatment of either TRAIL-sensitive or resistant human glioma cells with temozolomide (TMZ) and MSC-TRAIL resulted in a significant apoptotic effect compared to the administration of each agent alone [256]. Authors observed upregulation of DR5 expression and down-regulation of anti-apoptotic proteins such as XIAPs and cFLIP with a substantial increase in caspase activation. They confirmed the same results in vivo survival experiments and bioluminescence imaging analysis. Recently Huang et al evaluated the combination of sTRAIL-armed MSC and radiotherapy (RT) as sensitizing treatment for an immunotherapeutic approach [257]. Radiotherapy exhibited antitumor immunity via the cGAS/STING axis for type I interferon (IFN) production [258]. The authors observed that combined treatment with MSC-sTRAIL and RT significantly reduced cell viability and enhanced apoptosis by inducing TRAIL-dependent cell death also in STING-deficient colorectal cancer cells. The combination of MSC-sTRAIL and RT significantly remodeled TME and created an immunogenic setting (PD-L1 downregulation on cancer cells) where an immunotherapeutic approach with anti-PD1 should be evaluated.

Also our group evaluated the synergistic activity of a combinatory approach with Nab-paclitaxel and AD-MSC delivering sTRAIL in pancreatic model [176]. Pancreatic cancer cells were incubated with sTRAIL containing supernatants for up to 3 months to select resistant populations. Although fluorescence activated cell sorting (FACS) analysis reported no difference in TRAIL receptor in WT and TRAIL resistant clones, in the latter one the expression of pro-survival genes such as BCL-XL, NFKB1 and NFKB2 was reported, identifying this one as the main mechanism involved in TRAIL resistance. Then to evaluate the synergistic effect of the combination, BXPC3 PA clones were treated with sTRAIL containing supernatant and Nab-PTX (5 ng/mL) for 24 h optaining a death rate of 51.8±2.0% Afterwards the role of a previous sensitizing treatment with Nab-PTX was investigated, determining an increase death rate of 65.8±1.8% in combination with sTRAIL-containing supernatant. In vivo model, orthotopic models of mice bearing BXPC3 s-TRAIL resistant clones were treated weekly by 20 mg/kg intraperitoneal Nab-PTX and/or peri-tumoral injection of 1 million sTRAIL-AD-MSC 1 day later or with

sTRAIL-AD-MSC alone or Nab-PTX alone. We observed no difference in tumor size in mice treated with RR001 or Nab-PTX alone but, on the other side, a marked reduction of tumor diameters such as CK7 cells in immunohistochemical (IHC) analysis with reported stroma deterioration in mice treated with the combination approach.

2 AIMS OF THE STUDY

RR001 is an autologous human cell-based medicinal product, based on AD-MSCs genetically modified to produce high amounts of anti-cancer soluble molecule Tumor Necrosis Factor-related Apoptosis-inducing Ligand (sTRAIL). RR001 is indicated for the treatment of cancers expressing high levels of TRAIL receptors.

The therapeutic potential of combinatory approaches based on combination of GEM or Nab-PTX and TRAIL has been widely explored and reported in literature both in vitro and in vivo models [211, 212, 219-223, 225, 230, 231, 234, 236]. Recently, our group has firstly demonstrated the synergistic anticancer activity of Nab-PTX and sTRAIL MSCs combination against PDAC in pre-clinical models [176].

Here, for the first time, we explored the effectiveness and the molecular basis of the trio combinatory approach with GEM, Nab-PTX and RR001 against three different PDAC cell lines characterized by differing sensitivity to TRAIL, GEM and Nab-PTX in 2D and 3D models. In addition, we investigated the cytotoxic impact of this triple combination (GEM + Nab-PTX + RR001) on a artificial PDAC microenvironment recreated in vitro by the addition of primary human stromal cells in a 3D bioreactor.
Finally, in an orthotopic PDAC mouse model, we further prove the efficacy of RR001, when given in combination with GEM + Nab-PTX, also evaluating the feasibility of the route of administration and considering the any toxicity of this synergistic approach.

3 MATERIALS AND METHODS

Cell culture

Three human PDAC cell lines (wild-type BxPC-3, sTRAIL resistant BxPC-3, and MIA PaCa-2) were used. Wild-type BxPC-3 (WT BxPC-3; Interlab Cell Line Collection, ICLC, Genova, Italy) and sTRAIL-resistant BxPC-3 (sT-resistant BxPC-3) [4] were cultured in RPMI (Gibco-Life Technologies, Grand Island, NY, USA) with 10% heat-inactivated fetal bovine serum (FBS; Gibco-Life Technologies, Grand Island, NY, USA), 1% L-glutamine (Euroclone, Milan, Italy), and 1% penicillin/streptomycin (Sigma-Aldrich, Saint Louis, MO, USA). MIA PaCa-2 (ATCC, LGC Standards S.r.l., Milan, Italy) were maintained in DMEM (Gibco-Life Technologies, Grand Island, NY, USA), 10% FBS, 2.5% horse serum (Euroclone, Milan, Italy), 1% pen/strep, and 1% L-glutamine. Authentication of PDAC cell lines was performed by the Leibniz Institute DSMZ–German Collection of Microorganisms and Cell Cultures (GmbH, Braunschweig, Germany).

MSC were isolated from lipoaspirate specimens of individuals undergoing aesthetic liposuction after approval from a local ethics committee. Cells were maintained in α-MEM (Gibco-Life Technologies, Grand Island, NY, USA) supplemented with 2.5% human platelet lysate (Macopharma, Tourcoing, France), 1% L-glutamine, 0.5% ciprofloxacin (Fresenius Kabi Italia S.r.l., Verona, Italy), and 0.2% heparin (Sigma-Aldrich, Saint Louis, MO, USA). AD-MSC transduced with a lentiviral vector coding for sTRAIL gene (AD-MSC sTRAIL – Patent Pending Rigenerand Srl) or empty vector as a control (AD-MSC EMPTY) were obtained as described in Spano et al [177].

Luciferase transduction of PDAC cell lines

PDAC cell lines were engineered to express a luciferase protein (Lentiviral particles for Firefly Luciferase, GeneCopoeia, MD, USA) per manufacturer instructions. Photon emissions from luciferase-positive (Luc+) PDAC cells were measured via IVIS Lumina XRMS (Perkin Elmer, Waltham, Massachusetts, USA) with Living Image software (v.4.3.1, Perkin Elmer), used to estimate the level of photon emission per cell.

GEM Nab-PTX dose response in WT and engineered MSC

AD-MSC WT or sTRAIL were seeded in 96-well plates at 2500 cells/well. Cells were treated with increasing concentrations of GEM (10 μM) and Nab-PTX (1 μM) for 24 and 48 hours. MSC viability was assessed via Cell Titer AQueous96 One Solution Cell Proliferation assay and GloMax Discover Microplate Reader.

ELISA

AD-MSC WT or sTRAIL were cultured with/without GEM (10 μM) and Nab-PTX (1 μM) for 48 hours. CM was collected and filtered through a 0.22-μm filter (Euroclone, Milan, Italy). sTRAIL levels from MSC supernatants were measured using a Quantikine Human TRAIL/TNFSF10 kit per manufacturer instructions (Bio-Techne, Minneapolis, MN, USA).

Combination assay

PDAC cells (BxPC-3; s TRAIL resistant BxPC-3, MIA PaCa-2 PATU8988T) were seeded in 96-well plates at 5000 cells/well (Day 1) and incubated the following day (Day 2) with increasing concentration of GEM (from 0-2000 u M) and Nab-PTX (from 0 to10 μM) based on 3 different schedules (simultaneous co-treatment or pre-treatment with one drug and 24h-delayed treatment with the other one). PDAC cell viability was assessed via Cell Titer AQueous96 One Solution Cell Proliferation assay (Promega, Madison, WI, USA) and quantified via GloMax Discover Microplate Reader (Promega, Madison, WI, USA). According to the cell viability percentage and to the combination index (for the evaluation of drugs interaction), the most synergistic doses and schedules for each cell line was identified**.**

Cytotoxicity assays

GEM & Nab-PTX + sTRAIL combinatory approach in 2D: PDAC cells were seeded in 96-well plates at 5000 cells/well (Day 1) and incubated the following day (Day 2) with 10 μM GEM and 1 μM Nab-PTX (BxPC-3, sTRAIL resistant BxPC-2; MIA PaCa-2) or 10 μM (PATU-8988T). At Day 3, PDAC cell lines were treated for 24 hours more with CM from AD-MSC sTRAIL containing increasing concentrations of sTRAIL (0–2500 pg/ml). PDAC cell viability was assessed via Cell Titer AQueous96 One Solution Cell

Proliferation assay (Promega, Madison, WI, USA) and quantified via GloMax Discover Microplate Reader (Promega, Madison, WI, USA).

GEM & Nab-PTX + RR001 (AD-MSC sTRAIL) combinatory assay in 3D: Luc+ PDAC cells were seeded in VITVO bioreactor (Rigenerand srl, Medolla, Italy) on Day 1, as described in Candini et al[178]. On Day 2, cells were treated with GEM (10 μM for WT BxPC-3, sTRAIL-resistant BxPC-3, MIA PaCa-2 and PATU8988T) and Nab-PTX (1 μM for WT BxPC-3 and sTRAIL-resistant BxPC-3, MIA PaCa-2 or 10 μM for PATU8988T) or plain medium for 24 hours. On Day 3, PDAC cells were co-cultured up to 72 hours with RR001 (AD-MSC sTRAIL) at different effector: target ratios (E:T = 1:10 and 1:30). Luciferin substrate (Promega, Madison, WI, USA) was added into co-culture at 10 mg/ml. Tumor cell mortality was quantified based on decrease of Luciferase signal via GloMax Discover Microplate Reader. VITVO loaded with PDAC cells alone or co-cultured with AD-MSC EMPTY were used as controls.

Primary human CAF viability assays Human PDAC tissues were collected from four patients (PZ1 – PZ4) undergoing surgery at the Complex Structure of Hepato-Bilio-Pancreatic Oncological Surgery and Liver Transplant Surgery (University Hospital of Modena), after informed consent. Human PDAC samples were digested through mechanical and enzymatic dissociation via Tumor Dissociation Kit and the gentleMACS Octo Dissociator (MACS; Miltenyi Biotec, Auburn, CA, USA), following manufacturer instructions. Digested cells were cultured in minimal essential medium with α-MEM containing 2.5% platelet lysate, 1% glutamine, 0.5% ciprofloxacin, and 0.2% heparin for 10 days to selectively isolate four primary CAF cell lines. CAFs were characterized immunophenotypically by flow cytometry [150]. Most isolated cells demonstrated the typical mesenchymal antigen expression profile, expressing CD73 (98 ± 1%), CD90 (99%), and CD105 (87 ± 12%) and lacking CD45, EPCAM, and HLA-DR markers, proving their stromal cell lineage and confirming the absence of leukocyte or epithelial contaminant subpopulations. CAFs at low passage (no more than 5) were used for 3D in vitro studies.

Primary CAF were tested for sensitivity to sTRAIL, alone or in combination with GEM & Nab-PTX. Cells were seeded in a 96-well plate at 2500 cells/well in cell culture medium. Cells were next treated with CM from AD-MSC sTRAIL containing sTRAIL 1000 pg/ml or were pre-treated with GEM (10 μM) and Nab-PTX (1 Mm) for 24 hours

and incubated with sTRAIL (1000 pg/ml) for 24 hours. CAF viability was assessed via CellTiter-Glo reagent per manufacturer instructions and quantified via GloMax Discover Microplate Reader.

Cytotoxicity studies on 3D PDAC avatar

Luc+ WT BxPC-3, s TRAIL resistant BxPC-3 or MIA PaCa-2 cells and primary CAF cells were loaded in VITVO bioreactor to recreate in vitro an artificial tissue mimicking PDAC microenvironment. The realistic tumor/stroma ratio, observed in patient derived PDAC samples[187], was reproduced in VITVO by seeding 55% of tumor cells and 45% of stromal elements.

3D PDAC avatars were treated with GEM (10 μM) and Nab-PTX (1 μM) or plain medium for 24 hours. The next day, PDAC avatars were co-cultured up to 72 hours with RR001 (AD MSC sTRAIL) at different E:T ratios (1:10 or 1:30). Luciferin substrate (Promega) was added into co-culture at 10 mg/ml. Tumor cell mortality was quantified based on the decrease of Luciferase signal via GloMax® Discover Microplate Reader. VITVO loaded with PDAC cells and CAF elements alone were used as controls.

In vivo studies

Development of PDAC orthotopic mouse model and GEM & Nab-PTX dose selection:

PDAC orthotopic model: $1x10^6$ MIA-PaCa-2 Luc+ cells in 30 μl of 1:1 Matrigel (Corning) and PBS suspension were injected in the pancreas of 12 NOD-SCID mice. Five to 6-week-old mice were anesthetized with Isofluorane (Baxter, IL, USA) and the left flank was shaved. Before surgery, mice were administered with ketoprofen (3 mg/kg). The abdominal skin was lift with forceps and a 1-cm incision with sterile micro scissors was made at the level of the spleen. The underlying muscle was incised to enter the abdominal cavity without injury to the underlying organs. Spleen and pancreatic body were gently exposed to the outside of the peritoneal cavity by using a pair of blunt-nose forceps and tumor cells were slowly injected into the tail of pancreas by a 19G syringe. A fluid-filled region should be formed within the pancreatic parenchyma. After injection, syringe was carefully removed to avoid cell leakage from the site of injection and pancreas and spleen were returned to the peritoneal cavity with blunt forceps. Abdominal muscle layer and the skin layer were sequentially closed with interrupted 4-0 polysorb

sutures (Ethicon, Cincinnati, Ohio, USA). Tumor engraftment was evaluated by bioluminescence 7 days after cells injection by IVIS Lumina XRMS system and confirmed by ultrasound at day 11. Tumors were monitored weekly by Vevo 2100 Imaging System. Before the start of treatments, mice were randomized in three groups according to tumor volume.

According with the results reported in literature, two different combination doses of GEM and Nab-PTX that can be translated in our in vivo combinatory approach with RR001 have been identified [259-263]. These doses correspond to GEM 50 mg/kg + PTX 7.5 mg/kg or GEM 50 mg/kg + PTX 50 mg/kg respectively. Based on published preclinical data, both these combination doses provide a relevant antitumor effect in PDAC models without affecting animal survival or provoking relevant side effect. Tumor engraftment was evaluated by bioluminescence 7 days after injection by the IVIS Lumina XRMS system. Tumors were monitored weekly using the ultrasound Vevo 2100 Imaging System (FUJIFILM VisualSonics Inc., Bothell, WA, USA). Before treatment, mice were randomized into three groups by tumor volume. GEM (50 mg/kg) and PTX (7.5 or 50 mg/kg) were administered i.p at day 14 and 21. Tumor volume were quantified by Vevo Lab 3.1.0 software (FUJIFILM VisualSonics Inc.) and formalin-fixed, paraffin-embedded (FFPE) tumor sections and organs (liver, spleen, kidney) were evaluated via hematoxylin-and-eosin staining (H&E, Carlo Erba) to analyze tissue structure and histology.

In vivo efficacy of trio combination GEM + Nab-PTX + RR001 in PDAC orthotopic model: an orthotopic mouse model was used to assess the therapeutic impact of the GEM & Nab-PTX + RR001 (AD-MSC sTRAIL) combinatory approach after approval by the National Ministry of Health and the local Institutional Animal Care and Use Committee (502/2018-PR. 02/07/2018). 1x106 WT MIA PaCa-2 Luc+ cells in 30 µl of 1:1 Matrigel (Corning, New York, USA) and PBS (Gibco-Life Technologies, Grand Island, NY, USA) suspension were injected into the pancreas of 61 NOD-SCID mice, as previously reported. Tumor engraftment was evaluated by bioluminescence 7 days after injection by the IVIS Lumina XRMS system. Tumors were monitored weekly using the ultrasound Vevo 2100 Imaging System. Before treatment, mice were randomized into five groups by tumor volume. GEM (50 mg/kg) & PTX (7,5 mg/gr) was administered intraperitoneally (i.p.) at Days 15 and 22, followed by an ultrasound-guided intratumor (i.t.) injection of RR001 (AD-MSC sTRAIL E:T = 1:30 or 1:10) suspended in 15 µl of

PBS at Day 23. AD-MSC sTRAIL were labeled using XenoLight DiR (8 μM; Perkin Elmer, Waltham, Massachusetts, USA), and their biodistribution inside the pancreas was monitored up to 48 hours after injection. Formalin-fixed, paraffin-embedded (FFPE) tumor sections and organs (liver, spleen, kidney) were evaluated via hematoxylin-and-eosin staining (H&E, Carlo Erba, Milan, Italy) and immunohistochemistry analysis (IHC) of human CK-8/18 (VENTANA-ROCHE), human MIT and KI67. CK-8/18 and KI67 expression was analyzed with ImageJ software (NIH, Bethesda, MD), considering all tumor fields per sample at 100X magnification for every individual animal.

BasescopeTM Assay

For the detection of AD-MSC sTRAIL in mice tumor samples, we employed the BaseScope™ Assay (ACD Bio-Techne, USA), a novel method of in situ hybridization for visualizing single RNA target molecules in slide-mounted FFPE samples. We designed a specific probe targeting the RNA transcript of the TRAIL transgene and a hybridization-based signal amplification system allowed the detection of TRAIL mRNA inside AD-MSC sTRAIL. The probe used for BASESCOPE is selective for TRAIL transgene since it target the junction between the yeast GCN4 isoleucine zipper trimer-forming domain (IL-Z)55 and the TRAIL receptor binding domain sequence (Apo2L; amino acid 114–281) [177]. This probe has been validated by ACD Bio-Techne and it does not detect human or mouse endogenous genes. Individual sTRAIL RNA transcripts appeared as distinct dots of red chromogen.

Statistics

Data were expressed as mean values ± standard error of the mean (SEM). An unpaired 2-tailed Student's t-test was used ($p \leq 0.05$ as statistically significant). Fisher's exact test was employed for tumor necrosis quantification in vivo.

4 RESULTS

Here we report the pre-clinical studies supporting the scientific rational for the treatment of PDAC patients with an intratumoral administration of RR001 (an autologous human cell-based medicinal product based on AD-MSCs genetically modified to deliver the anti-cancer molecule soluble TRAIL) after pre-treatment with GEM and Nab-PTX (GNP) combination therapy.

The rationale of this tri-combination approach is based on the molecular mechanisms previously described that support the synergistic approach of Nab-PTX and GEM with TRAIL pro-apoptotic activity (see 1.5, 1.6 and 1.7) and on previous studies revealing that pretreatment with GNP increased the expression of the key functional TRAIL receptor DR5 on the surface of TRAIL resistant cancer cell [264, 265].

The anticancer efficacy of trio combination GNP + RR001 was studied *in vitro* using both 2D and 3D models and *in* an orthotopic xenograft PDAC mouse model.

4.1 SELECTION OF THE MOST APPROPRIATED DOSAGE OF GEM + NAB-PTX TO BE USED IN COMBINATION WITH RR001

Preliminary 2D experiments *in vitro* for the screening of the most appropriate treatment schedule and chemotherapeutics doses were performed to evaluate the antitumor impact of trio combinatory approach with GNP+RR001.

Firstly, the synergistic interaction between GEM and Nab-PTX was assessed by the evaluation of the cytotoxic effect of the treatment with both drugs on four different PDAC cell lines (BxPC-3 WT; MiaPaCa-2; PATU-8988T and sTRAIL resistant BxPC-3). Eighty different concentrations of the two drugs were crossed, and treatments were performed with 3 different schedules (simultaneous co-treatment or pre-treatment with one drug and 24h-delayed treatment with the other one). According to the cell viability percentage and to the combination index (for the evaluation of drugs interaction), the most synergistic doses and schedules for each cell line were identified (**Figure 8**). For all four different PDAC cell lines cotreatment with GNP had the most synergistic impact. In addition, for each tumor cell line the half maximal inhibitory concentration (IC50) dose of drug combination was identified: for BxPC-3 WT, MiaPaCa-2 and sTRAIL resistant

BxPC-3 IC50 corresponded to 10µm GEM + 1µm Nab-PTX. For PATU8988T IC50 dose was 10µm GEM + 10µm Nab-PTX (**Table 3**).

4.2 PRE-TREATMENT WITH GEM AND NAB-PTX DOESN'T INTERFERE WITH AD-MSC S-TRAIL VIABILITY AND S-TRAIL PRODUCTION

To assess whether the anti-proliferative and cytotoxic impact displayed by GNP could affect the AD-MSC sTRAIL viability, thus compromising the therapeutic efficacy of a combinatory approach with RR001, we performed a cell viability assay. The doses of GEM and Nab-PTX here used were the ones selected in previous studies on PDAC cell lines and that will be used in 3D model.

Cell viability assay showed that after 24 h of co-treatment with GEM (10 µM) and Nab-PTX (1 µM), 69±2% of AD-MSCs and 64±5% of AD-MSCs sTRAIL were still viable. At 48 hours a slight reduction in metabolic activity of both cell types was observed but however activity remained higher than 40% (AD-MSC = 41%; AD-MSC sTRAIL = 45%). This event is probably due to a block in the AD-MSC replicative potential, due to the mechanism of action of both cytostatic agents, rather than the apoptosis induction (**Figure 9**).

Furthermore, sTRAIL released by AD-MSCs sTRAIL was not compromised by co-treatment with GEM and Nab-PTX. The ELISA analysis of the supernatant collected from the AD-MSCs sTRAIL after 48 hours of co-treatment confirmed the presence 693 ± 24 pg / ml of sTRAIL (**Figure 10**). This value was completely in line with the production of sTRAIL obtained from genetically modified AD-MSCs grown in standard culture media which ranges from 233 to 872 pg/ml (536 $\pm$ 234 pg/ml) (**Figure 10**).

4.3 GEM AND NAB-PTX SYNERGIZE WITH RR001 TO INDUCE APOPTOSIS IN BOTH TRAIL SENSITIVE AND RESISTANT PDAC CELL LINES

We assessed in 2D the cytotoxic effect of the combinatorial approach GNP+RR001, combining the chosen schedules and doses of the two drugs with increasing concentrations of sTRAIL (from 50 to 2500 pg/ml; CM of AD-MSC sTRAIL). Starting from lower dose of sTRAIL (50 and 250 pg/ml respectively), the trio combination provoked on BxPC-3 WT and MIA PaCa-2 a statistically significant reduction of cell

viability compared to sTRAIL alone (** $p<0.05$ and * $p<0.02$) thus enhancing its cytotoxic impact. Notably, the combinatorial approach was also able to overcome sTRAIL resistance in BxPC-3 resistant to sTRAIL. For PATU-8988T cell line, sTRAIL doses higher than 750 pg/ml combined with GNP induced a statistically significant reduction of cell viability compared to both sTRAIL and chemotherapeutics alone**.** (**Figure 11**)

4.4 RR001 IN COMBINATION WITH GEM AND NAB-PTX INDUCE CYTOXICITY ON PRIMARY STROMAL CELLS FROM PDAC SAMPLES

In the attempt to determine the impact of trio-combinatory approach on PDAC stromal compartment, which can represent up to 70% of tumor burden, four primary samples of human stromal cells (namely, CAF) have been isolated from patients affected by PDAC by enzymatic digestion starting from tumor samples [187]. Then primary CAFs have been isolated from histological specimen of patients affected by PDAC by enzymatic digestion. Isolated cells were cultured in selective culture media in order to isolate stromal cellular elements. Ten days after *in vitro* culture, microscope observation revealed a cell population exclusively composed by spindle shape cells displaying the typical fibroblast morphology in all 4 samples. By 2D system, the sensitivity to GNP plus sTRAIL was investigated in all PDAC stromal samples. A significant cytotoxic effect of GNP was registered in all four stromal samples (> 60 % cell death). More important, tumor priming with GNP remarkably enhances the sensitivity of PDAC cells to RR001, leading to a significant synergistic antitumor effect in 3 out of 4 stromal samples (**Figure 12**).

4.5 THE COMBINATION OF RR001, GEM AND NAB-PTX INDUCE SIGNIFICANT ANTITUMOR IMPACT IN 3D PDAC CELL LINE CULTURES

We have already demonstrated by 2D *in vitro* data the synergism and the benefit of RR001 with both the combination GEM and Nab-PTX (see 4.3). Data to support the choice of the clinical dose and the rationale of the trio combinatory approach (GNP followed by RR001) in PDAC patients were investigated using 3 dimensional (3D) models. Cell lines were selected as being responsive or unresponsive to GNP or RR001

and expressing different (favorable and less favorable) TRAIL functional/decoy receptor ratios: BxPC-3 WT, BxPC-3 resistant to sTRAIL, MiaPaca-2, PATU-8988T.

3D culture systems have potential to provide more physiologic environments for cell culture in drug discovery and toxicology than classical bidimensional (2D) culture systems and to mimic an in vivo-like context enabling testing in a human avatar environment; 3D culture leads to a different modulation of gene expression, ultimately influencing the antigenic profile of the cells and closely mimicking an in vivo environment [266, 267]. In the case of RR001 development, this 3D culture system allows to recreate a three-dimensional tumor cell culture in vitro mimicking the in vivo tumor burden. This system has been used to generate proof of concept data for the use of RR001 in combination with chemotherapy agents, to study the therapeutic impact of trio-combo treatment based on GNP+RR001 as well as to identify the dose of RR001 associated with the most significant anticancer impact.

To do this, four different Luciferase expressing PDAC cell lines (BxPC-3 WT; MIA PaCa-2; PATU-8988T and sTRAIL resistant BxPc-3), representing the heterogeneity of PDAC patients in terms of TRAIL functional/decoy receptor ratios, sensitivity to TRAIL and chemotherapeutics (**Table 4**), were loaded into VITVO bioreactor and growth in 3D system. When the 3D culture was established, PDAC cells were pre-treated with the doses and treatment schedule of GEM and Nab-PTX previously defined (see sections 4.1.and 4.3).

For BxPC-3 WT, BxPC-3 resistant to sTRAIL and MiaPaca-2 cell lines, a combination with 10 µM GEM and 1 µM Nab-PTX was selected for the 3D *in vitro* experiments based on 2D dose-response experiments while for PATU8988T the concentration of Nab-PTX was increased at 10 µM. After 24h, RR001 at different doses (E:T= 1:10 or 1:30) was added. The cytotoxic impact of trio-combo on PDAC cells was quantified based on the decrease of BLI signal.

The following controls were used: GNP alone, GNP + AD-MSC transduced with lentiviral empty vector (AD-MSC EV) 1:10, RR001 alone 1:10 and 1:30, AD-MSC EV alone. For BxPC-3 WT cells, an high cytotoxic effect induced by GNP (75±4% cell death after 48h) and a slightly less prominent cytotoxic effect by RR001 alone were observed. The trio combination was confirmed as the most effective approach with more than 95% tumor cell death after 48h with both the two tested doses (E:T 1:30 and 1:10) (**Figure 13**).

Also, in BxPC-3 sTRAIL resistant cells, it was observed a high cytotoxic effect induced by GNP (67±1% cell viability after 48h), a very low cytotoxic effect induced by RR001 alone, and a synergistic antitumor effect for the trio combination, with more than 89% of tumor cell death after 48h with both the tested doses (E:T 1:30 and 1:10). (**Figure 14**)
For MiaPaca-2 cells, we observed a very low cytotoxic effect induced by GNP (no effect after 48h and around 20% cell mortality after 72h), a high and dose-dependent cytotoxic effect of RR001 alone (> 86±3% cell mortality for 1:10), and a synergistic anti-tumor effect for the trio combination (E:T 1:30 and 1:10), with more than 95% of tumor cells death after 72h at the two tested doses **(Figure 15).** Also in PATU-8988T cell line, characterized by chemo and TRAIL resistance, a synergistic antitumor effect after 72 h for the trio combo at E:T ratio of 1:10 was observed with more than 90% of tumor cell death. As we expected, no effect induced by GNP alone and a moderate cytotoxic effect by RR001 1:10 alone at 72 h were detected (**Figure 16**).

4.6 THE COMBINATION OF RR001, GEM AND NAB-PTX INDUCE SIGNIFICANT EFFECT IN PDAC AVATARS

We previously assessed the efficacy of the trio-combination approach on PDAC cell lines (both in 2D and 3D systems) and PDAC stromal cells (in 2D). One of the main peculiarities of PDAC is the essential bond between cancer cells and stroma that represents almost 70% of the tumor [187].
To mimic PDAC microenvironment we generated an additional 3D model by mixing malignant cells and primary stromal elements. We replicated the tumor/stroma ratio compartment that was observed by histological analysis on 50 surgical specimen of human PDAC samples and in accordance with a lot of previous reports (the amount of stroma in the tumor mass was 75%, approximately 45% composed by stromal elements and 30% by collagen fibers) [66, 268].
For this set of experiments, BxPC-3 WT, MiaPaCa-2 and sTRAIL resistant BxPC-3 were used. BxPC-3 WT lines had an high sensitivity to both chemotherapeutics ad RR001. MiaPaCa-2 and sTRAIL resistant BxPC-3 simulated the worst scenario in terms of response to GNP and RR001. Two additional stroma samples (ID: PZ2 and PZ4) were selected according to their sensitivity to GNP + RR001 as observed in the 2D system. Tumor and stromal cells were loaded into 3D bioreactor to generate an artificial PDAC tissue and pre-treated by GNP for 24h, then the culture medium was washed-out before

the addition of RR001. The percentage of tumor cells mortality was measured after 24h, 48h or 72h of treatment with RR001 using E:T ratios 1:10 and 1:30. The following controls were used: GNP alone, GNP + AD-MSC transduced by a lentiviral empty vector (AD-MSC EV) 1:10, RR001 alone 1:10 and 1:30, AD-MSC EV alone.

In PDAC avatar generated using BxPC-3 WT and primary stromal cells (ID: PZ2 and PZ4), data revealed a high cytotoxic effect induced by GNP (tumor cell mortality higher than 75±1% after 48h) and a synergistic antitumor effect for the trio combo 1:30 and 1:10 with more than 95±1% tumor cell death at 48 and 72h for the two tested doses. For each time point and dose tested, the cytotoxic effect displayed by GNP+RR001 was significantly higher than the one obtained by GNP or RR001 alone, thus further confirming the suitability of the proposed RR001 doses (1:30 and 1:10) in the combinatory approach even in presence of human PDAC stromal compartment. On the contrary, the reduced cytotoxic effect displayed by RR001 alone particularly in presence of stromal cells, is probably due to both the presence of stromal compartment that impacted RR001 distribution and the reduced number of AD-MSC sTRAIL loaded into the 3D system when the E:T ratio is calculated considering the amount of tumor cells only (**Figure 17**).

In PDAC avatar generated using s TRAIL resistant BxPC-3 and primary stromal cells (ID: PZ2 and PZ4), data showed a moderate cytotoxic effect induced by GNP (61±2% tumor cell mortality after 48h), and a synergistic antitumor effect for the trio combo 1:30 and 1:10 provoked tumor cell mortality after 48h higher than 86±1% at the two tested doses. For each time point and dose tested, the cytotoxic effect displayed by GNP + RR001 was significantly higher than the one obtained by GNP (**Figure 18**). Stromal compartment does not interfere with the ability of GNP in reverting TRAIL resistance in PDAC cells.

In PDAC avatar generated using MIA PaCa-2 and primary stromal cells (ID: PZ2 and PZ4), data revealed a moderate cytotoxic effect induced by GNP after 72h (2±1 % MiaPaCa-2 cell death after 24 and 48h, and 47±1 % after 72h) and confirmed the synergistic impact for the trio combinatory approach at 48 and 72h for both tested doses. The lower dose of RR001 (corresponding to 1:30 E:T), when combined with GNP, was able to kill up to 70±5% of MiaPaCa-2 cells in 72h, while the trio combo at the higher dose of RR001 (1:10) provoked an higher cytotoxic impact with 96±2% of PDAC cell

death. For each dose tested at 48 and 72h, the antitumor impact displayed by GNP + RR001 (1:10) was always higher than the one obtained by GNP or RR001 alone, thus confirming the efficacy of the combinatory approach on MiaPaCa-2 cells even when co-cultured with primary PDAC stromal elements (**Figure 19**).

4.7 ESTABLISHMENT OF A PREDICTIVE ORTHOTOPIC PDAC MOUSE MODEL AND IN VIVO GEM + NAB-PTX DOSE SELECTION

A PDAC orthotopic xenotransplant murine model was developed to mimic the clinical situation and identify the effective dose of GNP to be associated with RR001 to induce synergistic antitumor impact without provoking relevant side effects.

Based on published preclinical data, both combination of GEM 50 mg/kg + PTX 7.5 mg/kg or GEM 50 mg/kg + PTX 50 mg/kg provided a relevant antitumor effect in PDAC models without affecting animal survival or provoking relevant side effect [259-262]. Twenty 6 weeks-old NOD-SCID mice were injected into the pancreatic tail through abdominal surgery with $1x10^6$ MiaPaca2 PDAC cells (luciferase labeled) in 30 µl of cell suspension mixed with matrigel at day 0.

Only 1 mouse was sacrificed just after surgery because of spleen bleeding. Of the 19 mice left, 2 did not develop any intrapancreatic tumor and 1 was excluded from the study because at the randomization time the tumor was too small. Hence, 80% of the surgeries were successful (16 mice). Bioluminescence (BLI) signal was measured 7 days post MiaPaca2 injection to verify tumor engraftment (IVIS LUMINA III-Perkin Elmer). All operated mice displayed a bioluminescent signal. Treatments with GEM+PTX were performed intraperitoneally at day 14 and day 21 after surgery. US imaging allowed analysis of the tumor volumes. At both chosen concentrations (GEM 50 mg/kg + PTX 7.5 mg/kg; GEM 50 mg/kg + PTX 50 mg/kg), treatments significantly counteracted tumor cell growth compared to untreated control (**Figure 20A**). The mean tumor volumes ± sem in the last time point before sacrifice (day 28) were 39.2±8.6 mm^3 in the control group (N=4), versus 21.5±6.0 mm^3 in the group treated with GEM 50 mg/kg + PTX 7.5 mg/kg (N=4) and 8.9±1.3 mm^3 in the group treated with GEM 50 mg/kg + PTX 50 mg/kg (N=4). The antitumor effect in both treated groups was confirmed by histological analysis (by hematoxylin and eosin staining) (**Figure 20B**). Indeed, treated tumors displayed a compromised architecture, with loss of compactness in respect to control tumors and with presence of necrotic areas.

In order to assess the safety of the two regimens tested in vivo, animal weight (as marker of animal health) was registered and histological analysis by hematoxylin and eosin staining was performed on liver, kidney and spleen collected from mice at sacrifice (**Figure 21A**). As shown in **Figure 21A**, treated groups showed body weight trends comparable to that of control group, with no reduction of body weight due to possible toxic effects of the combinatorial regimen GNP.

The possible toxic effect of GNP at both chosen concentrations of paclitaxel was evaluated also at histological level (**Figure 21B**). Liver, spleen and kidney of treated animals were carefully checked for necrotic or fibrotic areas as well as for the presence of inflammatory infiltrating cells. No tissue damage nor inflammation were observed in the organs of any treated group, if compared with control group. In summary, the combinatorial regimen of GNP did not show any toxic effect on treated mice, even at the highest dose of PTX.

GNP (at both concentrations) determined a significant reduction of tumor volume growth and, at the histological level, tumor architecture was compromised. Importantly, treated mice did not display a weight decrease and no toxic effect was observed in organs histology. In light of the results of this pivotal study, the regimen with PTX at the concentration of 7.5 mg/kg was chosen, because it displayed a good antitumor effect, but tumors were not too small for the US-guided injection procedure of RR001. Indeed, too small tumors could hamper the targeting of the tumor with the syringe needle.

4.8 THE COMBINATION OF RR001 AND GNP INDUCE SIGNIFICANT ANTITUMOR EFFECT IN ORTHOTOPIC PDAC MOUSE MODEL

We evaluated the activity of the trio-combinatory regimen in a large cohort of mice (N=61). In light of the results of the previous reported studies, the regimen with GEM +PTX at the concentration of 50 mg/kg and 7.5 mg/kg respectively was chosen, because it displayed a good antitumor effect without relevant animal toxicity.

Sixty-one 6 weeks-old NOD-SCID mice were injected into the pancreatic tail through abdominal surgery with $1x10^6$ MiaPaca2 PDAC cells (luciferase labeled) in 30 µl of cell suspension mixed with matrigel at day 0. Tumor engraftment was analyzed by Ultrasound (US) imaging. Treatment with GNP (GEM 50 mg/kg + PTX 7.5 mg/kg) was performed at day 14 and day 21 after surgery as previously reported. RR001 was administered intra-

tumorally by an eco-guided injection at day 22 and RR001 cells were labelled with the infrared fluorescent agent DiR in order to track their presence inside tumor. (**Figure 22**). Tumor volumes were monitored over time by ultrasound (US) imaging. At the last time-point before sacrifice, the group GNP + RR001 1:10 showed a significant reduction of tumor volume compared to CTL group, RR001 1:10 group and GNP+RR001 1:30 group without any difference respect to GNP group. A significant difference of tumor volume was observed also between RR001 1:10 group and GNP+RR001 1:30 group revealing the combinatory strategy as the most effective. The mean tumor volumes ± sem were the following: CTL, 80± 12.8 (N=13); GNP, 31.5± 4.5 (N=13); RR001 1:10, 67.8±8.1 (N=13); GNP+RR001 1:30, 34.4±11 (N=11); GNP+RR001 1:10, 24.3±11 (N=11). (**Figure 23**)

After the sacrifice, tumors were collected for the histological analyses. To evaluate tumor architecture and tumor cells morphology, hematoxylin and eosin staining was performed (**Figure 24**). Tumors of the control group were extremely compact. On the contrary, a variable level of alteration of tumor architecture and degeneration of tumor tissue were observed in treated tumors. In particular, the groups treated with the GNP plus RR001 approaches (at both concentrations of cells) displayed tumors with the highest level of tissue degeneration and necrosis. In order to compare the tumor burden among groups, anti-CK8/18 immunohistochemistry (epithelial tumor marker) was performed. The amount of positive area was then quantified by ImageJ (two slides for each tumor; for each slide, all fields at 100X magnification were analyzed) (**Figure 25 A**). Notably, a significant reduction in CK8/18 positive cells was observed in the group treated with GNP in combination with RR001 1:10 in respect to all other groups. Tumor amount was significantly lower also in the group of mice treated with GNP+RR001 1:30 in respect to CTL group (**Figure 25 B**).

To evaluate the amount of proliferative neoplastic cells in tumors, an anti-Ki67 IHC (two slides per samples) was performed and all fields 100X per slide were processed with ImageJ. As shown in **Figure 26**, significative differences were observed in Ki-67 expression between control group and all treated groups. Particularly, groups treated with the combinatorial regimens GNP + RR001 1:30 and 1:10 not only displayed a significative lower amount of Ki67 positive cells in respect to CTL but also towards the single agent treatments, RR001 and GNP alone.

At sacrifice, intrapancreatic tumor, spleen, liver and kidney were collected. These metastases appeared as white patches and were mostly found on the spleen and were analyzed for the histological detection of metastases with hematoxylin and eosin staining. (**Figure 27 A**). Metastases were noticed in 34% of the mice, unexpectedly GNP group displayed the highest number of mice with metastases (77%), even more than the control group (38%). A significative lower incidence of metastasis was detected in all the groups treated with RR001 compared to GNP treatment and this effect was particularly relevant in group treated with the combinatorial regimen GNP + RR001 1:10 (9%) (*p=0.005, **Figure 27 B**). Anti-CK8/18 immunohistochemistry on consecutive spleen slides confirmed the tumor origin of the metastatic areas (**Figure 27 C**).

RR001 biodistribution was assessed using labelled fluorescent agent DiR and the IVIS imaging system (PerkinElmer). Fluorescence signal was registered up to 48 hours in mice treated by DiR labelled AD-MSC sTRAIL and no significant reduction in fluorescence intensity were detected over the time, indicating that AD-MSC sTRAIL stably persisted into the PDAC orthotopic xenograft (**Figure 28 A**). No other tissues showed fluorescence, meaning that AD-MSC sTRAIL did not relocate in other tissue or organs. In addition, a new histological method was employed in order to study the localization and survival of AD-MSC sTRAIL inside tumors 7 days after their eco-guided intratumor injection. Basescope is a ACD in situ hybridazion system that allows the detection of sTRAIL mRNA inside RR001 cells. All tumors of RR001 1:10 and GNP+RR001 groups were analyzed (1 slice per tumor) (**Figure 28 B**), and 2 representative tumors of CTL and GEM+NP groups were inserted as negative controls. In general, no large groups or high number of RR001 cells were detected. Indeed, when present, RR001 were found as small groups of cells beside the tumor (I and IV, **Figure 28 B**), or as few cells (II and V) or single cells (III-VI) in necrotic areas inside the tumor. However, AD-MSC s TRAIL cells appeared vital (both for their morphology and the high amount of sTRAIL mRNA per cell). The evaluation of the presence of AD-MSC s TRAIL by Basescope was extended also to mice spleen (**Figure 28 C**). No positive cells were found in any of the analyzed samples, probably because RR001 cells are not prone to penetrate spleen tissue.

4.9 COMBINATORIAL REGIMEN RR001, GEM AND NAB-PTX DOES NOT PROVOKE ANY TOXICITY IN PDAC MOUSE MODEL

In order to assess the possible toxic effects of treatments, the body weight of mice was monitored during the study and animal tissues were analyzed by H&E. As shown in **Figure 29 A**, no differences in body weight were observed between treated groups, including mice treated with GNP+RR001, and control group.

Taking into account the potential liver toxicity displayed by standard chemotherapeutic drugs and the reported sensitivity of hepatocytes towards some TRAIL forms, hepatic tissue of treated mice was carefully checked for necrotic or fibrotic areas as well as for the presence of inflammatory infiltrating cells [269]. Neither tissue damage nor inflammation was observed in liver tissue of any treated group if compared with control group (**Figure 29 B**). Similarly, neither signs of tissue damage nor inflammation were detected in renal structures, including renal glomeruli. In addition, toxicity was also assessed in the pancreas of treated mice, but neither the exocrine nor the endocrine components were damaged. Summarizing, tissue lesions could not be observed in any of the evaluated organs after the treatment with GNP, RR001, or the combination of them (at both E:T ratios) in vivo. No toxicity was observed in any treated group in respect to control group. Magnification 100X, scale bar 200 μm.

5 DISCUSSION

Pancreatic cancer accounts for only 3% of all cancers but it's the fourth leading cause of cancer death in both men and women causing 7% of all cancer deaths [4]. Pancreatic cancer affects men and women equally, with a peak of incidence around the age of 60 [270]. In last decade, despite a significant increase in incidence rate, no evident progress in the management of the disease were achieved and actually 1-year OS is about 24% and only 9% of patients are alive after 5 years from diagnosis [2]. A radical surgical approach is feasible in less than 20% of patients and even in those ones the well-known PDAC propensity for early metastatic spread and chemo-resistance limits patient outcomes [271]. Chemo-resistance is a multifactorial process involving pancreatic cancer cells, cancer stem cells and the TME [113]. In particular the high fibrotic stroma represents a barrier for tumor growth but at the same time it limits the effective transport of chemotherapeutic agents compromising the efficacy of systemic treatment [62]. The architecture of the tumor stroma is dynamic and influenced by the constant interaction between stroma components (ECM, CAFs, immune cells) and pancreatic cancer cells [70]. In the light of these main limitations the research for new systemic approaches or new anti-cancer molecules has evolved in last years. TRAIL is a pro-apoptotic molecule naturally produced by human body that could induce its anti-cancer activity following both extrinsic and intrinsic pathway with limited effect against normal cells [193]. The role of TRAIL activity alone in clinical setting is limited by the acquired TRAIL resistance and the poor bioavailability requiring frequent infusions. Several studies have investigated the mechanisms underneath acquired TRAIL resistance: reduced expression of DR4/5, down-regulation of pro-apoptotic proteins, and up-regulation of inhibitors of apoptosis (IAP) family proteins and anti-apoptotic proteins [208, 209, 272]. To overcome these unsatisfactory results, combinatory approaches based on systemic chemotherapy and TRAIL-based target therapy are emerging [273].

In the current study, we evaluated the safety and the efficacy of a trio combinatory approach with GEM, Nab-PTX and RR001, a human cell-based medicinal product based on AD-MSCs genetically modified to produce the anti-cancer molecule sTRAIL, both in vitro and vivo PDAC model. The choice of this combination chemotherapy was based on the efficacy of this regimen in locally advanced and metastatic PDAC [216, 274].

The choice of AD-MSC as TRAIL vehicle was based on AD-MSC peculiarity: they can reach the tumor site incorporating into the tumor architecture as stromal MSCs or CAFs with poorly immunogenic activity permitting a durable production of sTRAIL [143, 144]. We explored the role of this combination in PDAC setting due to high expression of TRAIL functional and decoy receptors on both tumor and stromal cells [187, 200, 201]. Secondary, in PDAC, promising results with the combination of Nab-PTX or GEM and TRAIL-based therapy were reported.

Few preclinical data were reported in combination with GEM suggesting that the activation of TRAIL intrinsic pathway associated with GEM activity on mitochondrial membrane permeabilization could enhance an apoptotic process mediated by caspase cascade [231]. Also in clinical setting, in a phase I trial the activity of anti-DR4 Mapatumumab was enhanced in combination with GEM + cisplatin obtaining partial response in 20% of patients and stable disease after 6 cycles in almost 30% of patients [238].

The synergistic activity of Nab-PTX and rhTRAIL was reported in vitro and in vivo in Mia-Paca-2 cell line and orthotopic model [225]. Also, our group demonstrated in vitro and vivo model of PDAC the synergistic activity of a combinatory approach with AD-MSC producing TRAIL and Nab-PTX, however for the first time in this study the efficacy of the trio-combination GEM & Nab-PTX + AD-MSC sTRAIL was explored [176].

For this reason, in a first phase we assessed the most promising doses and schedules of GEM and Nab-PTX on four different PDAC cell lines (BxPC-3 WT; MiaPaCa-2; PATU-8988T and sTRAIL resistant BxPC-3) to best represent the well-known PDAC tumor heterogeneity. The simultaneous co-treatment with 10μm of GEM + 1μm of Nab-PTX obtained the IC50 in BxPC-3 WT, MiaPaCa-2 and sTRAIL resistant BxPC-3 cell lines while for PATU8988T, characterized by marked chemo-resistance [176], IC50 dose was set on 10μm GEM + 10μm Nab-PTX. Then, to assess whether the anti-proliferative and cytotoxic impact displayed by GEM & Nab-PTX when used in combination could affect the AD-MSC sTRAIL viability, we evaluated the impact of pre-treatment with chemotherapeutics on AD MSC sTRAIL viability. Previously the effect of PTX alone or in combination with sTRAIL-containing supernatant was investigated on AD-MSC confirming a reduction of AD-MSC metabolic activity and proliferation with little impact on viability in both setting [176, 275]. The same group investigated also GEM effect on MSCs derived both from BM or from pancreas: MSC showed a very high resistance to GEM even at the highest concentration tested (100,000 ng/mL) with only 20-30%

reduction of cell viability [165]. We obtained the same results with GNP combination confirming in cell viability assay that after 24 h of co-treatment with GEM (10 μM) and Nab-PTX (1 μM), 69±2% of AD-MSC and 64±5% of AD-MSC sTRAIL were still viable and that after 48 hours activity remained higher than 40% (AD-MSC = 41%; AD-MSC sTRAIL = 45%) without compromising s-TRAIL release (693 ± 24 pg / ml), not inferior to previously reported data and from genetically modified AD-MSCs grown in standard culture media which ranges from 233 to 872 pg/ml (536±234 pg/ml) [176]. We hypothesized that the reduction of AD-MSC availability after 48 hours was probably due to a block in the AD-MSC replicative potential, due to the mechanism of action of both cytostatic agents, rather than apoptosis.

We confirmed the efficacy of the trio-combinatory approach testing GEM + Nab-PTX (with the previous chosen doses) and increasing concentration of sTRAIL (from 50 to 2500 pg/ml) in the previous mentioned different PDAC cell lines (BxPC-3 WT; MiaPaCa-2; PATU-8988T and sTRAIL resistant BxPC-3) in 2D and 3D in vitro models. Previously Elia et al reported cell death rate of 56.5% and 39.2% with GEM 100 μM and TRAIL at 100 ng/ml in BxPC3 and MiaPaCa-2 cells respectively [276]. In our experience in BxPC-3 WT and Mia Paca-2 cell lines, we obtained significant results with the combination of GEM (10 μM) and Nab-PTX (1 μM) + sTRAIL (50 pg/ml and 250 pg/ml respectively) compared to sTRAIL alone or GNP alone with cell death rate of almost 90%. In sTRAIL resistant BxPC-3 lines, in the same way as previously reported with the combination of Nab-PTX and sTRAIL [176], also the trio-combinatory approach was able to overcome sTRAIL resistance. For PATU-8988T cell line sTRAIL doses higher than 750 pg/ml combined with GEM and Nab-PTX induced a statistically significant reduction of cell viability compared to both sTRAIL and chemotherapeutics alone**.**

Our trio-combinatory approach aims to revert the well-known PDAC chemo-resistance targeting both PDAC cancer cells and stroma. Indeed, the cold and fibrotic tumor stroma is one of the main causes of systemic therapy failure [62]. Previous reports highlighted the intrinsic resistance of CAFs to both TRAIL mediated apoptosis and gemcitabine activity through SDF-1/SATB-1 pathway [277-279]. Conversely, Nab-PTX activity on tumor stroma enhances the intra-tumor concentration of GEM through increase in vascularization and inactivation of the cytidine deaminase, an enzyme involved in the catabolism of GEM [261, 263].

For the first time we hypothesized that the synergistic activity of GNP, in combination with AD-MSC sTRAIL, may induce cytotoxic effect not only on PDAC cancer cells but also on stromal elements since we demonstrated the GNP ability of reverting TRAIL resistance mechanisms and the high expression of TRAIL receptor DR5 on PDAC stroma [187, 195]. To confirm this suggestion, we evaluated the activity of the trio-combination on CAF populations isolated from 4 primary samples through enzymatic digestion. A significant cytotoxic effect of GNP was registered in all four stromal samples (> 60 % cell death) and, in particular, tumor priming with GNP remarkably enhances the sensitivity of PDAC cells to sTRAIL, leading to a significant synergistic antitumor effect in 3 out of 4 stromal samples.

This synergistic effect on both tumor and stromal cells was validated with VITVO 3D technology (Material and Methods). We were able to evaluate for the first time the trio-combinatory regimen efficacy in PDAC avatar: a 3D model generated to mimic PDAC TME by mixing malignant and primary stromal cells. We replicated the tumor/stroma ratio compartment that was observed by histological analysis on 50 surgical specimen of human PDAC samples previously conducted by Rigenerand and in accordance with a lot of previous reports (the amount of stroma in the tumor mass was 75%, approximately 45% composed by stromal elements and 30% by collagen fibers) [66, 268]. The efficacy of the trio-combo approach was confirmed on both sTRAIL sensitive lines (BxPC-3 WT) and sTRAIL resistant lines (BxPC-3 resistant and MiaPaCa-2 cells) even when co-cultured with primary PDAC stromal elements. In particular in BxPC-3 WT line + stromal cells we observed a tumor cell death rate of 95% at 48 and 72 h at both RR001 tested doses (1:10, 1:30) significantly higher than the one obtained by GNP or RR001 alone and not lower than previously reported data in VITVO for BxPC-3 WT cells alone. Also, in PDAC avatar generated using sTRAIL resistant BxPC-3 cell line and primary stromal cells (ID: PZ2 and PZ4), for each time point and dose tested, the cytotoxic effect displayed by GNP + RR001 (tumor cell mortality after 48h higher than 86±1% at the two tested doses) was significantly higher than the one obtained by GNP without any interference by stromal components.

For MiaPaca-2 avatar, the antitumor impact displayed by GEM + Nab-PTX + RR001 was always higher than the one obtained by GEM + Nab-PTX or RR001 alone, thus confirming the efficacy of the combinatory approach on MiaPaCa-2 cells even when co-cultured with primary PDAC stromal elements. We observed 2±1 % cell death after 24 and 48h, and 47±1 % after 72h for chemotherapy alone vs 70±5% in combination the

lowest dose of RR001 (1:30). The trio combo at the higher dose of RR001 (1:10) provoked an higher cytotoxic impact with 96±2% of PDAC cell death.

To confirm the preliminary in vitro results previously reported, we evaluated the effective dose of GEM + Nab-PTX and the animal toxicities of the trio combinatorial treatment in an orthotopic model of PDAC developed with MiaPaca2 cells injection in mice pancreatic tail (16 mice). We selected an orthotopic PDAC model because the implantation of PDAC cell subcutaneously or in other organ cannot simulate the pathophysiological and system-biological features of PDAC as well as the orthotopic models [280, 281].
We evaluated after 7 days from MiaPaca2 injection the effective tumor engraftment by BLI signal analysis and then we confirmed the efficacy of GEM - PTX treatment at both chosen concentrations ($p < 0,05$ with GEM 50 mg/kg + PTX 7.5 mg/kg; $p < 0,001$ with GEM 50 mg/kg + PTX 50 mg/kg). Treatments with GEM + PTX was performed intraperitoneally at day 14 and day 21 after MiaPaca2 injection. The antitumor effect in both treated groups was confirmed by histological analysis (by hematoxylin and eosin staining) obtaining compromised tumor architecture with loss of compactness in respect to control tumors. We reported no reduction of body weight due to possible toxic effects of chemotherapy nor tissue damage and inflammation in liver, spleen and kidney. In light of the results of this pivotal study, the regimen with PTX at the concentration of 7.5 mg/kg was chosen, because it displayed a good antitumor effect with low PTX dosage.
The next step was the addiction of RR001 to GEM 50 mg/kg + PTX 7.5 mg/kg in a large cohort of mice (61 mice). We selected an intratumoral (IT) injection approach based on previous report of gene therapy in gastrointestinal tumor [34, 282-284]. Recently Humbert et al reported that intra-tumoral injection of TLR9 agonist could convert an ‘immune cold’ into an ‘immune hot’ tumor and Bria et al revealed a potent antitumor activity of IT injection of IMO-2125 (Toll-like receptor 9 agonist) in combination with anti-PD1 in immunotherapy-resistant PDAC models through the modulation of immune microenvironment, fostered the interest for new combination strategies for the treatment of cold and immunotherapy refractory tumors [285, 286].
We observed that IT approach allowed a better integration of AD-MSC sTRAIL inside the TME compared to percutaneous injection. In addiction IT favors RR001 persistence and distribution in intra-tumoral area.
Treatments with GNP was performed intraperitoneally at day 14 and day 21 after MiaPaca2 injection. RR001 was administered IT by an eco-guided injection at day 22

and RR001 cells were labelled with the infrared fluorescent agent DiR in order to track their presence inside tumor. Tumor engraftment and cancer volumes were monitored over time by US imaging. At the last time-point before sacrifice, we confirmed that both GNP+RR001 1:10 and GNP+RR001 1:30 strategies obtained significant reduction of tumor volume compared to CTL group (CTL vs GNP+RR001 1:30 p=0.004; CTL vs GNP+RR001 1:10 p=0.0006) and RR001 1:10 alone group (RR001 1:10 vs GNP+RR001 1:30 p=0.001; RR001 1:10 vs GNP+RR001 1:10 p=0.00009). We confirmed this cytotoxic effect also in histological analyses after sacrifice. Tumors of the control group were extremely compact highlighting the presence of high fibrotic stroma. Conversely, tumor from GNP + RR001 groups displayed higher level of tissue degeneration associated with significative lower amount of Ki67 positive cells in respect to RR001 alone group.

At sacrifice unexpectedly, GNP group displayed the highest number of mice with liver metastases (80% of cases) even more than the control group (38%). Recently the same suggestion was reported in a retrospective analysis on 44 borderline PDAC treated with GEM-Nab-PTX regimen in neoadjuvant setting. The authors revealed that low stromal ratio induced by neoadjuvant chemotherapy promoted early liver metastasis in patients with borderline PDAC provided new insights into the complexity of stromal biology [287]. A significative lower incidence of metastasis was detected in all the groups treated with RR001 compared to GNP treatment and this effect was particularly relevant in group treated with the combinatorial regimen GNP + RR001 1:10 (9%) (p=0.005).

We evaluated RR001 biodistribution using labelled fluorescent agent DiR and the IVIS imaging system: AD-MSC sTRAIL stably persisted into the PDAC xenograft with no evidence of fluorescence in other tissues. This report confirmed previous works from Yaochitel et al and Murai et al in mice: after intrapancreatic injection of AD-MSC or BM-MSC, there was no evidence of extrapancreatic MSC diffusion. These data confirmed the feasibility and the efficacy of the intrapancreatic administration of RR001 [288, 289].

The safety profile of our trio-combinatory approach was the same as our previous experience with AD-MSC sTRAIL + Nab-PTX [176]. No differences in body weight were observed between treated groups, including mice treated with GNP+RR001, and control group. Tissue lesions could not be observed in any of the evaluated organs after the treatment with GNP, RR001, or the combination of them (at both E:T ratios) in vivo.

The last step of my research was the design of a phase I trial. Firstly, we evaluated the clinical dosage of RR001. RR001 significantly differs from rhTRAIL (rhApo2L/TRAIL, Amgen) previously tested into clinics: sTRAIL is a multimeric molecule and secondary, in RR001 sTRAIL is released by autologous human cells. In a phase I study involving 71 patients with advanced or metastatic solid tumors or lymphoma, rhApo2L/TRAIL treatment appeared safe and well tolerated at doses up to 30 mg/kg daily for 5 days every 3 weeks. Adverse events were mostly mild and readily managed with supportive care and/or symptomatic treatment [290]. More recently multiple myeloma subjects were treated daily with a new multimeric TRAIL variant (2.5 mg/kg, intravenously) during 14 consecutive days of each 21-day cycle for 2 cycles with manageable treatment-related adverse events, including a reversible liver toxicity [291].

With all these and other assumptions we designed a phase I/IIa trial in LAPC aim to determine the safety, feasibility and dose finding of intra-tumoral injection of RR001 administered by ultrasound (US) guided injections in combination with standard of care therapy GNP. Secondly the trial will explore the efficacy of this combination (radiological or histological for operated patients) researching liquid and tissue predictive biomarkers: the levels of sTRAIL, tumor/stromal ratio and lymphocytes infiltration before and after RR001 in histological specimens.

6 FIGURES

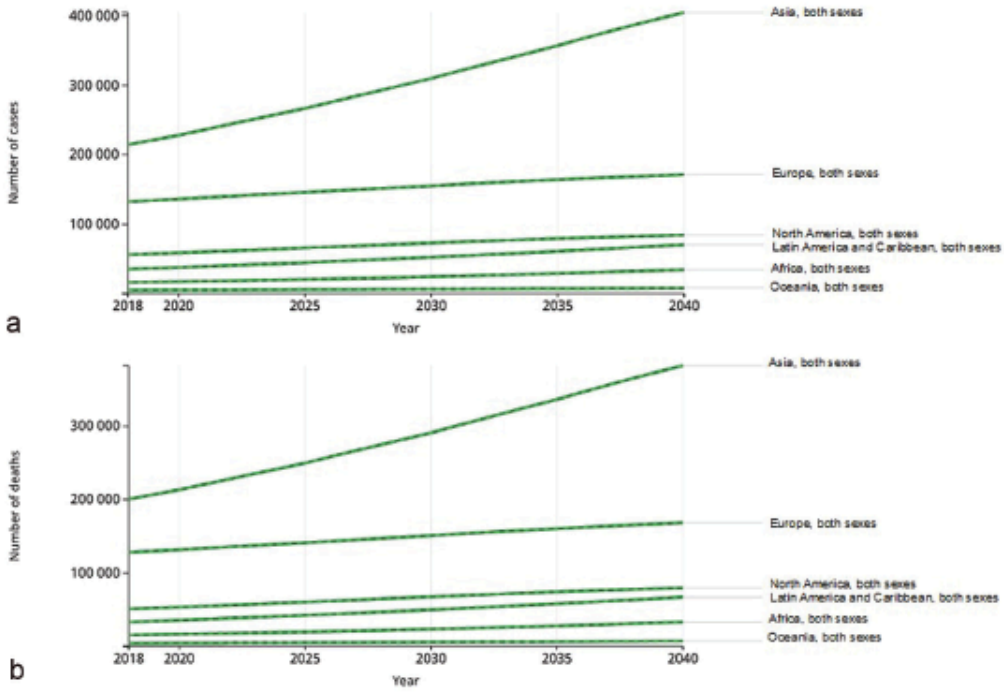

***Figure 1*. Trends in pancreatic cancer incidence and mortality predicted for the years 2018 to 2040. Adapted from [1]**

Figure 2. **Molecular classes and transcriptional networks defining PDAC**.

a, Unsupervised analysis of RNA-seq identified 4 PDAC classes: squamous (blue); ADEX (abnormally differentiated endocrine exocrine; brown); pancreatic progenitor (yellow); and immunogenic (red). Adapted from [13]

Resectable: R	• SMV/PV: no tumor contact or unilateral narrowing • SMA, CA, CHA: no tumor contact
Borderline resectable: BR	Subclassified according to SMV/PV involvement alone or arterial invasion.
BR-PV (SMV/PV involvement alone)	• SMV/PV: tumor contact 180° or greater or bilateral narrowing/occlusion, not exceeding the inferior border of the duodenum. • SMA, CA, CHA: no tumor contact/invasion
BR-A (arterial involvement)	• SMA, CA: tumor contact of less than 180° without showing deformity/stenosis. • CHA: tumor contact without showing tumor contact of the PHA and/or CA. (The involvement of the aorta is categorized as unresectable. Presence of variant arterial anatomy is not taken into consideration)
Unresectable: UR	Subclassified according to the status of distant metastasis
Locally advanced: LA	• SMV/PV: bilateral narrowing/occlusion, exceeding the inferior border of the duodenum. • SMA, CA: tumor contact/invasion of 180 or more degree#. • CHA: tumor contact/invasion showing tumor contact/invasion of the PHA and/or CA. • AO: tumor contact or invasion
Metastatic: M	• Distant metastasis $.

SMV: superior mesenteric vein, PV: portal vein, SMA: superior mesenteric artery, CA: celiac artery, CHA: common hepatic artery, PHA: proper hepatic artery, #: In the cases with CA invasion of 180° or more without involvement of the aorta and with intact and uninvolved gastroduodenal artery thereby permitting a distal pancreatectomy with enbloc celiac axis resection (DP-CAR) [21], some members prefer this criteria to be in the BR-A category. $: including macroscopic para aortic and extra abdominal lymph node metastasis.

Figure 3. **International consensus of classification of PDAC resecability [25]**

Study	Phase	Clinical indication	Treatment				End-points
			Strategy	Vector	Route	Combined therapy	Results/side effects
	I	PDAC	Immunotherapy	Allogeneic lymphocytes	IT injection (EUS)	None	No major complications and the median survival was 13.2 months with two partial responders and one minor response.
	I/II	Metastatic PDAC	Gene Therapy Suicide Gene (Cytochrome P450)	Transfected allogeneic human 293 kidney cells	IT injection	In combination with low-dose ifosfamide	Tumor regression/stabilization Median survival doubled
	I	PDAC	Gene Therapy	ONYX-015 (Replication-Selective Adenovirus)	IT injection (EUS)	In combination with GEM	No clinical pancreatitis occurred despite mild, transient elevations in lipase levels in a minority of patients. No side effects via transgastric delivery.
	I	PDAC	Gene Therapy Immunotherapy (TNFalpha)	2nd generation adenovector carrying the transgene	IT injection (EUS)	In combination with 5-Fluorouracil and radiotherapy	Mild side effect; well tolerated treatment; locoregional control of treated tumors; longer progression free survival
	I	Liver cancer, **PDAC**, colorectal cancer	Gene therapy Immunotherapy (IL-12)	Adenovirally Transfected autologous dendritic cells	IT injection (US, EUS and CT-guided)	None	Well tolerated treatment; progression in most patients. Partial response
(Hiroka et al. 2018)[i] [34]	I	LAPC PDAC	Gene Therapy	HF10 oncolytic virus	IT injection (EUS)	In combination with GEM and Erlotinib	Well tolerared, 5 patients (out of 9) with grade III myelosuppression and hepatic dysfunction. 2 patients reach complete response
(Barton et al. 2020)[284]	I	Metastatic PDAC	double-suicide gene therapy (yCD/mutTK) + IL-12	2nd generation adenovector carrying the transgene	IT injection (EUS)	In combination with FOLFIRINOX or GEM/nabPTX	Well tolerated, no DLT reached (12 patients)
(Lee et al. 2020)[33]	I	LAPC PDAC	double-suicide gene therapy (yCD/mutTK)	Adenovirus	IT injection (EUS)	In combination with GEM	Well tolerated; one patient showed a partial response and 8 showed stable disease at 12 weeks (9 total)

***Table 1*. Major published cell and gene therapy clinical studies with intra-tumor delivery against PDAC** -

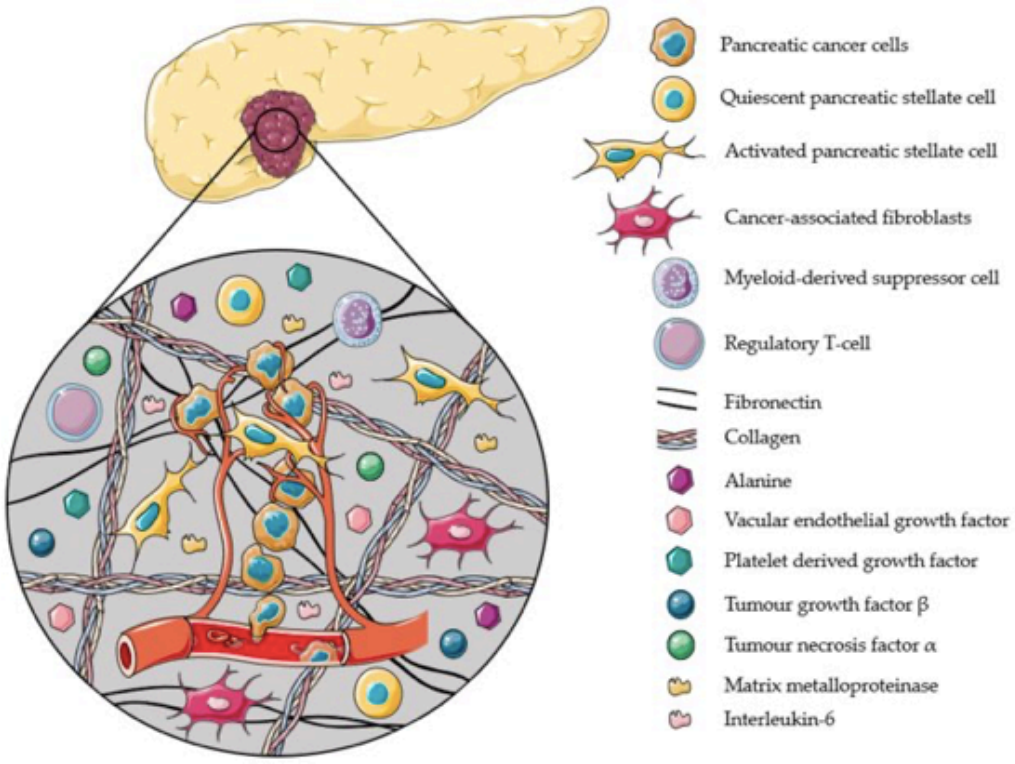

Figure 4. **Composition of pancreatic stroma. Adapted from [63]**

Schematic representation of the TME of PDAC and its dense desmoplastic stroma. Pancreatic stellate cells (PSCs), as main type of cancer-associated fibroblasts in this case, account for nearly 50% of the total stroma and are typically activated in PDAC. PSCs recruit immunosuppressive cells (e.g., MDSC and T-reg) and secrete extracellular matrix molecules (e.g., collagen and fibronectin), immunosuppressive (e.g., TGF-β) and inflammatory (e.g., IL-6 and TNF-α) cytokines, pro-angiogenic factors (e.g., VEGF), matrix metalloproteinases (e.g., MMP-2 and MMP-9), growth factors (e.g., PDGF), and non-essential amino acids (e.g., alanine). The complexity of this TME due to PSCs causes PDAC to acquire crucial properties like rapid growth, high invasion and metastatic potential, survival in hypoxic and low-nutrient conditions, and resistance to therapy.

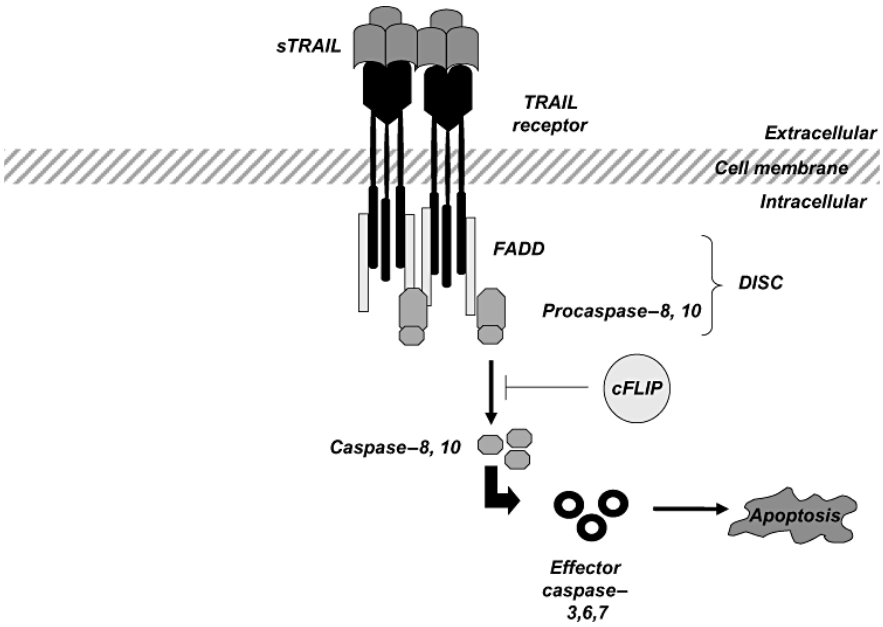

***Figure 5*. TRAIL as pivotal anti-cancer mechanism. Adapted from [192].**

TRAIL binds to five receptors, including four membrane-bound receptors (i.e., DR4, DR5, TRAIL-R3, and TRAIL-R4) and one soluble receptor (OPG). Only binding to DR4 or DR5 results in receptor trimerization and recruitment of FADD via the DDs of DR4 or DR5. After further recruitment of caspase-8, these proteins form a complex named DISC, which can activate caspase-8. In type I cells, caspase-8 activates caspase-3 and triggers apoptosis via the extrinsic pathway. However, in type II cells, the intrinsic pathway is triggered via caspase-8/BID/ tBID, and consequently, BAX/BAK on the mitochondrial membrane is activated to induce the release of cytochrome c, which promotes the formation of the apoptosome with APAF1 and procaspase-9. Subsequently, activation of caspase-9 and caspase-3 is induced.

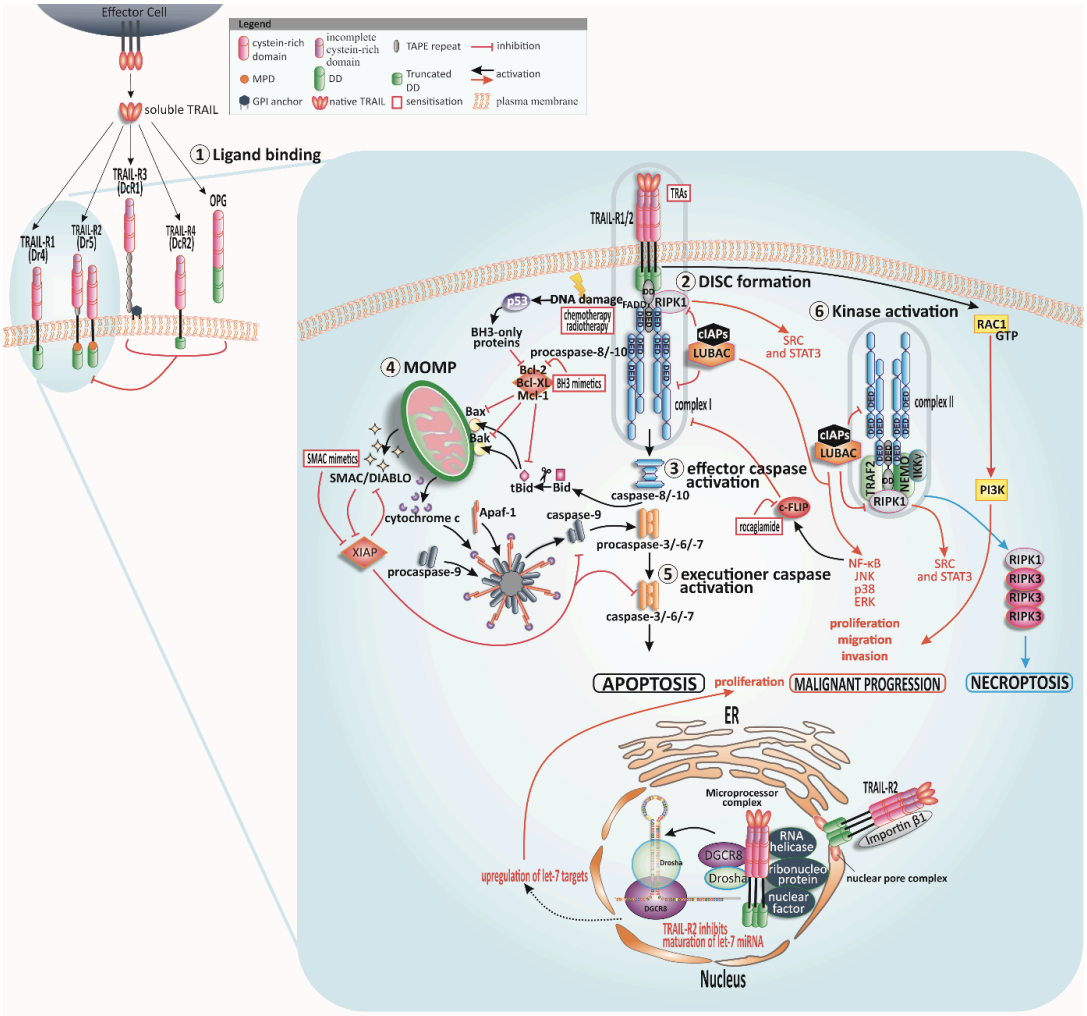

Figure 6. **TRAIL extrinsic and intrinsic apoptosis pathways. Adapted from [210]**

TRAIL can bind to four membrane-bound TRAIL receptors (TRAIL-Rs) and one soluble receptor ①. Following TRAIL binding to TRAIL-R1 or TRAIL-R2, the death-inducing signalling complex (DISC) is assembled ②. In type I cells, the signal of DISC-released caspase-8 is sufficient for activation of further downstream caspases and apoptosis induction ③, whereas the DISC signal is amplified via mitochondria in type II cells ④. Cleaved and thereby truncated Bid (tBid) activates the mitochondria-associated B-cell CLL/lymphoma 2 (Bcl-2)-family members Bcl-2-associated X protein (Bax) and Bcl-2 antagonist or killer (Bak) resulting in mitochondrial outer membrane permeabilisation (MOMP) and finally cytochrome c and second mitochondrial activator of caspases/direct inhibitor of apoptosis-binding protein with low isoelectric point (pI) (SMAC/DIABLO) release. The apoptosome comprising apoptotic protease activating factor-1 (Apaf-1), cytochrome c, and caspase-9, presents the activation platform for caspase-9 which leads

eventually to the activation of executioner caspases ⑤. p53 is activated in response to stress signals such as DNA damage and promotes Bcl-2 homology (BH)3-only proteins resulting in MOMP. TRAIL-receptor-interaction can provoke the formation of a second cytosolic complex ⑥, retaining Fas-associated protein with death domain (FADD) and caspase-8 and recruiting receptor-interacting serine/threonine-protein kinase 1 (RIPK1), TNF receptor-associated factor 2 (TRAF2), and nuclear factor kappa-light-chain-enhancer of activated B cells (NF-κB) essential modifier (NEMO) TRAF2 recruits cellular inhibitor of apoptosis protein 1/2 (cIAP1/2) which in turn trigger the ubiquitination of RIPK1 and therefore recruitment of linear ubiquitin chain assembly complex (LUBAC). LUBAC poly-ubiquitinylates RIPK1. RIPK1 is the stimulus for tyrosine-protein kinase Src and signal transducer and activator of transcription 3 (STAT3) promoting migration and invasion. Complex I and complex II induce NF-κB, p38 mitogen-activated protein kinase (p38 MAPK), c-JUN N-terminal kinase (JNK) and extracellular signal-regulated kinase (ERK) pathways. LUBAC is present in both complexes, responsible for caspase-8 activation and recruitment of the inhibitor of κB (IκB) kinase (IKK) complex, and consequently activation of NF-κB. In case of blocked caspase-8, the necrosome is formed by the interaction of RIPK1 and RIPK3. Independently of FADD and complex I and II, the membrane-proximal domain (MPD) of TRAIL-R2 can activate Ras-related C3 botulinum toxin substrate 1 (Rac1) to promote migration and invasion. TRAIL-R2 can also occur in the nucleus where it interacts with ribonucleoprotein complexes involved in the maturation of microRNAs (miRNAs) of the let-7 family. These miRNAs interact with and constrain mRNAs of several regulators of mitogenic pathways such as Ras and c-Myc thereby encouraging proliferation of tumour cells.

Cancer type	Intervention	Dosage	Outcome	Phase (Status)	Reference
Soluble recombinant human TRAIL (rhTRAIL)/Dulanermin					
Advanced cancer	Soluble recombinant human Apo2L/TRAIL (rhTRAIL)	0.5-30 mg/kg/d intravenously (IV) on days 1 to 5 of each 21-day cycle	rhTRAIL was safe and well tolerated; dose escalation up to serum concentrations on par with preclinical anti-tumor efficacy	I (Ongoing as of 2010)	(Herbst et al., 2010a)
Stage IV non-small-cell lung cancer (NSCLC)	Recombinant human Apo-2 ligand (Injection)	150 µg/kg/d IV, on days 1 to 7 of each 21-day cycle	(Ongoing)	III (Active, not recruiting)	*NCT03083743
In combination with the potential sensitizer(s)					
Advanced NSCLC (with no prior treatment)	Combination of rhTRAIL with paclitaxel, carboplatin and bevacizumab (PCB)	Paclitaxel, carboplatin (IV), and bevacizumab (IV) on day 1 followed by 4 or 8 mg/kg/d dulanermin (IV) for 5 days or 20 mg/kg/d dulanermin (IV) for 2 days of each 21-day cycle	Well tolerated with no increase in toxicity; overall response rate was 58%; the median progression-free survival (PFS) time was 7.2 months	Ib (Ongoing with long term follow-up as of 2008)	(Soria et al., 2010)
Follicular and low-grade $CD20^+$, B-cell Non-Hodgkin's Lymphoma (NHL)	Combination of dulanermin with rituximab	4 or 8 mg/kg/d dulanermin (IV) on days 1 to 5 of each 21-day cycle; 375 mg/m^2 rituximab (IV) weekly for up to 8 doses	Improved PFS with combination therapy (17.9 months) compared to dulanermin alone (6.9 months)	Ib, II (Terminated with results)	*NCT00400764
Advanced NSCLC	Combination of dulanermin with paclitaxel and carboplatin (PC) and bevacizumab (PCB)	PC (IV) with dulanermin 8 mg/kg/d for 5 days (Squamous NSCLC); PCB (IV) with dulanermin 8 mg/kg/d for 5 days or 20 mg/kg/d for 2 days (Nonsquamous NSCLC)	Grade ≥3 adverse events were common; elevated caspase-cleaved cytokeratin-18 after dulanermin treatment; did not improve patient outcomes.	II (Ongoing as of 2009)	(Soria et al., 2011)
Stage IIIb to IV NSCLC	Combination of dulanermin with vinorelbine and cisplatin	Vinorelbine (25 mg/m^2) (IV) on days 1 and 8; cisplatin (30 mg/m^2) (IV) on days 2 to 4 for up to six cycles plus dulanermin (75 µg/kg) (IV) on days 1 to 14 in every 21 days	Significantly improved PFS and objective response rate (ORR); similar adverse events AE profile across placebo and treatment	III (Completed in 2012)	(Ouyang et al., 2017)
Locally advanced, recurrent, or metastatic colorectal cancer	Dulanermin administered in combination with the FOLFOX regimen and bevacizumab	Drug: FOLFOX regimen IV repeating dose (Dose not stated) Drug: bevacizumab IV repeating dose (Dose not stated) Drug: dulanermin IV repeating dose (Dose not stated)	No results posted	1 (Completed in 2014)	*NCT00873756

Table 2. **Published clinical trials using rhTRAIL/Apo2L alone or in combination with chemotherapy. Adapted from [189]**

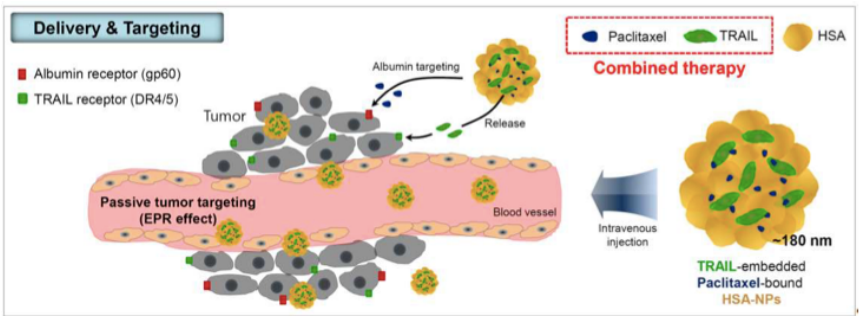

Figure 7. **Activity of TRAIL/PTX. Adapted from [225]**

One-pot/one-step formulation of paclitaxel (PTX)-bound albumin nanoparticles with embedded tumor necrosis factor-related apoptosis-inducing ligand (TRAIL/PTX HSA-NP) for the treatment of pancreatic cancer.

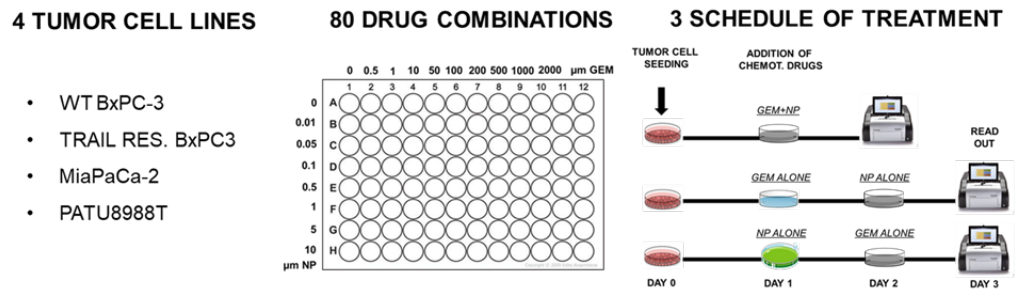

***Figure 8*. Experimental layout of drug combination assay to identify the combination index, the most synergistic doses and the schedules for GEM and Nab-PTX.**

PDAC CELL LINE	SCHEDULE OF TREATMENT	IC50 GEMCITABINE + Nab-PTX DOSE
BxPC-3	CO-TREATMENT	10 µM GEM+ 1 µM Nab-PTX
MIAPaCa-2	CO-TREATMENT	10 µM GEM+ 1 µM Nab-PTX
PATU8988T	CO-TREATMENT	10 µM GEM+ 10 µM Nab-PTX
BxPC-3 TRAIL RESISTANT	CO-TREATMENT	10 µM GEM+ 1 µM Nab-PTX

***Table 3*. Schedule of treatment and dose of drug combination for BxPC-3 WT, MIA PaCa-2 and sTRAIL resistant BxPC-3.**

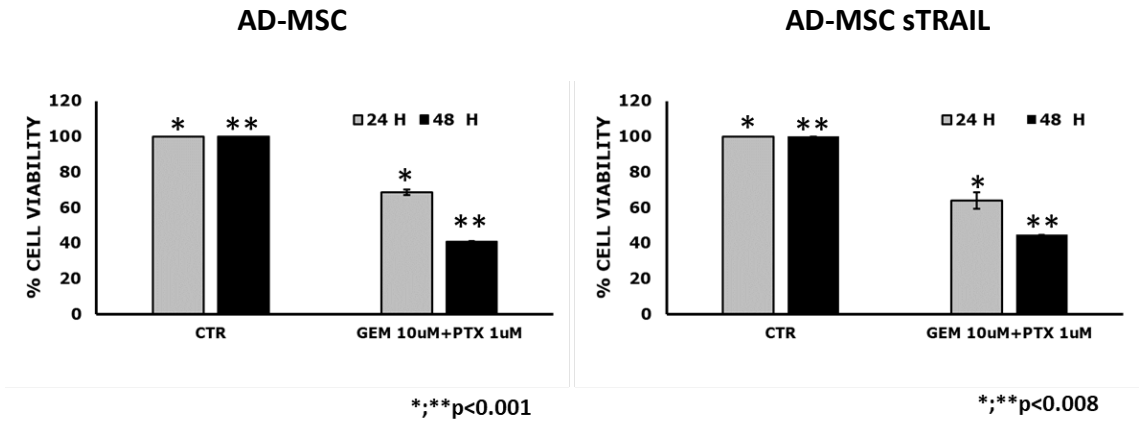

***Figure 9*. Cell viability assay on AD-MSCs sTRAIL and AD-MSCs wild type treated with GEM+Nab-PTX.**

Cell viability assay showed that after 24 h of co-treatment with GEM (10 µM) and Nab-PTX (1 µM), 69±2% of AD-MSCs and 64±5% of AD-MSCs sTRAIL were still viable. At 48 hours a slight reduction in metabolic activity of both cell types was observed but however activity remained higher than 40% (AD-MSC = 41%; AD-MSC sTRAIL = 45%).

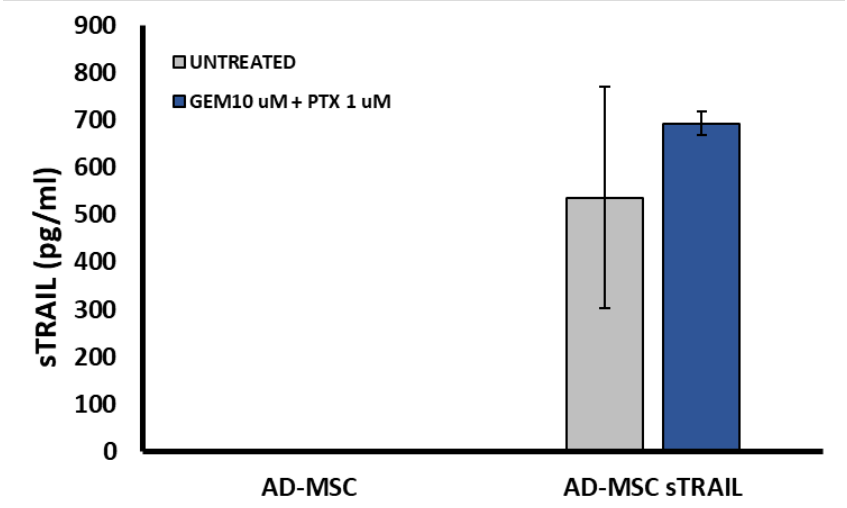

***Figure 10*. Quantification by ELISA of engineered AD-MSCs sTRAIL release before and after the treatment with GEM + Nab-PTX. EV AD-MSC sTRAIL production was under detection limit (UDL).**

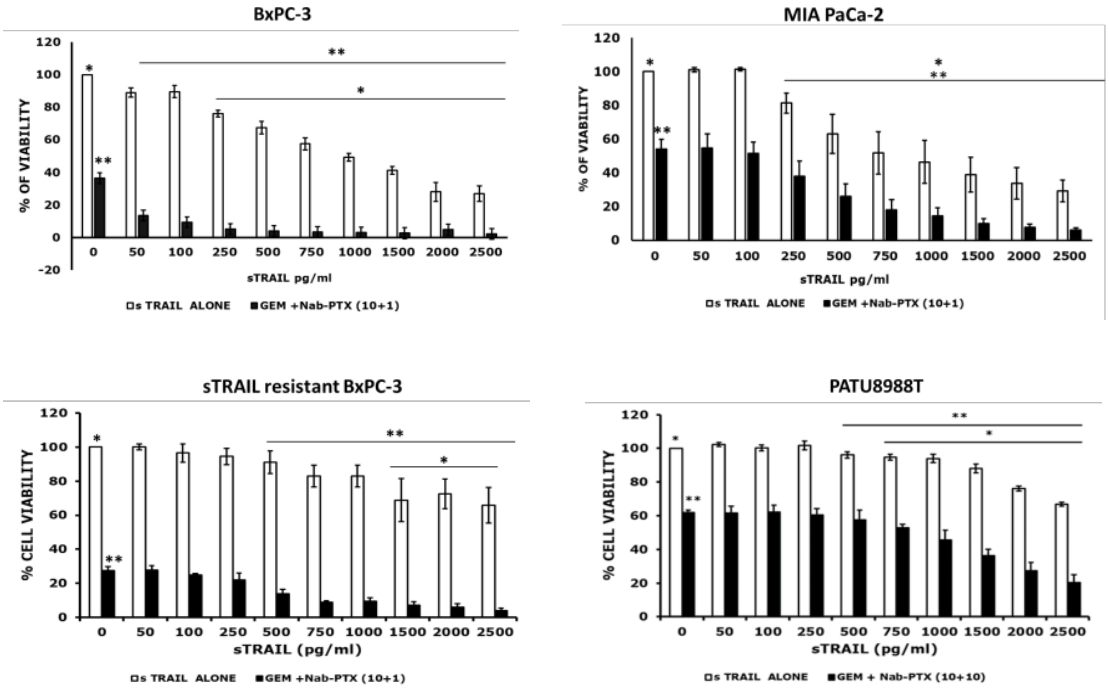

Figure 11. **Gemcitabine + Nab-Paclitaxel synergize with RR001 to induce apoptosis on PDAC cells.**

Cytotoxicity assay performed by Cell Titer AQueous96 One Solution Cell Proliferation assay (Promega) on BxPC-3, MIA PaCA-2, sTRAIL resistant BxPC-3 and PATU-8988T. BxPC-3, MIA PaCA-2, sTRAIL resistant BxPC-3 and PATU-8988T were pre-treated with GEM (10 µM) and Nab-PTX (1 µM or 10 µM for PATU) for 24 h and subsequently treated for further 24 h with conditioned media collected from RR001 and containing from 50 to 2500 pg/ml sTRAIL respectively. (** $p<0.05$ and * $p<0.02$).

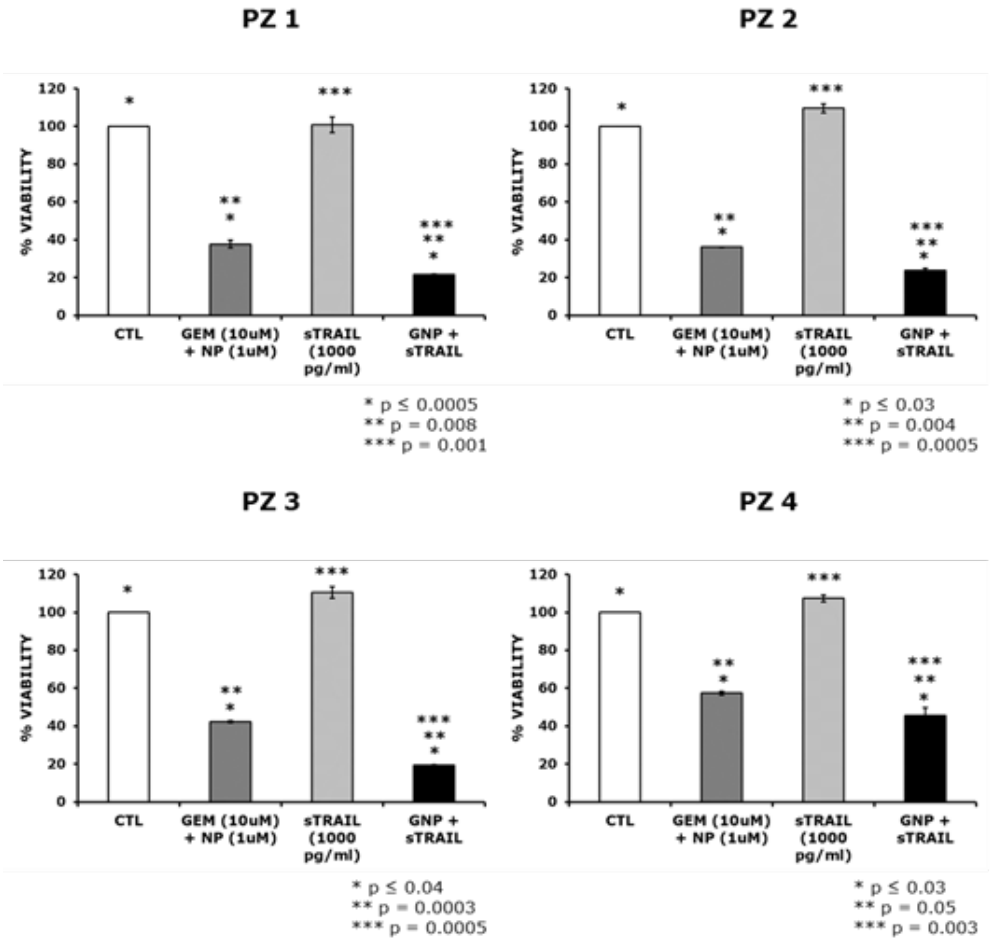

Figure 12. **Gemcitabine + Nab-Paclitaxel and RR001 cooperate to induce cell apoptosis in primary PDAC stromal cells.**

Stromal cells obtained from four PDAC samples (ID:PZ1-PZ4) were treated with GEM (10 μM) and Nab-PTX (1 μM) for 24 h and further 24h in co-treatment with RR001 (1000 pg/ml). Culture media alone (CTL), GEM + Nab-PTX alone or RR001 alone were used as control. P value by T test.

	TRAIL RECEPTORS EXPRESSION				SENSITIVITY TO TREATMENTS (IC50 in 2D)		
PDAC CELL LINE	DR4	DR5	DcR1	DcR2	sTRAIL	GEM	Nab-PTX
BxPC-3 WT	+	+++	ND	ND	**HIGH** (IC50:250 pg/ml)	**HIGH** (IC50:0.5 μM)	**HGH** (IC50: 0.5 μM)
MiaPaCa-2	+	+++	ND	+	**MODERATE** (IC50:500 pg/ml)	**RESISTANT** (IC50>2000 μM)	**HIGH** (IC50:0.1 μM)
PATU-8988T	+++	+++	ND	++	**RESISTANT** (IC50>2500 pg/ml)	**MODERATE** (IC50>50 μM)	**MODERATE** (IC50:10 μM)
BxPC-3 sTRAIL RESISTANT	+	+++	ND	ND	**RESISTANT** (IC50>2500 pg/ml)	**MODERATE** (IC50>1 μM)	**RESISTANT** (IC50>10 μM)

***Table 4*. Levels of TRAIL receptors and sensitivity to treatments in four different PDAC cell lines TRAIL receptors expression.**

Not detectable (nd); <20% (+); 20%<x<60% (++); >60% (+++). Sensitivity to sTRAIL (conditioned medium collected from AD-MSCs sTRAIL): IC50 ≤500 pg/ml (high); IC50≥ 500 pg/ml (moderate); IC50≥ 500 pg/ml (resistant). Sensitivity to GEM: IC50 ≤0.5 μM (high); IC50≥ 1 μM (moderate); IC50≥ 2000 μM (resistant). Sensitivity to Nab-PTX: IC50 ≤0.1 μM (high); IC50≤10 μM (moderate); IC50 >10μM (resistant).

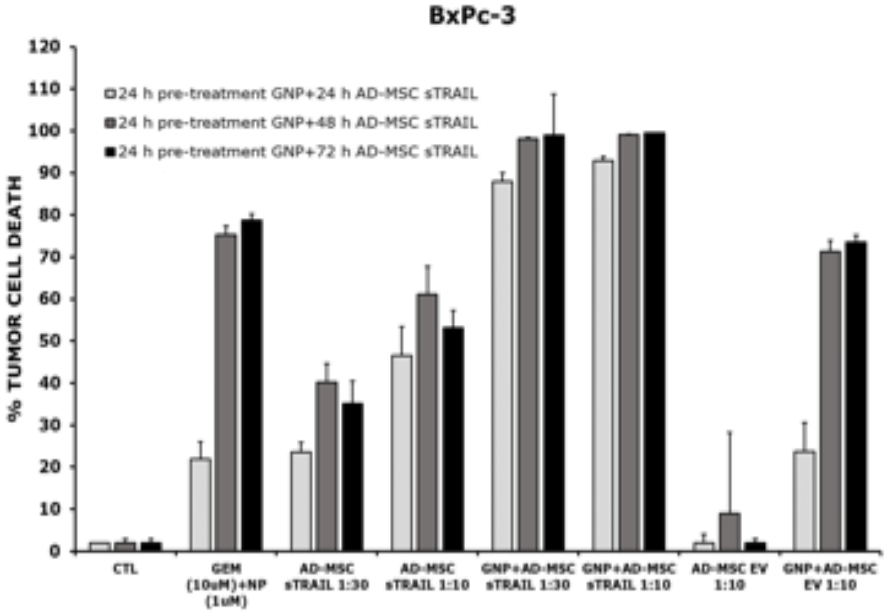

p<0.01

***Figure 13*. BxPC-3 WT cell death induced by GEM + Nab-PTX + RR001 analysed by 3D assays.**

AD-MSCs sTRAIL were co-cultured with tumor cells (TC), pre-treated or not with Gem+Nab-PTX (GNP), in the 3D system at different ratios (1:10 and 1:30). Culture medium (CTL) and AD-MSCs EV at 1:10 ratio were used as negative control. P values by t-test.

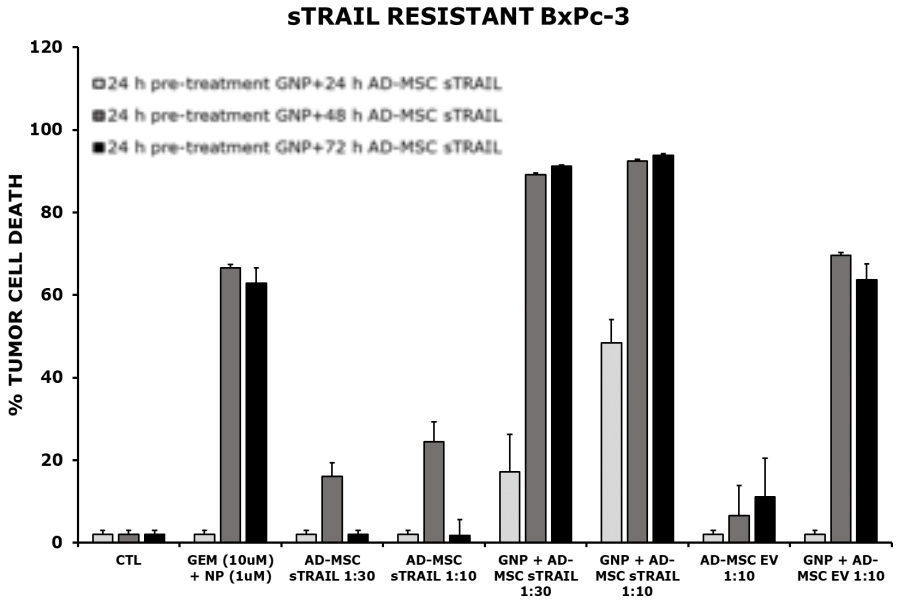

p<0.05

***Figure 14*. sTRAIL resistant BxPC-3 cell death induced by GEM + Nab-PTX + RR001 analysed by 3D assays.**

AD-MSCs sTRAIL were co-cultured with tumor cells (TC), pre-treated or not with GEM + Nab-PTX (GNP), in the 3D system at different ratios (1:10 and 1:30). Culture medium (CTL) and AD-MSCs EV at 1:10 ratio were used as negative control. P values by t-test.

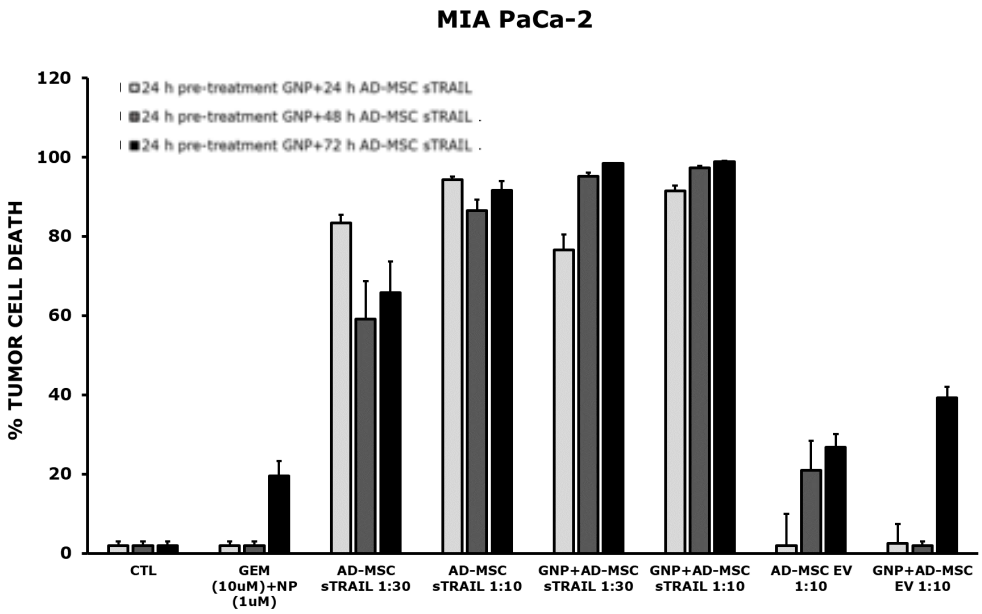

p<0.03

***Figure 15*. MiaPaca-2 cell death induced by GEM+Nab-PTX+RR001 analysed by 3D assays.**

AD-MSCs sTRAIL were co-cultured with tumor cells (TC), pre-treated or not with GEM + Nab-PTX (GNP), in the 3D system at different ratios (1:10 and 1:30). Culture medium (CTL) and AD-MSC EV at 1:10 ratio were used as negative control. P values by t-test.

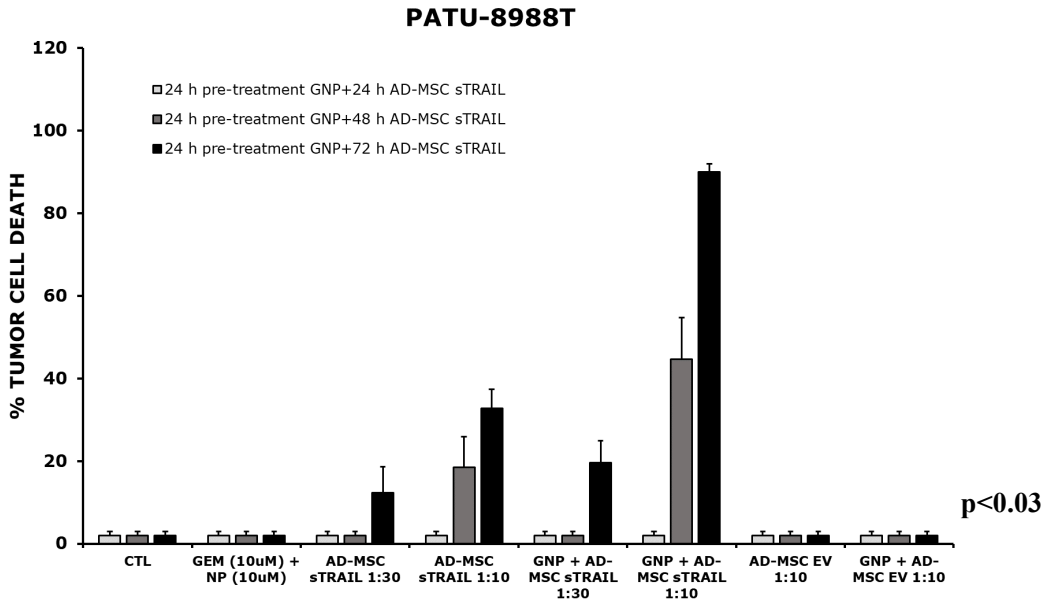

***Figure 16*. PATU-8988T cell death induced by GEM+Nab-PTX+RR001 analysed by 3D assays.**

AD-MSCs sTRAIL were co-cultured with tumor cells (TC), pre-treated or not with GEM + Nab-PTX, in the 3D system at different ratios (1:10 and 1:30). Culture medium (CTL) and AD-MSC EV at 1:10 ratio were used as negative control. P values by t-test.

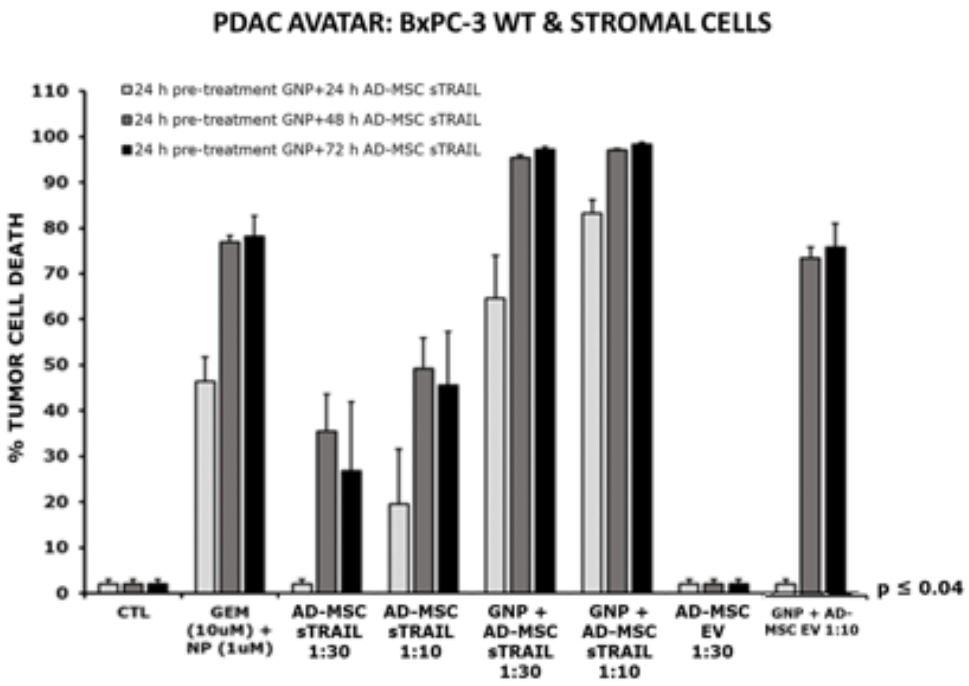

***Figure 17*. BxPC-3 WT cell death induced by GEM + Nab-PTX + RR001 analyzed by 3D assays involving stromal compartment .**

BxPC-3 mixed with stromal cells were loaded into the 3D system and pre-treated or not with GEM + Nab-PTX for 24h. AD-MSCs sTRAIL were then added at different ratios (1:10 and 1:30) calculated considering the amount of tumor cell only. Culture medium (CTL) and AD-MSCs EV at 1:10 ratio were used as negative control. P values by t-test.

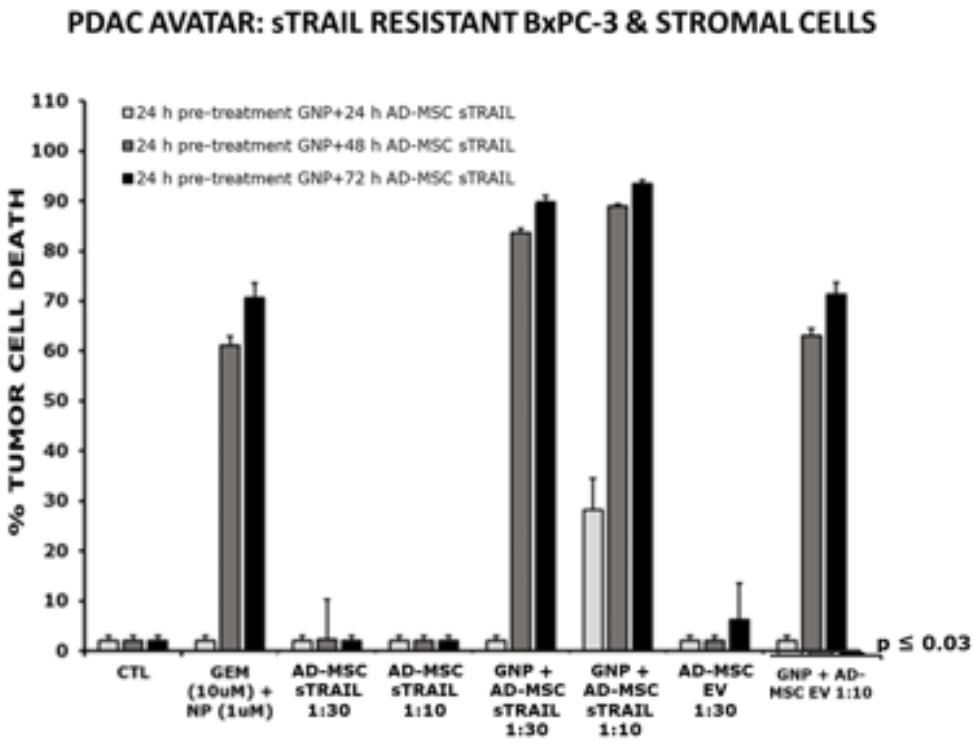

***Figure 18*. sTRAIL resistant BxPC-3 cell death induced by GEM+Nab-PTX+RR001 analysed by 3D assays involving stromal compartment (45%).**

sTRAIL resistant BxPC-3 mixed with stromal cells were loaded into the 3D and pre-treated or not with Gem + Nab-PTX for 24h. AD-MSCs sTRAIL were then added at different ratios (1:10 and 1:30) calculated considering the amount of tumor cell only. Culture medium (CTL) and AD-MSCs EV at 1:10 ratio were used as negative control. P values by t-test.

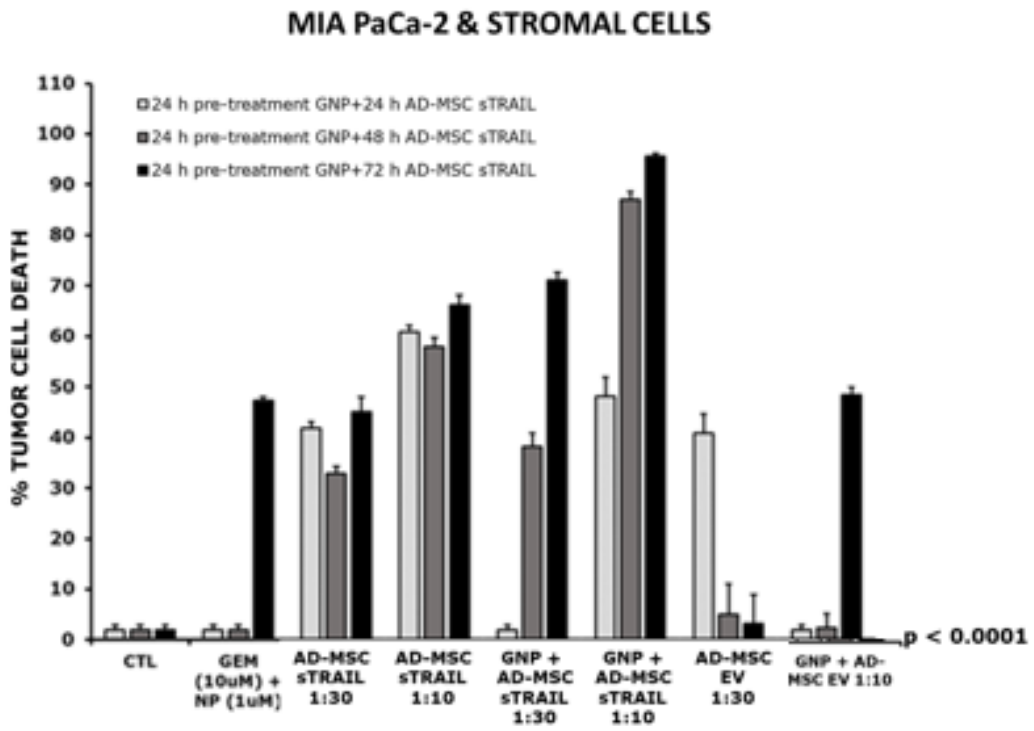

***Figure 19*. MIA PACA-2 cell death induced by GEM + Nab-PTX/RR001 analyzed by 3D assays involving stromal compartment.**

MIA PACA-2 mixed with stromal cells were loaded into the 3D system and pre-treated or not with GEM + Nab-PTX for 24h. AD-MSCs sTRAIL were then added at different E:T ratios (1:10 and 1:30) calculated considering the amount of tumor cell only. Culture medium (CTL) and AD-MSCs EMPTY at 1:10 ratio were used as negative control. P values by t-test.

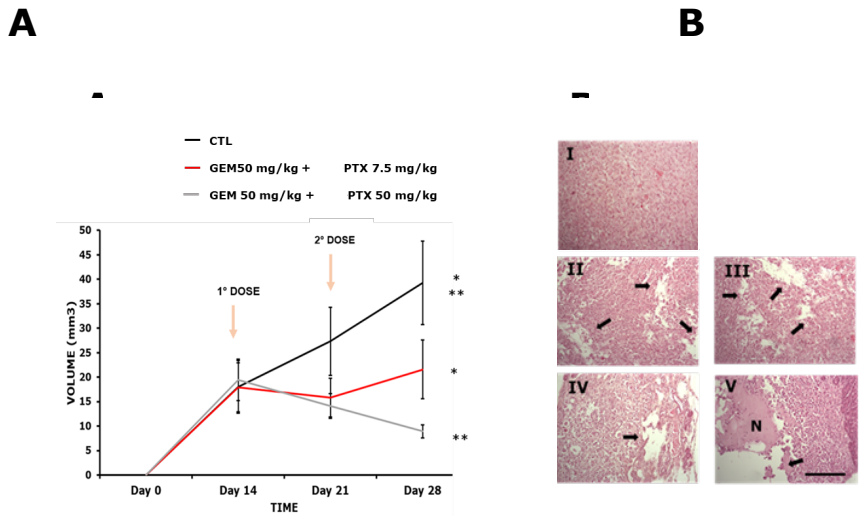

***Figure 20*. Change of tumor volume over time and histological analysis.**

A. Tumor volume was measured through US scans from the day of tumor implant to the day of sacrifice. Treated groups showed a significant reduction of tumor volume compared to the control group. T test at 28 days, *p<0.05; **p<0.001. **B.** Histological analysis of intrapancreatic tumors by hematoxylin and eosin staining: I, CTL; II-III, GEM 50 mg/kg+PTX 7.5 mg/kg; IV-V, GEM 50 mg/kg+PTX 50 mg/kg. Black arrows indicate areas with loss of compactness, N indicates a necrotic area. Magnification 100X, scale bar 200 um.

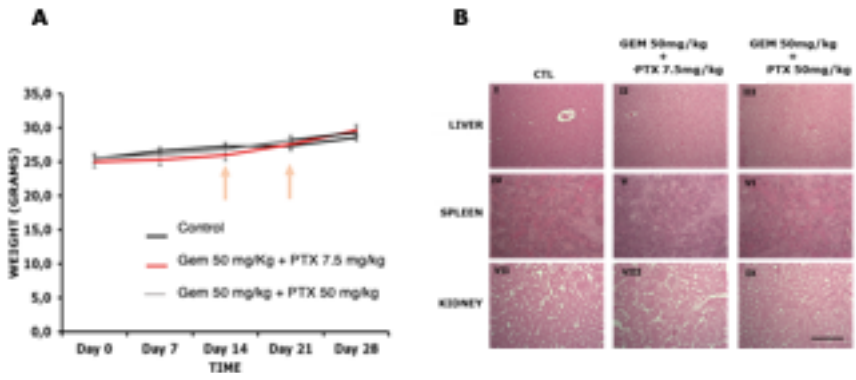

***Figure 21*. Safety profile of GEM + Nab-PTX treatment in orthotopic PDAC mouse model.**

A. Mice body weight measurement. No reduction in body weight was observed for all treated groups in respect to control. **B.** Histological analysis by hematoxylin and eosin staining of liver, spleen and kidney of mice treated with GEM + Nab-PTX. No toxicity was observed in any treated group in respect to control group. Magnification 100X, scale bar 200 um.

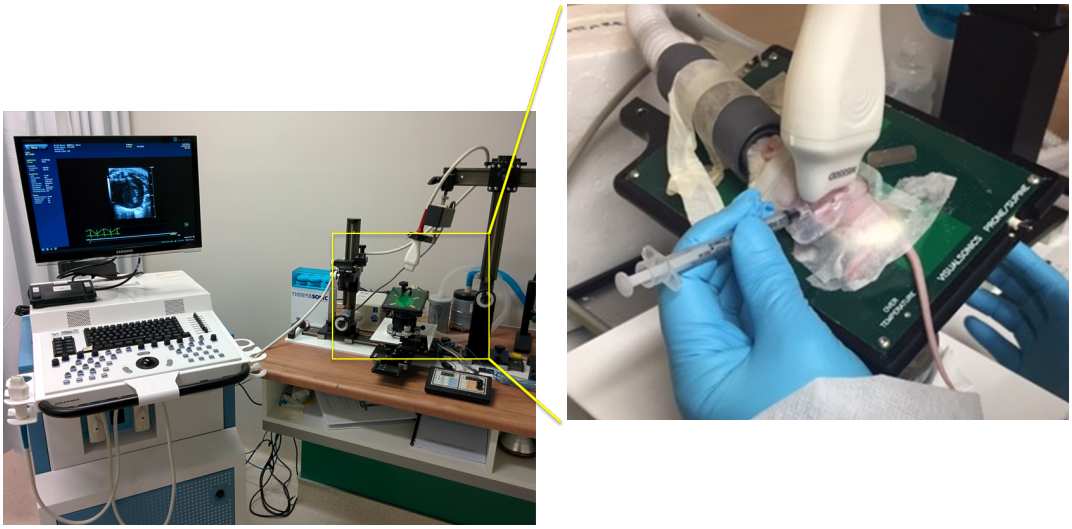

B

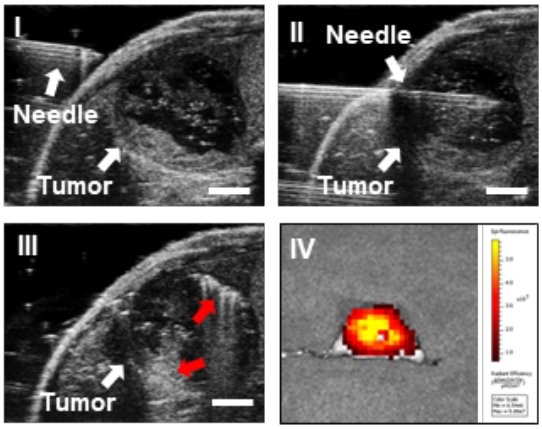

***Figure 22*: US guided intratumoral RR001 injections.**

A. VisualSonics Vevo® 2100 Imaging System. Inset image shows the moment of intratumor MSCs sTRAIL administration by eco-guided system. **B**. Representative images of MSC s TRAIL ultrasound-guided injection in orthotopic pancreatic tumor. I, the syringe needle is entering mouse skin; II, the needle is inside the tumor; III, MSC s TRAIL (red arrows) are located inside the tumor after injection. Scale bar 2 mm. IV, Representative fluorescence image of a mouse pancreas with intrapancreatic tumor explanted 7 days after injection of MSCs sTRAIL labeled by DiR.

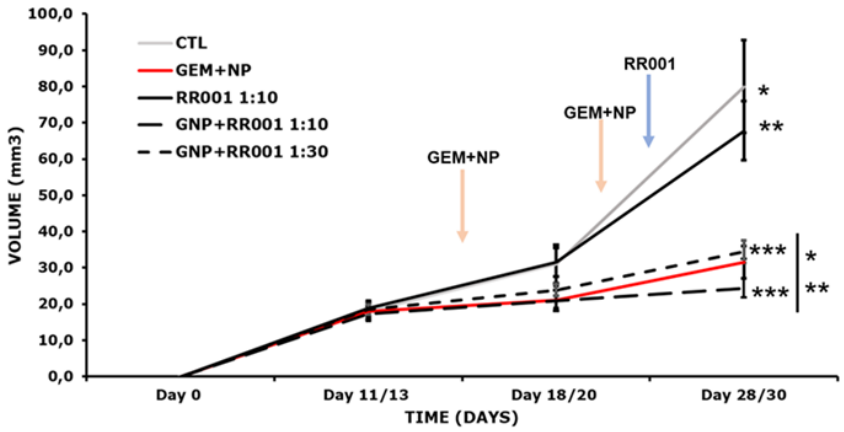

Figure 23: **Change of tumor volume over time.**

Tumor volume was measured through US scans from the day of tumor implant to the day of sacrifice. T test at 30 days: CTL vs GEM+NP p=0.001; CTL vs GNP+RR001 1:30 p=0.004; CTL vs GNP+RR001 1:10 p=0.0006; RR001 1:10 vs GEM+NP p=0.0006; RR001 1:10 vs GNP+RR001 1:30 p=0.001; RR001 1:10 vs GNP+RR001 1:10 p=0.00009; GNP+RR001 1:10 vs GNP+RR001 1:30 p=0.01. *,**,***$p<0.05$.

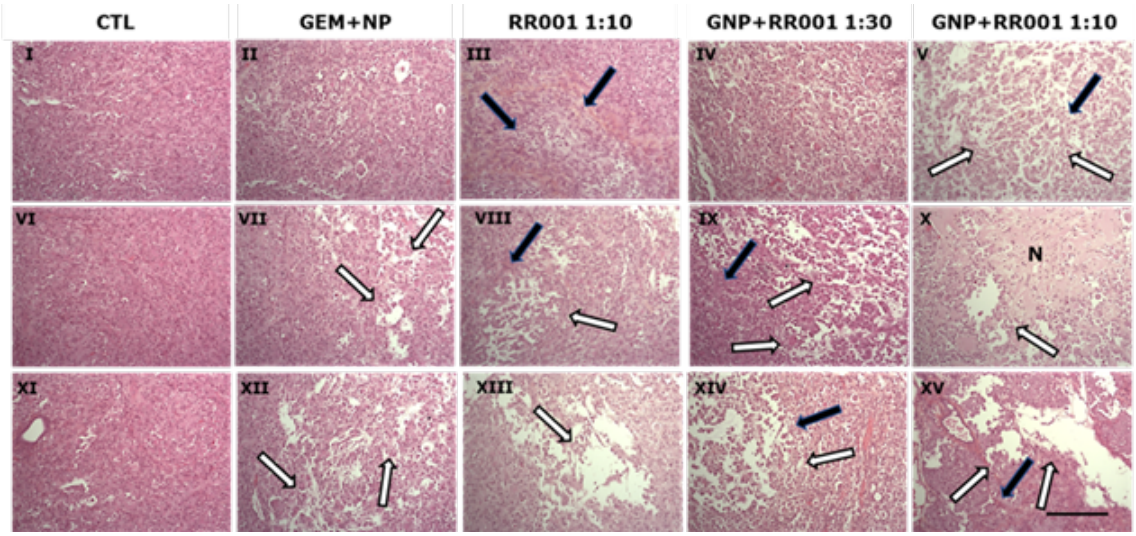

Figure 24. **Histological analysis of tumor architecture.**

Representative images of hematoxylin and eosin staining. Tissue degeneration was observed in treated groups, especially in the groups treated with the combination of GEM, Nab-PTX and RR001. White arrows indicate tumor tissue in degeneration, black arrows indicate stromal-like cells. N indicates a necrotic area. Magnification 100X, scale bar 200 um.

.

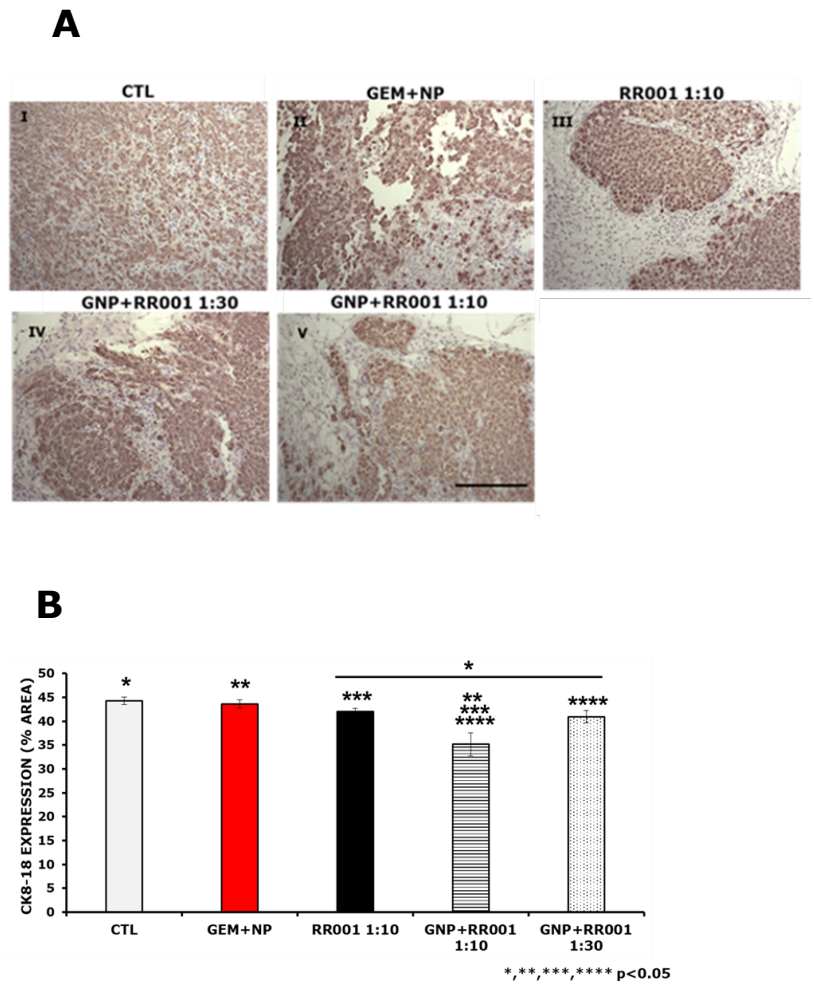

***Figure 25*: Histological analysis of PDAC tumor amount with CK8/18.**

A. Representative images of the immunohistochemistry anti-CK8/18 on intrapancreatic tumors. Positive areas (brown DAB) represent human PDAC tumor. Magnification 100X, scale bar 200 um. B. Histogram representing the quantification of CK8/18 positive areas within the different groups. For each tumor, two slides were evaluated. T test: * $p<0.05$

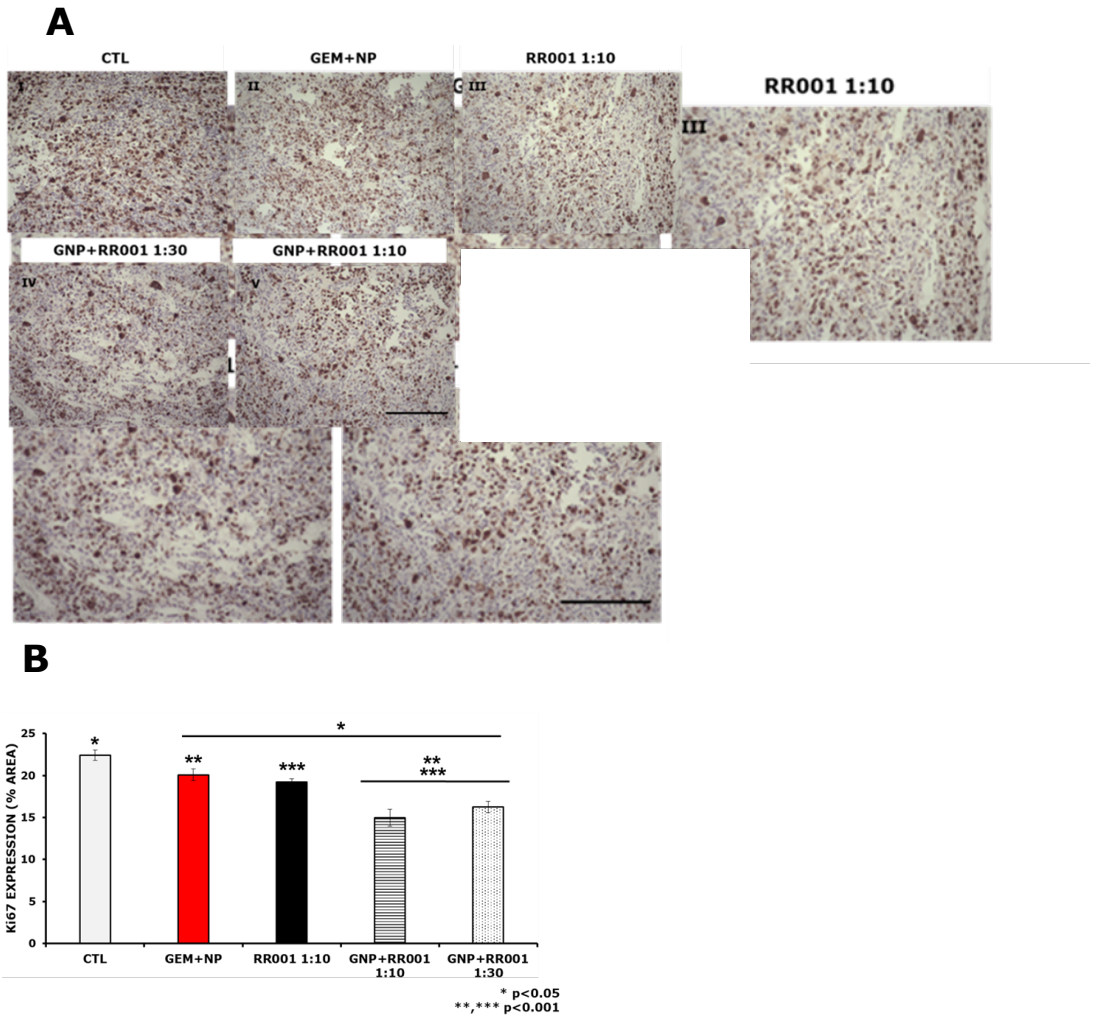

***Figure 26*: Histological analysis of tumor cells proliferation in PDAC with Ki67.**

A. Representative images of the anti-Ki67 immunohistochemistry on intrapancreatic tumors. Positive areas (brown DAB) represent proliferative tumor cells in PDAC. Magnification 100X, scale bar 200 um. **B**. Histogram representing the quantification of Ki67 positive areas within the different groups. For each tumor, two slides were evaluated. T test: *p<0.05, *;** p<0.001.

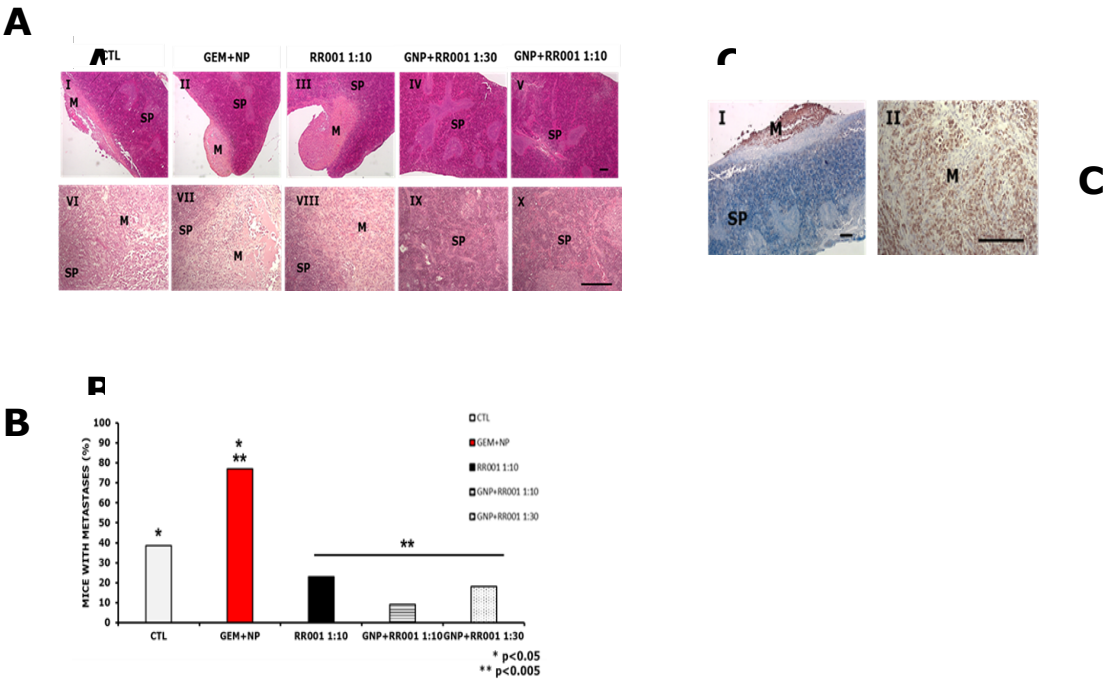

***Figure 27*: Abdominal metastases.**

A. Histological detection and quantification of spleen metastases. In the upper panel (I-V) , representative images of hematoxylin and eosin staining on mice spleens. M, metastasis; SP, spleen. Magnification 25X; lower panel (VI-X): magnification 100X. Scale bar 200 um. **B**. Graph represents the quantification of mice with spleen metastasis in the experimental groups. The groups which had the highest number of mice with metastases were GEM+NP and the control group, followed by the group treated with RR001 1:10 as single treatment and the group GNP+RR001 1:30. A lower tumor dissemination was visible in all the group treated with RR001 with a particularly relevant impact in GNP+RR001 1:10 compared to GNP alone. T test, *p<0.05; **p<0.005. **C**. Representative images of CK8/18 immunohistochemistry on mice metastatic. No brown positive signal can be found in isotype control. M, metastasis; SP, spleen. I: magnification 25X, scale bar 200 um; II: magnification 100X, scale bar 200 um.

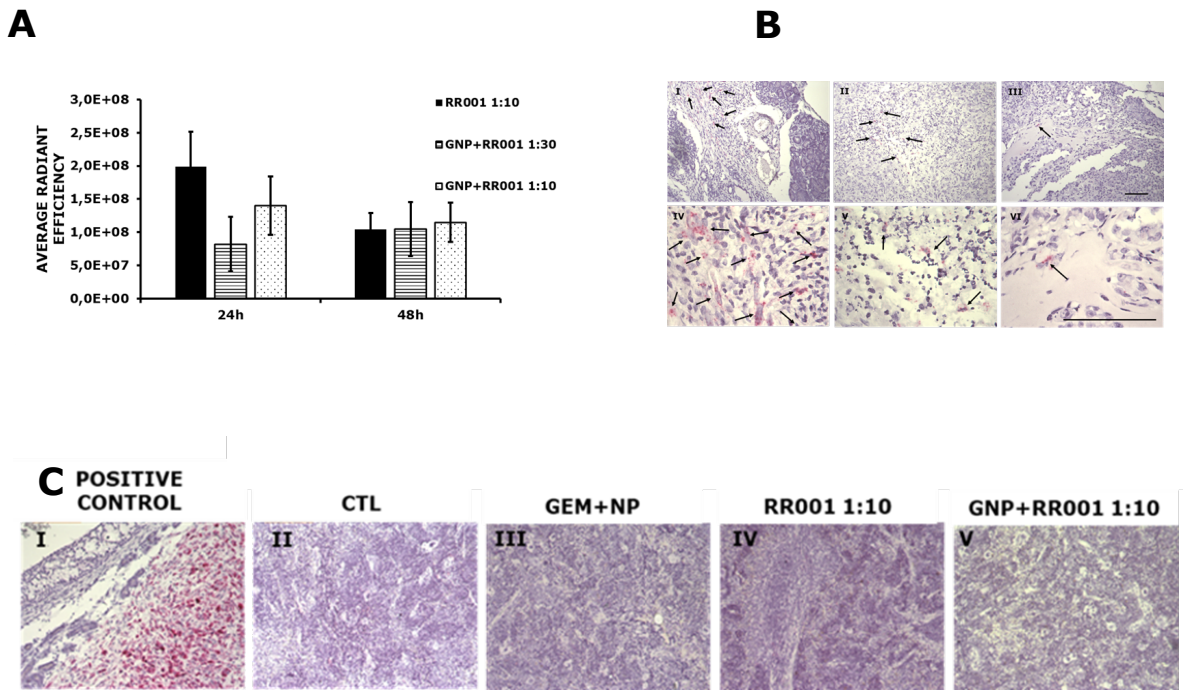

***Figure 28*. RR001 (AD-MSCs sTRAIL cells) biodistribution.**

A. Mean of fluorescence signal intensity monitored until 48 hours post RR001 injection in PDAC tumors, reported as average radiant efficiency. The fluorescence signal did not decrease significantly 48 hours post RR001 injection (T test). **B**. RR001 detection in tumors by Basescope in situ hybridization system. Representative examples of RR001 biodistribution 7 days after its intratumor injection in mice of RR001 1:10 and GNP+RR001 1:10 groups. Positive cells (red signals in the cytoplasm) represent RR001 cells. I and IV: group of RR001 cells beside intrapancreatic tumor. II and V: RR001 cells in a necrotic area inside the tumor. III and VI: a single RR001 cell inside the tumor. No RR001 cells were detected in CTL nor GEM+NP groups. GNP+RR001 1:30 group was not analyzed. Black arrows, RR001 cells. Upper panel (I-III): magnification 100X; lower panel (IV-VI): magnification 400X. Scale bar 200 um. **C**. RR001 detection in spleen by Basescope in situ hybridization system. No positive cells (red signals in the cytoplasm) were found in the spleen of animals 7 days after the intratumor injection of RR001. I, positive control: a group of RR001 cells 1 day after their intrapancreatic injection. Magnification 100X; scale bar 200 um.

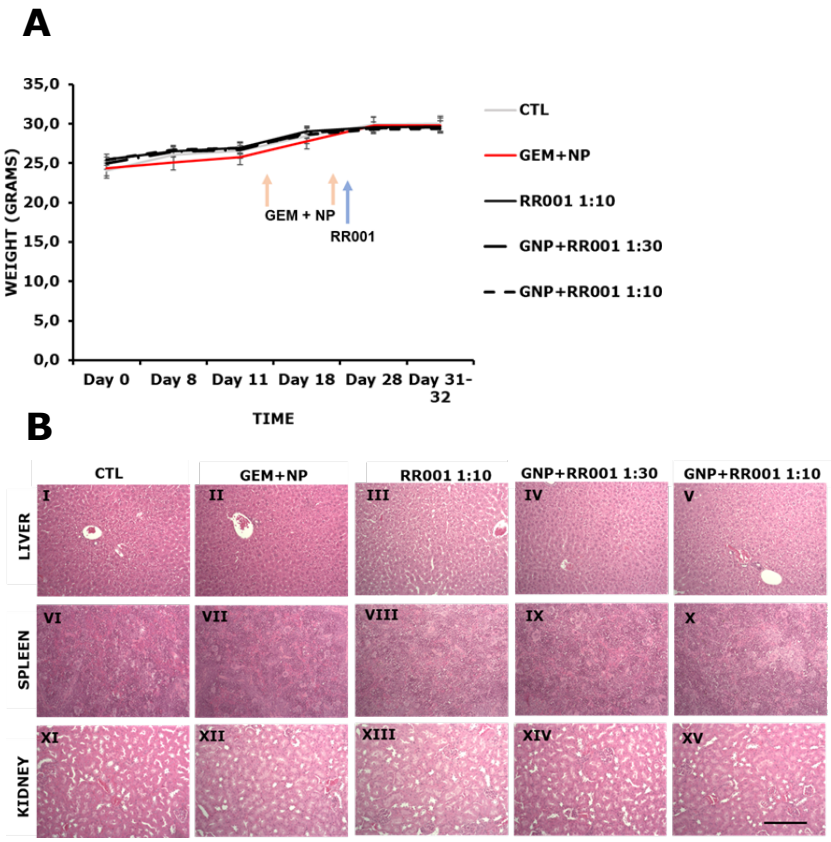

***Figure 29*. Safety profile of GNP+RR001 combinatorial treatment.**

A. Mice body weight measurement. No reduction in body weight was detected in any treated group in respect to control. B. Histological analysis by hematoxylin and eosin staining of liver, spleen and kidney of mice. No toxicity was observed in any treated group in respect to control group. Magnification 100X, scale bar 200 um.

7 REFERENCES

1. Sung, H., et al., *Global Cancer Statistics 2020: GLOBOCAN Estimates of Incidence and Mortality Worldwide for 36 Cancers in 185 Countries.* CA Cancer J Clin, 2021. **71**(3): p. 209-249.
2. Huang, J., et al., *Worldwide Burden of, Risk Factors for, and Trends in Pancreatic Cancer.* Gastroenterology, 2021. **160**(3): p. 744-754.
3. Hu, C., et al., *Association Between Inherited Germline Mutations in Cancer Predisposition Genes and Risk of Pancreatic Cancer.* JAMA, 2018. **319**(23): p. 2401-2409.
4. Rawla, P., T. Sunkara, and V. Gaduputi, *Epidemiology of Pancreatic Cancer: Global Trends, Etiology and Risk Factors.* World J Oncol, 2019. **10**(1): p. 10-27.
5. Pishvaian, M.J., et al., *Overall survival in patients with pancreatic cancer receiving matched therapies following molecular profiling: a retrospective analysis of the Know Your Tumor registry trial.* Lancet Oncol, 2020. **21**(4): p. 508-518.
6. Pilarski, R., *The Role of.* Am Soc Clin Oncol Educ Book, 2019. **39**: p. 79-86.
7. Peretti, U., et al., *Germinal BRCA1-2 pathogenic variants (gBRCA1-2pv) and pancreatic cancer: epidemiology of an Italian patient cohort.* ESMO Open, 2021. **6**(1): p. 100032.
8. Slater, E.P., et al., *PALB2 mutations in European familial pancreatic cancer families.* Clin Genet, 2010. **78**(5): p. 490-4.
9. Golan, T., et al., *Overall survival and clinical characteristics of pancreatic cancer in BRCA mutation carriers.* Br J Cancer, 2014. **111**(6): p. 1132-8.
10. O'Reilly, E.M., et al., *Randomized, Multicenter, Phase II Trial of Gemcitabine and Cisplatin With or Without Veliparib in Patients With Pancreas Adenocarcinoma and a Germline.* J Clin Oncol, 2020. **38**(13): p. 1378-1388.
11. Talia Golan, P.H., Michele Reni, Eric Van Cutsem, Teresa Macarulla, Michael J. Hall, Joon Oh Park, Daniel Hochhauser, Dirk Arnold, Do-Youn Oh, Anke C. Reinacher-Schick, Giampaolo Tortora, Hana Algül, Eileen Mary O'Reilly, David McGuinness, Karen Cui, Katia Schlienger, Gershon Y. Locker, Hedy L. Kindler, *Overall survival from the phase 3 POLO trial: Maintenance olaparib for germline BRCA-mutated metastatic pancreatic cancer*. 2021: 2021 Gastrointestinal Cancers Symposium.
12. andrew_aguirre@dfci.harvard.edu, C.G.A.R.N.E.a. and C.G.A.R. Network, *Integrated Genomic Characterization of Pancreatic Ductal Adenocarcinoma.* Cancer Cell, 2017. **32**(2): p. 185-203.e13.
13. Bailey, P., et al., *Genomic analyses identify molecular subtypes of pancreatic cancer.* Nature, 2016. **531**(7592): p. 47-52.
14. Waddell, N., et al., *Whole genomes redefine the mutational landscape of pancreatic cancer.* Nature, 2015. **518**(7540): p. 495-501.
15. Mizrahi, J.D., et al., *Pancreatic cancer.* Lancet, 2020. **395**(10242): p. 2008-2020.
16. Tempero, M.A., et al., *Pancreatic Adenocarcinoma, Version 2.2021, NCCN Clinical Practice Guidelines in Oncology.* J Natl Compr Canc Netw, 2021. **19**(4): p. 439-457.
17. Neoptolemos, J.P., et al., *A randomized trial of chemoradiotherapy and chemotherapy after resection of pancreatic cancer.* N Engl J Med, 2004. **350**(12): p. 1200-10.
18. Oettle, H., et al., *Adjuvant chemotherapy with gemcitabine and long-term outcomes among patients with resected pancreatic cancer: the CONKO-001 randomized trial.* JAMA, 2013. **310**(14): p. 1473-81.
19. Neoptolemos, J.P., et al., *Comparison of adjuvant gemcitabine and capecitabine with gemcitabine monotherapy in patients with resected pancreatic cancer (ESPAC-4): a*

multicentre, open-label, randomised, phase 3 trial. Lancet, 2017. **389**(10073): p. 1011-1024.
20. Conroy, T., et al., *FOLFIRINOX or Gemcitabine as Adjuvant Therapy for Pancreatic Cancer.* N Engl J Med, 2018. **379**(25): p. 2395-2406.
21. Yamada, D., et al., *Randomized phase II study of gemcitabine and S-1 combination therapy versus gemcitabine and nanoparticle albumin-bound paclitaxel combination therapy as neoadjuvant chemotherapy for resectable/borderline resectable pancreatic ductal adenocarcinoma (PDAC-GS/GA-rP2, CSGO-HBP-015).* Trials, 2021. **22**(1): p. 568.
22. Motoi, F., et al., *Randomized phase II/III trial of neoadjuvant chemotherapy with gemcitabine and S-1 versus upfront surgery for resectable pancreatic cancer (Prep-02/JSAP05).* Jpn J Clin Oncol, 2019. **49**(2): p. 190-194.
23. Ahmad, S.A., et al., *Surgical Outcome Results From SWOG S1505: A Randomized Clinical Trial of mFOLFIRINOX Versus Gemcitabine/Nab-paclitaxel for Perioperative Treatment of Resectable Pancreatic Ductal Adenocarcinoma.* Ann Surg, 2020. **272**(3): p. 481-486.
24. Ghanem, I., et al., *Neoadjuvant chemotherapy with or without radiotherapy versus upfront surgery for resectable pancreatic adenocarcinoma: a meta-analysis of randomized clinical trials.* ESMO Open, 2022. **7**(3): p. 100485.
25. Isaji, S., et al., *International consensus on definition and criteria of borderline resectable pancreatic ductal adenocarcinoma 2017.* Pancreatology, 2018. **18**(1): p. 2-11.
26. Versteijne, E., et al., *Meta-analysis comparing upfront surgery with neoadjuvant treatment in patients with resectable or borderline resectable pancreatic cancer.* Br J Surg, 2018. **105**(8): p. 946-958.
27. Versteijne, E., et al., *Neoadjuvant Chemoradiotherapy Versus Upfront Surgery for Resectable and Borderline Resectable Pancreatic Cancer: Long-Term Results of the Dutch Randomized PREOPANC Trial.* J Clin Oncol, 2022. **40**(11): p. 1220-1230.
28. van Dam, J.L., et al., *Neoadjuvant therapy or upfront surgery for resectable and borderline resectable pancreatic cancer: A meta-analysis of randomised controlled trials.* Eur J Cancer, 2022. **160**: p. 140-149.
29. Mollberg, N., et al., *Arterial resection during pancreatectomy for pancreatic cancer: a systematic review and meta-analysis.* Ann Surg, 2011. **254**(6): p. 882-93.
30. Chen, Z., et al., *Meta-analysis of FOLFIRINOX-based neoadjuvant therapy for locally advanced pancreatic cancer.* Medicine (Baltimore), 2021. **100**(3): p. e24068.
31. Philip, P.A., et al., *Nab-paclitaxel plus gemcitabine in patients with locally advanced pancreatic cancer (LAPACT): a multicentre, open-label phase 2 study.* Lancet Gastroenterol Hepatol, 2020. **5**(3): p. 285-294.
32. Kunzmann, V., et al., *Nab-paclitaxel plus gemcitabine versus nab-paclitaxel plus gemcitabine followed by FOLFIRINOX induction chemotherapy in locally advanced pancreatic cancer (NEOLAP-AIO-PAK-0113): a multicentre, randomised, phase 2 trial.* Lancet Gastroenterol Hepatol, 2021. **6**(2): p. 128-138.
33. Lee, J.C., et al., *Tolerability and safety of EUS-injected adenovirus-mediated double-suicide gene therapy with chemotherapy in locally advanced pancreatic cancer: a phase 1 trial.* Gastrointest Endosc, 2020. **92**(5): p. 1044-1052.e1.
34. Hirooka, Y., et al., *A Phase I clinical trial of EUS-guided intratumoral injection of the oncolytic virus, HF10 for unresectable locally advanced pancreatic cancer.* BMC Cancer, 2018. **18**(1): p. 596.
35. Suker, M., et al., *Efficacy and feasibility of stereotactic radiotherapy after folfirinox in patients with locally advanced pancreatic cancer (LAPC-1 trial).* EClinicalMedicine, 2019. **17**: p. 100200.
36. Ierardi, A.M., et al., *Percutaneous ablation therapies of inoperable pancreatic cancer: a systematic review.* Ann Gastroenterol, 2015. **28**(4): p. 431-9.

37. Lafranceschina, S., et al., *Systematic Review of Irreversible Electroporation Role in Management of Locally Advanced Pancreatic Cancer.* Cancers (Basel), 2019. **11**(11).
38. Girelli, R., et al., *Feasibility and safety of electrochemotherapy (ECT) in the pancreas: a pre-clinical investigation.* Radiol Oncol, 2015. **49**(2): p. 147-54.
39. Conroy, T., et al., *FOLFIRINOX versus gemcitabine for metastatic pancreatic cancer.* N Engl J Med, 2011. **364**(19): p. 1817-25.
40. Von Hoff, D.D., et al., *Increased survival in pancreatic cancer with nab-paclitaxel plus gemcitabine.* N Engl J Med, 2013. **369**(18): p. 1691-703.
41. Klein-Brill, A., et al., *Comparison of FOLFIRINOX vs Gemcitabine Plus Nab-Paclitaxel as First-Line Chemotherapy for Metastatic Pancreatic Ductal Adenocarcinoma.* JAMA Netw Open, 2022. **5**(6): p. e2216199.
42. Pusceddu, S., et al., *Comparative Effectiveness of Gemcitabine plus Nab-Paclitaxel and FOLFIRINOX in the First-Line Setting of Metastatic Pancreatic Cancer: A Systematic Review and Meta-Analysis.* Cancers (Basel), 2019. **11**(4).
43. Golan, T., et al., *Maintenance Olaparib for Germline.* N Engl J Med, 2019. **381**(4): p. 317-327.
44. Wang-Gillam, A., et al., *Nanoliposomal irinotecan with fluorouracil and folinic acid in metastatic pancreatic cancer after previous gemcitabine-based therapy (NAPOLI-1): a global, randomised, open-label, phase 3 trial.* Lancet, 2016. **387**(10018): p. 545-557.
45. Oettle, H., et al., *Second-line oxaliplatin, folinic acid, and fluorouracil versus folinic acid and fluorouracil alone for gemcitabine-refractory pancreatic cancer: outcomes from the CONKO-003 trial.* J Clin Oncol, 2014. **32**(23): p. 2423-9.
46. Schultheis, B., et al., *Gemcitabine combined with the monoclonal antibody nimotuzumab is an active first-line regimen in KRAS wildtype patients with locally advanced or metastatic pancreatic cancer: a multicenter, randomized phase IIb study.* Ann Oncol, 2017. **28**(10): p. 2429-2435.
47. Shukui Qin, Y.B., Zishu Wang, Zhendong Chen, Ruihua Xu, Jianming Xu, Hongmei Zhang, Jia Chen, Ying Yuan, Tianshu Liu, Lin Yang, Haijun Zhong, Donghui Chen, Lin Shen, Chunyi Hao, Deliang Fu, Ying Cheng, Jianwei Yang, Xian hong Bai, Jin Li, *Nimotuzumab combined with gemcitabine versus gemcitabine in K-RAS wild-type locally advanced or metastatic pancreatic cancer: A prospective, randomized-controlled, double-blinded, multicenter, and phase III clinical trial.* 2022, 2022 ASCO Annual Meeting II.
48. Fusco, M.J., et al., *Identification of Targetable Gene Fusions and Structural Rearrangements to Foster Precision Medicine in.* JCO Precis Oncol, 2021. **5**.
49. *Sotorasib Tackles KRASG12C-Mutated Pancreatic Cancer.* Cancer Discov, 2022. **12**(4): p. 878-879.
50. Ou, S.I., et al., *First-in-Human Phase I/IB Dose-Finding Study of Adagrasib (MRTX849) in Patients With Advanced.* J Clin Oncol, 2022: p. JCO2102752.
51. Philip, P.A., et al., *A Phase III open-label trial to evaluate efficacy and safety of CPI-613 plus modified FOLFIRINOX (mFFX) versus FOLFIRINOX (FFX) in patients with metastatic adenocarcinoma of the pancreas.* Future Oncol, 2019. **15**(28): p. 3189-3196.
52. Alistar, A., et al., *Safety and tolerability of the first-in-class agent CPI-613 in combination with modified FOLFIRINOX in patients with metastatic pancreatic cancer: a single-centre, open-label, dose-escalation, phase 1 trial.* Lancet Oncol, 2017. **18**(6): p. 770-778.
53. Royal, R.E., et al., *Phase 2 trial of single agent Ipilimumab (anti-CTLA-4) for locally advanced or metastatic pancreatic adenocarcinoma.* J Immunother, 2010. **33**(8): p. 828-33.
54. O'Reilly, E.M., et al., *Durvalumab With or Without Tremelimumab for Patients With Metastatic Pancreatic Ductal Adenocarcinoma: A Phase 2 Randomized Clinical Trial.* JAMA Oncol, 2019. **5**(10): p. 1431-1438.

55. Lutz, E.R., et al., *Immunotherapy converts nonimmunogenic pancreatic tumors into immunogenic foci of immune regulation.* Cancer Immunol Res, 2014. **2**(7): p. 616-31.
56. Lutz, E., et al., *A lethally irradiated allogeneic granulocyte-macrophage colony stimulating factor-secreting tumor vaccine for pancreatic adenocarcinoma. A Phase II trial of safety, efficacy, and immune activation.* Ann Surg, 2011. **253**(2): p. 328-35.
57. Le, D.T., et al., *Evaluation of ipilimumab in combination with allogeneic pancreatic tumor cells transfected with a GM-CSF gene in previously treated pancreatic cancer.* J Immunother, 2013. **36**(7): p. 382-9.
58. Beatty, G.L., et al., *Activity of Mesothelin-Specific Chimeric Antigen Receptor T Cells Against Pancreatic Carcinoma Metastases in a Phase 1 Trial.* Gastroenterology, 2018. **155**(1): p. 29-32.
59. Leidner, R., et al., *Neoantigen T-Cell Receptor Gene Therapy in Pancreatic Cancer.* N Engl J Med, 2022. **386**(22): p. 2112-2119.
60. Beatty, G.L., et al., *A phase I study of an agonist CD40 monoclonal antibody (CP-870,893) in combination with gemcitabine in patients with advanced pancreatic ductal adenocarcinoma.* Clin Cancer Res, 2013. **19**(22): p. 6286-95.
61. Grisendi, G., et al., *Tumor Stroma Manipulation By MSC.* Curr Drug Targets, 2016. **17**(10): p. 1111-26.
62. Hosein, A.N., R.A. Brekken, and A. Maitra, *Pancreatic cancer stroma: an update on therapeutic targeting strategies.* Nat Rev Gastroenterol Hepatol, 2020. **17**(8): p. 487-505.
63. Verloy, R., et al., *Cold Atmospheric Plasma Treatment for Pancreatic Cancer-The Importance of Pancreatic Stellate Cells.* Cancers (Basel), 2020. **12**(10).
64. Bachem, M.G., et al., *Pancreatic stellate cells--role in pancreas cancer.* Langenbecks Arch Surg, 2008. **393**(6): p. 891-900.
65. Bonnans, C., J. Chou, and Z. Werb, *Remodelling the extracellular matrix in development and disease.* Nat Rev Mol Cell Biol, 2014. **15**(12): p. 786-801.
66. Whatcott, C.J., et al., *Desmoplasia in Primary Tumors and Metastatic Lesions of Pancreatic Cancer.* Clin Cancer Res, 2015. **21**(15): p. 3561-8.
67. Öhlund, D., et al., *Type IV collagen stimulates pancreatic cancer cell proliferation, migration, and inhibits apoptosis through an autocrine loop.* BMC Cancer, 2013. **13**: p. 154.
68. Madsen, C.D., *Pancreatic cancer is suppressed by fibroblast-derived collagen I.* Cancer Cell, 2021. **39**(4): p. 451-453.
69. Munshi, H.G. and M.S. Stack, *Reciprocal interactions between adhesion receptor signaling and MMP regulation.* Cancer Metastasis Rev, 2006. **25**(1): p. 45-56.
70. Perez, V.M., J.F. Kearney, and J.J. Yeh, *The PDAC Extracellular Matrix: A Review of the ECM Protein Composition, Tumor Cell Interaction, and Therapeutic Strategies.* Front Oncol, 2021. **11**: p. 751311.
71. Betriu, N., et al., *Syndecans and Pancreatic Ductal Adenocarcinoma.* Biomolecules, 2021. **11**(3).
72. Seguin, L., et al., *Galectin-3, a Druggable Vulnerability for KRAS-Addicted Cancers.* Cancer Discov, 2017. **7**(12): p. 1464-1479.
73. Dallas, S.L., et al., *Fibronectin regulates latent transforming growth factor-beta (TGF beta) by controlling matrix assembly of latent TGF beta-binding protein-1.* J Biol Chem, 2005. **280**(19): p. 18871-80.
74. Arnold, S.A., et al., *Lack of host SPARC enhances vascular function and tumor spread in an orthotopic murine model of pancreatic carcinoma.* Dis Model Mech, 2010. **3**(1-2): p. 57-72.
75. Rice, A.J., et al., *Matrix stiffness induces epithelial-mesenchymal transition and promotes chemoresistance in pancreatic cancer cells.* Oncogenesis, 2017. **6**(7): p. e352.
76. Henke, E., R. Nandigama, and S. Ergün, *Extracellular Matrix in the Tumor Microenvironment and Its Impact on Cancer Therapy.* Front Mol Biosci, 2019. **6**: p. 160.

77. Smith-Mungo, L.I. and H.M. Kagan, *Lysyl oxidase: properties, regulation and multiple functions in biology.* Matrix Biol, 1998. **16**(7): p. 387-98.
78. Egeblad, M., M.G. Rasch, and V.M. Weaver, *Dynamic interplay between the collagen scaffold and tumor evolution.* Curr Opin Cell Biol, 2010. **22**(5): p. 697-706.
79. Tang, D.G., *Understanding and targeting prostate cancer cell heterogeneity and plasticity.* Semin Cancer Biol, 2022. **82**: p. 68-93.
80. Rossow, L., et al., *LOX-catalyzed collagen stabilization is a proximal cause for intrinsic resistance to chemotherapy.* Oncogene, 2018. **37**(36): p. 4921-4940.
81. Hodkinson, P.S., et al., *ECM overrides DNA damage-induced cell cycle arrest and apoptosis in small-cell lung cancer cells through beta1 integrin-dependent activation of PI3-kinase.* Cell Death Differ, 2006. **13**(10): p. 1776-88.
82. Nakagawa, Y., et al., *Overexpression of fibronectin confers cell adhesion-mediated drug resistance (CAM-DR) against 5-FU in oral squamous cell carcinoma cells.* Int J Oncol, 2014. **44**(4): p. 1376-84.
83. Eke, I., et al., *Cetuximab attenuates its cytotoxic and radiosensitizing potential by inducing fibronectin biosynthesis.* Cancer Res, 2013. **73**(19): p. 5869-79.
84. Nam, J.M., et al., *Breast cancer cells in three-dimensional culture display an enhanced radioresponse after coordinate targeting of integrin alpha5beta1 and fibronectin.* Cancer Res, 2010. **70**(13): p. 5238-48.
85. Raavé, R., T.H. van Kuppevelt, and W.F. Daamen, *Chemotherapeutic drug delivery by tumoral extracellular matrix targeting.* J Control Release, 2018. **274**: p. 1-8.
86. Schaaf, M.B., A.D. Garg, and P. Agostinis, *Defining the role of the tumor vasculature in antitumor immunity and immunotherapy.* Cell Death Dis, 2018. **9**(2): p. 115.
87. Jacobetz, M.A., et al., *Hyaluronan impairs vascular function and drug delivery in a mouse model of pancreatic cancer.* Gut, 2013. **62**(1): p. 112-20.
88. Chen, W. and P. Ten Dijke, *Immunoregulation by members of the TGFβ superfamily.* Nat Rev Immunol, 2016. **16**(12): p. 723-740.
89. Yingling, J.M., et al., *Preclinical assessment of galunisertib (LY2157299 monohydrate), a first-in-class transforming growth factor-β receptor type I inhibitor.* Oncotarget, 2018. **9**(6): p. 6659-6677.
90. Melisi, D., et al., *Galunisertib plus gemcitabine vs. gemcitabine for first-line treatment of patients with unresectable pancreatic cancer.* Br J Cancer, 2018. **119**(10): p. 1208-1214.
91. Melisi, D., et al., *Safety and activity of the TGFβ receptor I kinase inhibitor galunisertib plus the anti-PD-L1 antibody durvalumab in metastatic pancreatic cancer.* J Immunother Cancer, 2021. **9**(3).
92. McLeod, R., et al., *First-in-Human Study of AT13148, a Dual ROCK-AKT Inhibitor in Patients with Solid Tumors.* Clin Cancer Res, 2020. **26**(18): p. 4777-4784.
93. Rath, N., et al., *Rho Kinase Inhibition by AT13148 Blocks Pancreatic Ductal Adenocarcinoma Invasion and Tumor Growth.* Cancer Res, 2018. **78**(12): p. 3321-3336.
94. Gorchs, L., et al., *The vitamin D analogue calcipotriol promotes an anti-tumorigenic phenotype of human pancreatic CAFs but reduces T cell mediated immunity.* Sci Rep, 2020. **10**(1): p. 17444.
95. Moz, S., et al., *Vitamin D Prevents Pancreatic Cancer-Induced Apoptosis Signaling of Inflammatory Cells.* Biomolecules, 2020. **10**(7).
96. Ramanathan, R.K., et al., *Phase IB/II Randomized Study of FOLFIRINOX Plus Pegylated Recombinant Human Hyaluronidase Versus FOLFIRINOX Alone in Patients With Metastatic Pancreatic Adenocarcinoma: SWOG S1313.* J Clin Oncol, 2019. **37**(13): p. 1062-1069.
97. Van Cutsem, E., et al., *Randomized Phase III Trial of Pegvorhyaluronidase Alfa With Nab-Paclitaxel Plus Gemcitabine for Patients With Hyaluronan-High Metastatic Pancreatic Adenocarcinoma.* J Clin Oncol, 2020. **38**(27): p. 3185-3194.

98. Longo, V., et al., *Angiogenesis in pancreatic ductal adenocarcinoma: A controversial issue.* Oncotarget, 2016. **7**(36): p. 58649-58658.
99. Jiang, B., et al., *Stroma-Targeting Therapy in Pancreatic Cancer: One Coin With Two Sides?* Front Oncol, 2020. **10**: p. 576399.
100. Fukasawa, M. and M. Korc, *Vascular endothelial growth factor-trap suppresses tumorigenicity of multiple pancreatic cancer cell lines.* Clin Cancer Res, 2004. **10**(10): p. 3327-32.
101. Rougier, P., et al., *Randomised, placebo-controlled, double-blind, parallel-group phase III study evaluating aflibercept in patients receiving first-line treatment with gemcitabine for metastatic pancreatic cancer.* Eur J Cancer, 2013. **49**(12): p. 2633-42.
102. Kindler, H.L., et al., *Gemcitabine plus bevacizumab compared with gemcitabine plus placebo in patients with advanced pancreatic cancer: phase III trial of the Cancer and Leukemia Group B (CALGB 80303).* J Clin Oncol, 2010. **28**(22): p. 3617-22.
103. Van Cutsem, E., et al., *Phase III trial of bevacizumab in combination with gemcitabine and erlotinib in patients with metastatic pancreatic cancer.* J Clin Oncol, 2009. **27**(13): p. 2231-7.
104. Murphy, J.E., et al., *Total Neoadjuvant Therapy With FOLFIRINOX in Combination With Losartan Followed by Chemoradiotherapy for Locally Advanced Pancreatic Cancer: A Phase 2 Clinical Trial.* JAMA Oncol, 2019. **5**(7): p. 1020-1027.
105. Liu, H., et al., *Use of Angiotensin System Inhibitors Is Associated with Immune Activation and Longer Survival in Nonmetastatic Pancreatic Ductal Adenocarcinoma.* Clin Cancer Res, 2017. **23**(19): p. 5959-5969.
106. Ugel, S., et al., *Tumor-induced myeloid deviation: when myeloid-derived suppressor cells meet tumor-associated macrophages.* J Clin Invest, 2015. **125**(9): p. 3365-76.
107. Porembka, M.R., et al., *Pancreatic adenocarcinoma induces bone marrow mobilization of myeloid-derived suppressor cells which promote primary tumor growth.* Cancer Immunol Immunother, 2012. **61**(9): p. 1373-85.
108. Pinton, L., et al., *Activated T cells sustain myeloid-derived suppressor cell-mediated immune suppression.* Oncotarget, 2016. **7**(2): p. 1168-84.
109. Tariq, M., et al., *Macrophage Polarization: Anti-Cancer Strategies to Target Tumor-Associated Macrophage in Breast Cancer.* J Cell Biochem, 2017. **118**(9): p. 2484-2501.
110. Kim, S.Y. and M.G. Nair, *Macrophages in wound healing: activation and plasticity.* Immunol Cell Biol, 2019. **97**(3): p. 258-267.
111. Salmaninejad, A., et al., *Tumor-associated macrophages: role in cancer development and therapeutic implications.* Cell Oncol (Dordr), 2019. **42**(5): p. 591-608.
112. Liu, L., et al., *Low intratumoral regulatory T cells and high peritumoral CD8(+) T cells relate to long-term survival in patients with pancreatic ductal adenocarcinoma after pancreatectomy.* Cancer Immunol Immunother, 2016. **65**(1): p. 73-82.
113. Zeng, S., et al., *Chemoresistance in Pancreatic Cancer.* Int J Mol Sci, 2019. **20**(18).
114. Mishra, P., D. Banerjee, and A. Ben-Baruch, *Chemokines at the crossroads of tumor-fibroblast interactions that promote malignancy.* J Leukoc Biol, 2011. **89**(1): p. 31-9.
115. Patel, G.K., et al., *Exosomes confer chemoresistance to pancreatic cancer cells by promoting ROS detoxification and miR-155-mediated suppression of key gemcitabine-metabolising enzyme, DCK.* Br J Cancer, 2017. **116**(5): p. 609-619.
116. Richards, K.E., et al., *Cancer-Associated Fibroblasts Confer Gemcitabine Resistance to Pancreatic Cancer Cells through PTEN-Targeting miRNAs in Exosomes.* Cancers (Basel), 2022. **14**(11).
117. Horimoto, Y., et al., *Emerging roles of the tumor-associated stroma in promoting tumor metastasis.* Cell Adh Migr, 2012. **6**(3): p. 193-202.
118. Räsänen, K. and A. Vaheri, *Activation of fibroblasts in cancer stroma.* Exp Cell Res, 2010. **316**(17): p. 2713-22.

119. Mueller, L., et al., *Stromal fibroblasts in colorectal liver metastases originate from resident fibroblasts and generate an inflammatory microenvironment.* Am J Pathol, 2007. **171**(5): p. 1608-18.
120. Kidd, S., et al., *Origins of the tumor microenvironment: quantitative assessment of adipose-derived and bone marrow-derived stroma.* PLoS One, 2012. **7**(2): p. e30563.
121. Direkze, N.C., et al., *Bone marrow contribution to tumor-associated myofibroblasts and fibroblasts.* Cancer Res, 2004. **64**(23): p. 8492-5.
122. Geng, X., et al., *Cancer-Associated Fibroblast (CAF) Heterogeneity and Targeting Therapy of CAFs in Pancreatic Cancer.* Front Cell Dev Biol, 2021. **9**: p. 655152.
123. Helms, E.J., et al., *Mesenchymal Lineage Heterogeneity Underlies Nonredundant Functions of Pancreatic Cancer-Associated Fibroblasts.* Cancer Discov, 2022. **12**(2): p. 484-501.
124. Beckermann, B.M., et al., *VEGF expression by mesenchymal stem cells contributes to angiogenesis in pancreatic carcinoma.* Br J Cancer, 2008. **99**(4): p. 622-31.
125. Omary, M.B., et al., *The pancreatic stellate cell: a star on the rise in pancreatic diseases.* J Clin Invest, 2007. **117**(1): p. 50-9.
126. Rhim, A.D., et al., *Stromal elements act to restrain, rather than support, pancreatic ductal adenocarcinoma.* Cancer Cell, 2014. **25**(6): p. 735-47.
127. Catenacci, D.V., et al., *Randomized Phase Ib/II Study of Gemcitabine Plus Placebo or Vismodegib, a Hedgehog Pathway Inhibitor, in Patients With Metastatic Pancreatic Cancer.* J Clin Oncol, 2015. **33**(36): p. 4284-92.
128. Biffi, G., et al., *IL1-Induced JAK/STAT Signaling Is Antagonized by TGFβ to Shape CAF Heterogeneity in Pancreatic Ductal Adenocarcinoma.* Cancer Discov, 2019. **9**(2): p. 282-301.
129. Öhlund, D., et al., *Distinct populations of inflammatory fibroblasts and myofibroblasts in pancreatic cancer.* J Exp Med, 2017. **214**(3): p. 579-596.
130. Flint, T.R., et al., *Tumor-Induced IL-6 Reprograms Host Metabolism to Suppress Anti-tumor Immunity.* Cell Metab, 2016. **24**(5): p. 672-684.
131. Antoon, R., et al., *Pancreatic cancer growth promoted by bone marrow mesenchymal stromal cell-derived IL-6 is reversed predominantly by IL-6 blockade.* Cytotherapy, 2022. **24**(7): p. 699-710.
132. Mace, T.A., et al., *IL-6 and PD-L1 antibody blockade combination therapy reduces tumour progression in murine models of pancreatic cancer.* Gut, 2018. **67**(2): p. 320-332.
133. Yu, J.H. and H. Kim, *Role of janus kinase/signal transducers and activators of transcription in the pathogenesis of pancreatitis and pancreatic cancer.* Gut Liver, 2012. **6**(4): p. 417-22.
134. Nagathihalli, N.S., et al., *Signal Transducer and Activator of Transcription 3, Mediated Remodeling of the Tumor Microenvironment Results in Enhanced Tumor Drug Delivery in a Mouse Model of Pancreatic Cancer.* Gastroenterology, 2015. **149**(7): p. 1932-1943.e9.
135. Das, S., et al., *Tumor Cell-Derived IL1β Promotes Desmoplasia and Immune Suppression in Pancreatic Cancer.* Cancer Res, 2020. **80**(5): p. 1088-1101.
136. Zhang, D., et al., *Tumor-Stroma IL1β-IRAK4 Feedforward Circuitry Drives Tumor Fibrosis, Chemoresistance, and Poor Prognosis in Pancreatic Cancer.* Cancer Res, 2018. **78**(7): p. 1700-1712.
137. Bockorny, B., et al., *BL-8040, a CXCR4 antagonist, in combination with pembrolizumab and chemotherapy for pancreatic cancer: the COMBAT trial.* Nat Med, 2020. **26**(6): p. 878-885.
138. Chan, T.S., Y. Shaked, and K.K. Tsai, *Targeting the Interplay Between Cancer Fibroblasts, Mesenchymal Stem Cells, and Cancer Stem Cells in Desmoplastic Cancers.* Front Oncol, 2019. **9**: p. 688.

139. Horwitz, E.M. and M. Dominici, *How do mesenchymal stromal cells exert their therapeutic benefit?* Cytotherapy, 2008. **10**(8): p. 771-4.
140. Dominici, M., et al., *Minimal criteria for defining multipotent mesenchymal stromal cells. The International Society for Cellular Therapy position statement.* Cytotherapy, 2006. **8**(4): p. 315-7.
141. Bianco, P., et al., *"Mesenchymal" stem cells in human bone marrow (skeletal stem cells): a critical discussion of their nature, identity, and significance in incurable skeletal disease.* Hum Gene Ther, 2010. **21**(9): p. 1057-66.
142. Pittenger, M.F., et al., *Mesenchymal stem cell perspective: cell biology to clinical progress.* NPJ Regen Med, 2019. **4**: p. 22.
143. Mishra, V.K., et al., *Identifying the Therapeutic Significance of Mesenchymal Stem Cells.* Cells, 2020. **9**(5).
144. Golinelli, G., et al., *Arming Mesenchymal Stromal/Stem Cells Against Cancer: Has the Time Come?* Front Pharmacol, 2020. **11**: p. 529921.
145. Sordi, V., et al., *Bone marrow mesenchymal stem cells express a restricted set of functionally active chemokine receptors capable of promoting migration to pancreatic islets.* Blood, 2005. **106**(2): p. 419-27.
146. He, Q., C. Wan, and G. Li, *Concise review: multipotent mesenchymal stromal cells in blood.* Stem Cells, 2007. **25**(1): p. 69-77.
147. Gao, H., et al., *Activation of signal transducers and activators of transcription 3 and focal adhesion kinase by stromal cell-derived factor 1 is required for migration of human mesenchymal stem cells in response to tumor cell-conditioned medium.* Stem Cells, 2009. **27**(4): p. 857-65.
148. Zischek, C., et al., *Targeting tumor stroma using engineered mesenchymal stem cells reduces the growth of pancreatic carcinoma.* Ann Surg, 2009. **250**(5): p. 747-53.
149. Ahn, S.Y., *The Role of MSCs in the Tumor Microenvironment and Tumor Progression.* Anticancer Res, 2020. **40**(6): p. 3039-3047.
150. Grisendi, G., et al., *Understanding tumor-stroma interplays for targeted therapies by armed mesenchymal stromal progenitors: the Mesenkillers.* Am J Cancer Res, 2011. **1**(6): p. 787-805.
151. Paunescu, V., et al., *Tumour-associated fibroblasts and mesenchymal stem cells: more similarities than differences.* J Cell Mol Med, 2011. **15**(3): p. 635-46.
152. Huang, W.H., et al., *Mesenchymal stem cells promote growth and angiogenesis of tumors in mice.* Oncogene, 2013. **32**(37): p. 4343-54.
153. Wang, W., et al., *Involvement of Wnt/β-catenin signaling in the mesenchymal stem cells promote metastatic growth and chemoresistance of cholangiocarcinoma.* Oncotarget, 2015. **6**(39): p. 42276-89.
154. Cousin, B., et al., *Adult stromal cells derived from human adipose tissue provoke pancreatic cancer cell death both in vitro and in vivo.* PLoS One, 2009. **4**(7): p. e6278.
155. Otsu, K., et al., *Concentration-dependent inhibition of angiogenesis by mesenchymal stem cells.* Blood, 2009. **113**(18): p. 4197-205.
156. Jia, Z., et al., *Adipose Mesenchymal Stem Cell-Derived Exosomal microRNA-1236 Reduces Resistance of Breast Cancer Cells to Cisplatin by Suppressing SLC9A1 and the Wnt/β-Catenin Signaling.* Cancer Manag Res, 2020. **12**: p. 8733-8744.
157. Chulpanova, D.S., et al., *Application of Mesenchymal Stem Cells for Therapeutic Agent Delivery in Anti-tumor Treatment.* Front Pharmacol, 2018. **9**: p. 259.
158. Almeida-Porada, G., A.J. Atala, and C.D. Porada, *Therapeutic Mesenchymal Stromal Cells for Immunotherapy and for Gene and Drug Delivery.* Mol Ther Methods Clin Dev, 2020. **16**: p. 204-224.
159. Mastrolia, I., et al., *Challenges in Clinical Development of Mesenchymal Stromal/Stem Cells: Concise Review.* Stem Cells Transl Med, 2019. **8**(11): p. 1135-1148.
160. Kean, T.J., et al., *MSCs: Delivery Routes and Engraftment, Cell-Targeting Strategies, and Immune Modulation.* Stem Cells Int, 2013. **2013**: p. 732742.

161. De Becker, A. and I.V. Riet, *Homing and migration of mesenchymal stromal cells: How to improve the efficacy of cell therapy?* World J Stem Cells, 2016. **8**(3): p. 73-87.
162. Silva, L.H., et al., *Magnetic targeting as a strategy to enhance therapeutic effects of mesenchymal stromal cells.* Stem Cell Res Ther, 2017. **8**(1): p. 58.
163. Arbab, A.S., et al., *In vivo trafficking and targeted delivery of magnetically labeled stem cells.* Hum Gene Ther, 2004. **15**(4): p. 351-60.
164. Golinelli, G., et al., *Targeting GD2-positive glioblastoma by chimeric antigen receptor empowered mesenchymal progenitors.* Cancer Gene Ther, 2020. **27**(7-8): p. 558-570.
165. Bonomi, A., et al., *Gemcitabine-releasing mesenchymal stromal cells inhibit in vitro proliferation of human pancreatic carcinoma cells.* Cytotherapy, 2015. **17**(12): p. 1687-95.
166. Pascucci, L., et al., *Paclitaxel is incorporated by mesenchymal stromal cells and released in exosomes that inhibit in vitro tumor growth: a new approach for drug delivery.* J Control Release, 2014. **192**: p. 262-70.
167. Babajani, A., et al., *Recent Advances on Drug-Loaded Mesenchymal Stem Cells With Anti-neoplastic Agents for Targeted Treatment of Cancer.* Front Bioeng Biotechnol, 2020. **8**: p. 748.
168. Nawaz, M., *Extracellular vesicle-mediated transport of non-coding RNAs between stem cells and cancer cells: implications in tumor progression and therapeutic resistance.* Stem Cell Investig, 2017. **4**: p. 83.
169. Layek, B., et al., *Nano-Engineered Mesenchymal Stem Cells Increase Therapeutic Efficacy of Anticancer Drug Through True Active Tumor Targeting.* Mol Cancer Ther, 2018. **17**(6): p. 1196-1206.
170. Zhang, J., V. Kale, and M. Chen, *Gene-directed enzyme prodrug therapy.* AAPS J, 2015. **17**(1): p. 102-10.
171. Martinez-Quintanilla, J., et al., *Therapeutic efficacy and fate of bimodal engineered stem cells in malignant brain tumors.* Stem Cells, 2013. **31**(8): p. 1706-14.
172. Kucerova, L., et al., *Long-term efficiency of mesenchymal stromal cell-mediated CD-MSC/5FC therapy in human melanoma xenograft model.* Gene Ther, 2014. **21**(10): p. 874-87.
173. Studeny, M., et al., *Bone marrow-derived mesenchymal stem cells as vehicles for interferon-beta delivery into tumors.* Cancer Res, 2002. **62**(13): p. 3603-8.
174. Shah, K., *Mesenchymal stem cells engineered for cancer therapy.* Adv Drug Deliv Rev, 2012. **64**(8): p. 739-48.
175. Rossignoli, F., et al., *Inducible Caspase9-mediated suicide gene for MSC-based cancer gene therapy.* Cancer Gene Ther, 2019. **26**(1-2): p. 11-16.
176. Rossignoli, F., et al., *MSC-Delivered Soluble TRAIL and Paclitaxel as Novel Combinatory Treatment for Pancreatic Adenocarcinoma.* Theranostics, 2019. **9**(2): p. 436-448.
177. Spano, C., et al., *Soluble TRAIL Armed Human MSC As Gene Therapy For Pancreatic Cancer.* Sci Rep, 2019. **9**(1): p. 1788.
178. Candini, O., et al., *A Novel 3D In Vitro Platform for Pre-Clinical Investigations in Drug Testing, Gene Therapy, and Immuno-oncology.* Sci Rep, 2019. **9**(1): p. 7154.
179. Guiho, R., et al., *TRAIL delivered by mesenchymal stromal/stem cells counteracts tumor development in orthotopic Ewing sarcoma models.* Int J Cancer, 2016. **139**(12): p. 2802-2811.
180. Yan, C., et al., *Suppression of orthotopically implanted hepatocarcinoma in mice by umbilical cord-derived mesenchymal stem cells with sTRAIL gene expression driven by AFP promoter.* Biomaterials, 2014. **35**(9): p. 3035-43.
181. Whatcott, C., et al., *Tumor-stromal interactions in pancreatic cancer.* Crit Rev Oncog, 2013. **18**(1-2): p. 135-51.
182. Lang, F.F., et al., *Phase I Study of DNX-2401 (Delta-24-RGD) Oncolytic Adenovirus: Replication and Immunotherapeutic Effects in Recurrent Malignant Glioma.* J Clin Oncol, 2018. **36**(14): p. 1419-1427.

183. Kaczorowski, A., et al., *Delivery of improved oncolytic adenoviruses by mesenchymal stromal cells for elimination of tumorigenic pancreatic cancer cells.* Oncotarget, 2016. **7**(8): p. 9046-59.
184. Diaz Arguello, O.A. and H.J. Haisma, *Apoptosis-Inducing TNF Superfamily Ligands for Cancer Therapy.* Cancers (Basel), 2021. **13**(7).
185. Morizot, A., et al., *Chemotherapy overcomes TRAIL-R4-mediated TRAIL resistance at the DISC level.* Cell Death Differ, 2011. **18**(4): p. 700-11.
186. Neumann, S., et al., *Dominant negative effects of tumor necrosis factor (TNF)-related apoptosis-inducing ligand (TRAIL) receptor 4 on TRAIL receptor 1 signaling by formation of heteromeric complexes.* J Biol Chem, 2014. **289**(23): p. 16576-87.
187. Dall'Ora, M., et al., *TRAIL receptors are expressed in both malignant and stromal cells in pancreatic ductal adenocarcinoma.* Am J Cancer Res, 2021. **11**(9): p. 4500-4514.
188. Mohr, A., R. Yu, and R.M. Zwacka, *TRAIL-receptor preferences in pancreatic cancer cells revisited: Both TRAIL-R1 and TRAIL-R2 have a licence to kill.* BMC Cancer, 2015. **15**: p. 494.
189. Wong, S.H.M., et al., *The TRAIL to cancer therapy: Hindrances and potential solutions.* Crit Rev Oncol Hematol, 2019. **143**: p. 81-94.
190. Grisendi, G., et al., *Adipose-derived mesenchymal stem cells as stable source of tumor necrosis factor-related apoptosis-inducing ligand delivery for cancer therapy.* Cancer Res, 2010. **70**(9): p. 3718-29.
191. Bodmer, J.L., et al., *TRAIL receptor-2 signals apoptosis through FADD and caspase-8.* Nat Cell Biol, 2000. **2**(4): p. 241-3.
192. Zhong, H.H., et al., *TRAIL-based gene delivery and therapeutic strategies.* Acta Pharmacol Sin, 2019. **40**(11): p. 1373-1385.
193. Yuan, S. and C.W. Akey, *Apoptosome structure, assembly, and procaspase activation.* Structure, 2013. **21**(4): p. 501-15.
194. Lowe, S.W., et al., *p53 status and the efficacy of cancer therapy in vivo.* Science, 1994. **266**(5186): p. 807-10.
195. Lemke, J., et al., *TRAIL signaling is mediated by DR4 in pancreatic tumor cells despite the expression of functional DR5.* J Mol Med (Berl), 2010. **88**(7): p. 729-40.
196. Ganten, T.M., et al., *Prognostic significance of tumour necrosis factor-related apoptosis-inducing ligand (TRAIL) receptor expression in patients with breast cancer.* J Mol Med (Berl), 2009. **87**(10): p. 995-1007.
197. Sträter, J., et al., *Expression of TRAIL and TRAIL receptors in colon carcinoma: TRAIL-R1 is an independent prognostic parameter.* Clin Cancer Res, 2002. **8**(12): p. 3734-40.
198. Kriegl, L., et al., *Expression, cellular distribution, and prognostic relevance of TRAIL receptors in hepatocellular carcinoma.* Clin Cancer Res, 2010. **16**(22): p. 5529-38.
199. Sanlioglu, A.D., et al., *High TRAIL death receptor 4 and decoy receptor 2 expression correlates with significant cell death in pancreatic ductal adenocarcinoma patients.* Pancreas, 2009. **38**(2): p. 154-60.
200. Gallmeier, E., et al., *Loss of TRAIL-receptors is a recurrent feature in pancreatic cancer and determines the prognosis of patients with no nodal metastasis after surgery.* PLoS One, 2013. **8**(2): p. e56760.
201. Gundlach, J.P., et al., *Cytoplasmic TRAIL-R1 is a positive prognostic marker in PDAC.* BMC Cancer, 2018. **18**(1): p. 777.
202. Dimberg, L.Y., et al., *On the TRAIL to successful cancer therapy? Predicting and counteracting resistance against TRAIL-based therapeutics.* Oncogene, 2013. **32**(11): p. 1341-50.
203. Horak, P., et al., *Contribution of epigenetic silencing of tumor necrosis factor-related apoptosis inducing ligand receptor 1 (DR4) to TRAIL resistance and ovarian cancer.* Mol Cancer Res, 2005. **3**(6): p. 335-43.

204. Bin, L., et al., *Tumor-derived mutations in the TRAIL receptor DR5 inhibit TRAIL signaling through the DR4 receptor by competing for ligand binding.* J Biol Chem, 2007. **282**(38): p. 28189-94.
205. Zhang, Y. and B. Zhang, *TRAIL resistance of breast cancer cells is associated with constitutive endocytosis of death receptors 4 and 5.* Mol Cancer Res, 2008. **6**(12): p. 1861-71.
206. Grotzer, M.A., et al., *Resistance to TRAIL-induced apoptosis in primitive neuroectodermal brain tumor cells correlates with a loss of caspase-8 expression.* Oncogene, 2000. **19**(40): p. 4604-10.
207. Kim, E.H., S.U. Kim, and K.S. Choi, *Rottlerin sensitizes glioma cells to TRAIL-induced apoptosis by inhibition of Cdc2 and the subsequent downregulation of survivin and XIAP.* Oncogene, 2005. **24**(5): p. 838-49.
208. Goklany, S., et al., *Delivery of TRAIL-expressing plasmid DNA to cancer cells in vitro and in vivo using aminoglycoside-derived polymers.* J Mater Chem B, 2019. **7**(44): p. 7014-7025.
209. Liu, H., et al., *Improvement of Pharmacokinetic Profile of TRAIL via Trimer-Tag Enhances its Antitumor Activity in vivo.* Sci Rep, 2017. **7**(1): p. 8953.
210. Kretz, A.L., et al., *TRAILblazing Strategies for Cancer Treatment.* Cancers (Basel), 2019. **11**(4).
211. Jin, H., et al., *Apo2 ligand/tumor necrosis factor-related apoptosis-inducing ligand cooperates with chemotherapy to inhibit orthotopic lung tumor growth and improve survival.* Cancer Res, 2004. **64**(14): p. 4900-5.
212. Naka, T., et al., *Effects of tumor necrosis factor-related apoptosis-inducing ligand alone and in combination with chemotherapeutic agents on patients' colon tumors grown in SCID mice.* Cancer Res, 2002. **62**(20): p. 5800-6.
213. Li, Y.B., et al., *Radiosensitization of breast cancer cells by TRAIL-endostatin-targeting gene therapy.* Neoplasma, 2013. **60**(6): p. 613-9.
214. Ray, S. and A. Almasan, *Apoptosis induction in prostate cancer cells and xenografts by combined treatment with Apo2 ligand/tumor necrosis factor-related apoptosis-inducing ligand and CPT-11.* Cancer Res, 2003. **63**(15): p. 4713-23.
215. Fiveash, J.B., et al., *Enhancement of glioma radiotherapy and chemotherapy response with targeted antibody therapy against death receptor 5.* Int J Radiat Oncol Biol Phys, 2008. **71**(2): p. 507-16.
216. Goldstein, D., et al., *nab-Paclitaxel plus gemcitabine for metastatic pancreatic cancer: long-term survival from a phase III trial.* J Natl Cancer Inst, 2015. **107**(2).
217. Blagosklonny, M.V., et al., *Paclitaxel induces primary and postmitotic G1 arrest in human arterial smooth muscle cells.* Cell Cycle, 2004. **3**(8): p. 1050-6.
218. Demidenko, Z.N., et al., *Mechanism of G1-like arrest by low concentrations of paclitaxel: next cell cycle p53-dependent arrest with sub G1 DNA content mediated by prolonged mitosis.* Oncogene, 2008. **27**(32): p. 4402-10.
219. Huang, S., et al., *Improved melanoma suppression with target-delivered TRAIL and Paclitaxel by a multifunctional nanocarrier.* J Control Release, 2020. **325**: p. 10-24.
220. Gradishar, W.J., *Albumin-bound paclitaxel: a next-generation taxane.* Expert Opin Pharmacother, 2006. **7**(8): p. 1041-53.
221. Nimmanapalli, R., et al., *Pretreatment with paclitaxel enhances apo-2 ligand/tumor necrosis factor-related apoptosis-inducing ligand-induced apoptosis of prostate cancer cells by inducing death receptors 4 and 5 protein levels.* Cancer Res, 2001. **61**(2): p. 759-63.
222. Li, L., et al., *Paclitaxel enhances tumoricidal potential of TRAIL via inhibition of MAPK in resistant gastric cancer cells.* Oncol Rep, 2016. **35**(5): p. 3009-17.
223. Dorsey, J.F., et al., *Tumor necrosis factor-related apoptosis-inducing ligand (TRAIL) and paclitaxel have cooperative in vivo effects against glioblastoma multiforme cells.* Mol Cancer Ther, 2009. **8**(12): p. 3285-95.

224. Kim, M., et al., *TRAIL inactivates the mitotic checkpoint and potentiates death induced by microtubule-targeting agents in human cancer cells.* Cancer Res, 2008. **68**(9): p. 3440-9.
225. Min, S.Y., et al., *Facile one-pot formulation of TRAIL-embedded paclitaxel-bound albumin nanoparticles for the treatment of pancreatic cancer.* Int J Pharm, 2015. **494**(1): p. 506-15.
226. Soria, J.C., et al., *Randomized phase II study of dulanermin in combination with paclitaxel, carboplatin, and bevacizumab in advanced non-small-cell lung cancer.* J Clin Oncol, 2011. **29**(33): p. 4442-51.
227. Ouyang, X., et al., *Phase III study of dulanermin (recombinant human tumor necrosis factor-related apoptosis-inducing ligand/Apo2 ligand) combined with vinorelbine and cisplatin in patients with advanced non-small-cell lung cancer.* Invest New Drugs, 2018. **36**(2): p. 315-322.
228. Burris, H.A., 3rd, et al., *Improvements in survival and clinical benefit with gemcitabine as first-line therapy for patients with advanced pancreas cancer: a randomized trial.* J Clin Oncol, 1997. **15**(6): p. 2403-13.
229. Hylander, B.L., et al., *The anti-tumor effect of Apo2L/TRAIL on patient pancreatic adenocarcinomas grown as xenografts in SCID mice.* J Transl Med, 2005. **3**(1): p. 22.
230. Hylander, B.L., et al., *Tumor priming by Apo2L/TRAIL reduces interstitial fluid pressure and enhances efficacy of liposomal gemcitabine in a patient derived xenograft tumor model.* J Control Release, 2015. **217**: p. 160-9.
231. Zhao, B., et al., *Mechanisms of TRAIL and gemcitabine induction of pancreatic cancer cell apoptosis.* Asian Pac J Cancer Prev, 2011. **12**(10): p. 2675-8.
232. Suzuki, S., et al., *JNK suppression of chemotherapeutic agents-induced ROS confers chemoresistance on pancreatic cancer stem cells.* Oncotarget, 2015. **6**(1): p. 458-70.
233. Chen, S.H., et al., *Gemcitabine-induced pancreatic cancer cell death is associated with MST1/cyclophilin D mitochondrial complexation.* Biochimie, 2014. **103**: p. 71-9.
234. Sikic, B.I., et al., *A phase Ib study to assess the safety of lexatumumab, a human monoclonal antibody that activates TRAIL-R2, in combination with gemcitabine, pemetrexed, doxorubicin or FOLFIRI.* Journal of Clinical Oncology, 2007. **25**(18_suppl): p. 14006-14006.
235. Zhao, X., et al., *Small molecule inhibitor YM155-mediated activation of death receptor 5 is crucial for chemotherapy-induced apoptosis in pancreatic carcinoma.* Mol Cancer Ther, 2015. **14**(1): p. 80-9.
236. Kindler, H.L., et al., *A randomized, placebo-controlled phase 2 study of ganitumab (AMG 479) or conatumumab (AMG 655) in combination with gemcitabine in patients with metastatic pancreatic cancer.* Ann Oncol, 2012. **23**(11): p. 2834-2842.
237. Forero-Torres, A., et al., *Phase 2, multicenter, open-label study of tigatuzumab (CS-1008), a humanized monoclonal antibody targeting death receptor 5, in combination with gemcitabine in chemotherapy-naive patients with unresectable or metastatic pancreatic cancer.* Cancer Med, 2013. **2**(6): p. 925-32.
238. Oldenhuis, C., et al., *A phase I study with the agonistic TRAIL-R1 antibody, mapatumumab, in combination with gemcitabine and cisplatin.* Journal of Clinical Oncology, 2008. **26**(15_suppl): p. 3540-3540.
239. Tolcher, A.W., et al., *Phase I pharmacokinetic and biologic correlative study of mapatumumab, a fully human monoclonal antibody with agonist activity to tumor necrosis factor-related apoptosis-inducing ligand receptor-1.* J Clin Oncol, 2007. **25**(11): p. 1390-5.
240. Moniri, M.R., et al., *TRAIL-engineered pancreas-derived mesenchymal stem cells: characterization and cytotoxic effects on pancreatic cancer cells.* Cancer Gene Ther, 2012. **19**(9): p. 652-8.

241. Mohr, A., et al., *Targeting of XIAP combined with systemic mesenchymal stem cell-mediated delivery of sTRAIL ligand inhibits metastatic growth of pancreatic carcinoma cells.* Stem Cells, 2010. **28**(11): p. 2109-20.
242. Hylander, B.L., et al., *The anti-tumor effect of Apo2L/TRAIL on patient pancreatic adenocarcinomas grown as xenografts in SCID mice.* Journal of Translational Medicine, 2005. **3**: p. 22-22.
243. Sharma, R., et al., *Influence of the implantation site on the sensitivity of patient pancreatic tumor xenografts to Apo2L/TRAIL therapy.* Pancreas, 2014. **43**(2): p. 298-305.
244. Trauzold, A., et al., *Multiple and synergistic deregulations of apoptosis-controlling genes in pancreatic carcinoma cells.* Br J Cancer, 2003. **89**(9): p. 1714-21.
245. de Miguel, D., et al., *Onto better TRAILs for cancer treatment.* Cell Death Differ, 2016. **23**(5): p. 733-47.
246. Starnoni, M., M. Pinelli, and G. De Santis, *Surgical Wound Infections in Plastic Surgery: Simplified, Practical, and Standardized Selection of High-risk Patients.* Plast Reconstr Surg Glob Open, 2019. **7**(4): p. e2202.
247. Foppiani, E.M., et al., *Impact of HOXB7 overexpression on human adipose-derived mesenchymal progenitors.* Stem Cell Res Ther, 2019. **10**(1): p. 101.
248. Alice Davies, B.S., Krishna Kolluri, Doraid Alrifai, Rebecca Graham, Ben Weil, Rita Rego, Owen Bain, P. Stephen Patrick, Kim Champion, Alex Day, Bilyana Popova, Graham Wheeler, Dan Fullen, Tammy Kalbur, Martin Forster, Mark Lowdell, Sam Janes, *A phase I/II trial to assess the safety and efficacy of MSCTRAIL in the treatment of metastatic lung adenocarcinoma*. 2019, ASCO 2019.
249. Yu, R., et al., *Delivery of sTRAIL variants by MSCs in combination with cytotoxic drug treatment leads to p53-independent enhanced antitumor effects.* Cell Death Dis, 2013. **4**: p. e503.
250. Jo, E.B., et al., *Complete regression of metastatic de-differentiated liposarcoma with engineered mesenchymal stromal cells with dTRAIL and HSV-TK.* Am J Transl Res, 2020. **12**(7): p. 3993-4000.
251. Kim, S.W., et al., *Complete regression of metastatic renal cell carcinoma by multiple injections of engineered mesenchymal stem cells expressing dodecameric TRAIL and HSV-TK.* Clin Cancer Res, 2013. **19**(2): p. 415-27.
252. Mohr, A., et al., *MSC.sTRAIL Has Better Efficacy than MSC.FL-TRAIL and in Combination with AKTi Blocks Pro-Metastatic Cytokine Production in Prostate Cancer Cells.* Cancers (Basel), 2019. **11**(4).
253. Qiu, Y., et al., *Antitumor Activity of Cabazitaxel and MSC-TRAIL Derived Extracellular Vesicles in Drug-Resistant Oral Squamous Cell Carcinoma.* Cancer Manag Res, 2020. **12**: p. 10809-10820.
254. Park, S.A., et al., *Combination treatment with VPA and MSCs-TRAIL could increase anti-tumor effects against intracranial glioma.* Oncol Rep, 2021. **45**(3): p. 869-878.
255. Han, H.R., et al., *Evaluation of Combination Treatment Effect With TRAIL-secreting Mesenchymal Stem Cells and Compound C Against Glioblastoma.* Anticancer Res, 2019. **39**(12): p. 6635-6643.
256. Kim, S.M., et al., *Potential application of temozolomide in mesenchymal stem cell-based TRAIL gene therapy against malignant glioma.* Stem Cells Transl Med, 2014. **3**(2): p. 172-82.
257. Huang, K.C., et al., *Engineered sTRAIL-armed MSCs overcome STING deficiency to enhance the therapeutic efficacy of radiotherapy for immune checkpoint blockade.* Cell Death Dis, 2022. **13**(7): p. 610.
258. Storozynsky, Q. and M.M. Hitt, *The Impact of Radiation-Induced DNA Damage on cGAS-STING-Mediated Immune Responses to Cancer.* Int J Mol Sci, 2020. **21**(22).
259. Alvarez, R., et al., *Stromal disrupting effects of nab-paclitaxel in pancreatic cancer.* Br J Cancer, 2013. **109**(4): p. 926-33.

260. Borsoi, C., et al., *Gemcitabine enhances the transport of nanovector-albumin-bound paclitaxel in gemcitabine-resistant pancreatic ductal adenocarcinoma.* Cancer Lett, 2017. **403**: p. 296-304.
261. Frese, K.K., et al., *nab-Paclitaxel potentiates gemcitabine activity by reducing cytidine deaminase levels in a mouse model of pancreatic cancer.* Cancer Discov, 2012. **2**(3): p. 260-269.
262. Rajeshkumar, N.V., et al., *Superior therapeutic efficacy of nab-paclitaxel over cremophor-based paclitaxel in locally advanced and metastatic models of human pancreatic cancer.* Br J Cancer, 2016. **115**(4): p. 442-53.
263. Von Hoff, D.D., et al., *Gemcitabine plus nab-paclitaxel is an active regimen in patients with advanced pancreatic cancer: a phase I/II trial.* J Clin Oncol, 2011. **29**(34): p. 4548-54.
264. Hunter, T.B., et al., *Paclitaxel and TRAIL synergize to kill paclitaxel-resistant small cell lung cancer cells through a caspase-independent mechanism mediated through AIF.* Anticancer Res, 2011. **31**(10): p. 3193-204.
265. Gravett, A.M., A.G. Dalgleish, and J. Copier, *In vitro culture with gemcitabine augments death receptor and NKG2D ligand expression on tumour cells.* Sci Rep, 2019. **9**(1): p. 1544.
266. Breslin, S. and L. O'Driscoll, *The relevance of using 3D cell cultures, in addition to 2D monolayer cultures, when evaluating breast cancer drug sensitivity and resistance.* Oncotarget, 2016. **7**(29): p. 45745-45756.
267. Longati, P., et al., *3D pancreatic carcinoma spheroids induce a matrix-rich, chemoresistant phenotype offering a better model for drug testing.* BMC Cancer, 2013. **13**: p. 95.
268. Drifka, C.R., et al., *Highly aligned stromal collagen is a negative prognostic factor following pancreatic ductal adenocarcinoma resection.* Oncotarget, 2016. **7**(46): p. 76197-76213.
269. Lawrence, D., et al., *Differential hepatocyte toxicity of recombinant Apo2L/TRAIL versions.* Nat Med, 2001. **7**(4): p. 383-5.
270. Collaborators, G.P.C., *The global, regional, and national burden of pancreatic cancer and its attributable risk factors in 195 countries and territories, 1990-2017: a systematic analysis for the Global Burden of Disease Study 2017.* Lancet Gastroenterol Hepatol, 2019. **4**(12): p. 934-947.
271. Furukawa, K., et al., *Prognostic Factors in Patients With Recurrent Pancreatic Cancer: A Multicenter Database Analysis.* Anticancer Res, 2020. **40**(1): p. 293-298.
272. Je, H., et al., *Overcoming therapeutic efficiency limitations against TRAIL-resistant tumors using re-sensitizing agent-loaded trimeric TRAIL-presenting nanocages.* J Control Release, 2021. **331**: p. 7-18.
273. Thapa, B., R. Kc, and H. Uludağ, *TRAIL therapy and prospective developments for cancer treatment.* J Control Release, 2020. **326**: p. 335-349.
274. Cascinu, S., et al., *Nab-paclitaxel/gemcitabine combination is more effective than gemcitabine alone in locally advanced, unresectable pancreatic cancer - A GISCAD phase II randomized trial.* Eur J Cancer, 2021. **148**: p. 422-429.
275. Bonomi, A., et al., *Adipose tissue-derived stromal cells primed in vitro with paclitaxel acquire anti-tumor activity.* Int J Immunopathol Pharmacol, 2013. **26**(1 Suppl): p. 33-41.
276. Elia, A., et al., *Implication of 4E-BP1 protein dephosphorylation and accumulation in pancreatic cancer cell death induced by combined gemcitabine and TRAIL.* Cell Death Dis, 2017. **8**(12): p. 3204.
277. Szegezdi, E., et al., *Stem cells are resistant to TRAIL receptor-mediated apoptosis.* J Cell Mol Med, 2009. **13**(11-12): p. 4409-14.

278. Wei, L., et al., *Cancer-associated fibroblasts promote progression and gemcitabine resistance via the SDF-1/SATB-1 pathway in pancreatic cancer.* Cell Death Dis, 2018. **9**(11): p. 1065.
279. Liang, C., et al., *Complex roles of the stroma in the intrinsic resistance to gemcitabine in pancreatic cancer: where we are and where we are going.* Exp Mol Med, 2017. **49**(12): p. e406.
280. Pham, T.N.D., et al., *Preclinical Models of Pancreatic Ductal Adenocarcinoma and Their Utility in Immunotherapy Studies.* Cancers (Basel), 2021. **13**(3).
281. Zhan, B., et al., *Identification and causes of metabonomic difference between orthotopic and subcutaneous xenograft of pancreatic cancer.* Oncotarget, 2017. **8**(37): p. 61264-61281.
282. Leventhal, D.S., et al., *Immunotherapy with engineered bacteria by targeting the STING pathway for anti-tumor immunity.* Nat Commun, 2020. **11**(1): p. 2739.
283. Fröbom, R., et al., *Phase I trial evaluating safety and efficacy of intratumorally administered inflammatory allogeneic dendritic cells (ilixadencel) in advanced gastrointestinal stromal tumors.* Cancer Immunol Immunother, 2020. **69**(11): p. 2393-2401.
284. Barton, K.N., et al., *Phase I trial of oncolytic adenovirus-mediated cytotoxic and interleukin-12 gene therapy for the treatment of metastatic pancreatic cancer.* Mol Ther Oncolytics, 2021. **20**: p. 94-104.
285. Humbert, M. and S. Hugues, *Warming up the tumor microenvironment in order to enhance immunogenicity.* Oncoimmunology, 2019. **8**(1): p. e1510710.
286. Carbone, C., et al., *Intratumoral injection of TLR9 agonist promotes an immunopermissive microenvironment transition and causes cooperative antitumor activity in combination with anti-PD1 in pancreatic cancer.* J Immunother Cancer, 2021. **9**(9).
287. Kawahara, K., et al., *The effect of the low stromal ratio induced by neoadjuvant chemotherapy on recurrence patterns in borderline resectable pancreatic ductal adenocarcinoma.* Clin Exp Metastasis, 2022. **39**(2): p. 311-322.
288. Yaochite, J.N., et al., *Therapeutic efficacy and biodistribution of allogeneic mesenchymal stem cells delivered by intrasplenic and intrapancreatic routes in streptozotocin-induced diabetic mice.* Stem Cell Res Ther, 2015. **6**: p. 31.
289. Murai, N., et al., *Intrapancreatic injection of human bone marrow-derived mesenchymal stem/stromal cells alleviates hyperglycemia and modulates the macrophage state in streptozotocin-induced type 1 diabetic mice.* PLoS One, 2017. **12**(10): p. e0186637.
290. Herbst, R.S., et al., *Phase I dose-escalation study of recombinant human Apo2L/TRAIL, a dual proapoptotic receptor agonist, in patients with advanced cancer.* J Clin Oncol, 2010. **28**(17): p. 2839-46.
291. Leng, Y., et al., *Phase II open-label study of recombinant circularly permuted TRAIL as a single-agent treatment for relapsed or refractory multiple myeloma.* Chin J Cancer, 2016. **35**(1): p. 86.

Acknowledgements.

This work has been realized thanks to the close collaboration with Rigenerand s.r.l, now Evotec Modena. The RR001 technology, originally developed and optimized in the laboratory of Cell Therapies directed by Prof. Dominici at the University of Modena and Reggio Emilia, is now owned by Evotec group